PONTIFÍCIA UNIVERSIDADE CATÓLICA DE MINAS GERAIS
Post-graduation program in Mechanical Engineering

Cádmo Augusto Rodrigues Dias

ARTIFICIAL INTELLIGENCE AND DATA SCIENCE FOR OBJECTIVE AND SUBJECTIVE ASSESSMENTS IN A DiM 150 DYNAMIC VEHICLE SIMULATOR

Belo Horizonte
2025

Cádmo Augusto Rodrigues Dias

ARTIFICIAL INTELLIGENCE AND DATA SCIENCE FOR OBJECTIVE AND SUBJECTIVE ASSESSMENTS IN A DiM 150 DYNAMIC VEHICLE SIMULATOR

A thesis submitted to the Post-graduate Program in Mechanical Engineering of the Pontifícia Universidade Católica de Minas Gerais as a partial requirement for obtaining the title of Doctor in Mechanical Engineering.

Supervisor: Professor Jánes Landre Júnior, Ph.D.

Study field: Automotive Engineering

Belo Horizonte
2025

FICHA CATALOGRÁFICA
Elaborada pela Biblioteca da Pontifícia Universidade Católica de Minas Gerais

Dias, Cádmo Augusto Rodrigues
D541a Artificial intelligence and data science for objective and subjective assessments in a DiM 150 dynamic vehicle simulator / Cádmo Augusto Rodrigues Dias. Belo Horizonte, 2025.
113 f. : il.

Orientador: Jánes Landre Júnior

Tese (Doutorado) - Pontifícia Universidade Católica de Minas Gerais. Programa de Pós-Graduação em Engenharia Mecânica

1. Engenharia mecânica - Modelos matemáticos. 2. Automóveis - Dinâmica. 3. Automóveis - Métodos de simulação. 4. Inteligência artificial. 5. Redes neurais (Computação). 6. Linguagem de programação (Computadores). 7. Veículos - Inovações tecnológicas. I. Landre Júnior, Jánes. II. Pontifícia Universidade Católica de Minas Gerais. Programa de Pós-Graduação em Engenharia Mecânica. III. Título.

CDU: 629.113.027
Ficha catalográfica elaborada por Fabiana Marques de Souza e Silva - CRB 6/2086

Cádmo Augusto Rodrigues Dias

ARTIFICIAL INTELLIGENCE AND DATA SCIENCE FOR OBJECTIVE AND SUBJECTIVE ASSESSMENTS IN A DiM 150 DYNAMIC VEHICLE SIMULATOR

A thesis submitted to the Post-graduate Program in Mechanical Engineering of the Pontifícia Universidade Católica de Minas Gerais as a partial requirement for obtaining the title of Doctor in Mechanical Engineering.

Supervisor: Professor Jánes Landre Júnior, Ph.D.

Study field: Automotive Engineering

Professor Jánes Landre Júnior, Ph.D. – Pontifícia Universidade Católica de Minas Gerais, PUC Minas (Supervisor)

Professor Luis Henrique Andrade Maia , Ph.D. – Pontifícia Universidade Católica de Minas Gerais, PUC Minas (Examining committee)

Professor Claysson Bruno Santos Vimieiro, Ph.D. – Pontifícia Universidade Católica de Minas Gerais, PUC Minas (Examining committee)

Professor Juan Carlos Horta Gutiérrez, Ph.D. – Universidade Federal de Minas Gerais, UFMG (Examining committee)

Professor Márcio Eduardo Silveira, Ph.D. – Universidade Federal de São João del-Rei, UFSJ (Examining committee)

Belo Horizonte, July 4th, 2025

ACKNOWLEDGMENTS

To Eliana, my mother, and Íris, my aunt, who together sacrificed numerous personal achievements so that I could have the opportunity to study and attend university.

To my sisters, Nathália and Sarah,
as well as my friends, for their unwavering support.

To Professor Jánes, my supervisor, to whom I am grateful for his guidance, support, and friendship.

To all the teachers, professors, and every staff member at the institutions where I had the privilege to study.

To everyone who contributed to this (long) journey.

I also extend my gratitude to Stellantis LATAM for their cooperation in providing data for this research.

This study was financed in part by the Coordenação de Aperfeiçoamento de Pessoal de Nível Superior – Brasil (CAPES) - Finance Code 001.

“Bringing the gifts that my ancestors gave,
I am the dream and the hope of the slave.
I rise.”
(Still I Rise - Maya Angelou)

ABSTRACT

Data science (DS) and artificial intelligence (AI) techniques are integral to modern Engineering research, and this also holds for Automotive Engineering. In this context, given the growing need to analyze extensive datasets obtained from vehicle instrumentation and simulator use, this study aims to explore the relationship between drivers' subjective experiences regarding vehicle dynamic behavior and its objective metrics (OM). To make this feasible, resources such as artificial neural networks (ANN), with the aid of Python programming language employing libraries like NumPy, Pandas, and Scikit; four virtual car models developed in VI-CarRealTime (VI-CRT) software, and twenty-five human drivers using a dynamic simulator with nine degrees of freedom, the driver in motion VI-Grade DiM 150, were needed. By leveraging data from both virtual simulations and human drivers, the deep neural network (DNN) demonstrated its ability to standardize vehicle evaluations across individuals with varying experience levels, ensuring consistent and objective results, and presenting satisfactory accuracy of around 90%. While one of the key outcomes of this thesis is the capacity to evaluate the vehicle independently of driver subjectivity, another crucial one is the system’s ability to rely on less experienced drivers for vehicle classification. Also, another contribution is the significant reductions in vehicle development time and costs. Overall, this work advances vehicle evaluation by harmonizing subjective and objective assessments, fostering innovation in Automotive Engineering.

Keywords: Dynamic vehicle simulator. DiM 150. Artificial intelligence. Subjective assessments. Objective metrics.

RESUMO

As técnicas de ciência de dados e inteligência artificial são essenciais para a pesquisa em Engenharia moderna e, não diferentemente, isso também se aplica à Engenharia Automotiva. Nesse contexto, dada a crescente necessidade de analisar extensivos conjuntos de dados obtidos a partir da instrumentação de veículos e do uso de simuladores, este trabalho tem como objetivo explorar a relação entre as experiências subjetivas dos motoristas, em termos do comportamento dinâmico de veículos, com métricas objetivas. Para viabilizar essa análise, foram utilizados recursos como redes neurais artificiais, com o auxílio da linguagem de programação Python e bibliotecas como NumPy, Pandas e Scikit; quatro modelos virtuais de veículos desenvolvidos no software VI-CarRealTime; e vinte e cinco motoristas reais em um simulador dinâmico com nove graus de liberdade, o VI-Grade DiM 150. Ao explorar os dados provenientes de simulações virtuais e de motoristas reais, a rede neural profunda demonstrou sua capacidade de estimar as avaliações dos veículos entre pilotos com diferentes níveis de experiência, garantindo resultados consistentes e objetivos, com uma precisão satisfatória em torno de 90%. Embora uma das principais contribuições desta tese seja a capacidade de avaliar o veículo independentemente da subjetividade do motorista, outro resultado importante é a possibilidade de o sistema utilizar motoristas menos experientes para a classificação dos veículos. Adicionalmente, destaca-se a significativa redução no tempo de desenvolvimento e nos custos associados ao projeto de veículos. Em suma, este trabalho promove avanços na avaliação de veículos ao harmonizar avaliações subjetivas e objetivas, incentivando a inovação na engenharia automotiva.

Palavras-chave: Simulador dinâmico veicular. DiM 150. Inteligência artificial. Avaliações subjetivas. Métricas objetivas.

LIST OF FIGURES

LIST OF TABLES

LIST OF ABBREVIATIONS

AI	Artificial intelligence
ANN	Artificial neural network
BD	Big data
BNDES	Banco Nacional de Desenvolvimento Econômico e Social
BP	Backpropagation
CG	Center of gravity
DL	Deep learning
DLC	Double-lane change
DIL	Driver-in-the-loop
DS	Data science
DT	Digital twin
DNN	Deep neural network
EPS	Electric steering system
ESC	Electronic stability control
HIL	Hardware-in-the-loop
IoT	Internet of Things
K&C	Kinematics and compliance
MC	Motion cueing
MIL	Model-in-the-loop
ML	Machine Learning
OM	Objective metrics
RL	Reinforcement learning
SA	Subjective metrics
SIM Center	*Centro de Excelência em Simulação Dinâmica e Segurança Ativa de Veículos*
RNN	Recurrent neural networks
SUV	Sport utility vehicles
SWA	Steering wheel rotation angle
VI-CRT	VI-CarRealTime

LIST OF SYMBOLS

F_a	Damping force
$\dot{\Delta}_a$	Damper mass velocity
c_a	Damper constant
c_g	The position of the center of the peak (Gaussian function)
σ_g	Standard deviation (Gaussian function)
y	Non-linear output
x_n	External input signal
w	Weight (ANN)
f	Activation function
u	Input signal to the activation function
E	Mean square error
p	Number of training samples
k	Number of neurons present in the last layer
d	Desired output (ANN)
M_s	Sprung mass
M_{ns}	Unsprung mass
k	Stiffness
F	Spring force
Δ	Linear displacement
τ	Steering ratio
$\measuredangle$	Wheel steer angle
K	Understeer gradient
a_y	Lateral acceleration
L	Distance from front and rear-end axles
R	Turn radius
C_s	Sprung mass damper coefficient
K_s	Sprung mass stiffness coefficient
C_{ns}	Unsprung mass damper coefficient
K_{ns}	Unsprung mass stiffness coefficient
ns	Unsprung mass

F_c Force due body weight

F_r Force due wheel displacement

Z_{M_s} Sprung mass vertical displacement

$Z_{M_{ns}}$ Unsprung mass vertical displacement

Z Road vertical profile

$[m]$ Mass matrix

$[c]$ Damping matrix

$[k]$ Stiffness matrix

$\{z\}$ Displacement unidimensional matrix

$\{F\}$ Force unidimensional matrix

θ Track slope

a_x Longitudinal acceleration

b Distance between CG and front-end axle

c Distance between CG and rear-end axle

DA Drag force

d_h Distance between rear-end axle and towing point

Fx_f Front tractive force

F_{x_r} Rear tractive force

cg Centre of gravity

h_a Drag forces height

h_h Drag forces height

L Distance between axles

R_{h_x} Towing force (horizontal)

R_{h_z} Towing force (vertical)

R_{xf} Front-end axle rolling resistance

R_{xr} Rear-end rolling resistance

W Total weight

W_{fs} Total weight (front-end axle)

W_{fr} Total weight (rear-end axle)

θ Road slope

α Slip angle

F_{yf} Lateral force (front-end axle)

F_{yr} Lateral force (rear-end axle)

V_x Longitudinal speed

CONTENTS

1 INTRODUCTION

The use of virtual simulation has reshaped the landscape of Automotive Engineering, offering a controlled and efficient means to evaluate vehicles and their systems' performance in virtual environments (SCHURMANN *et al.*, 2023; SEREDYNSKI, 2020). At the pinnacle of this state-of-the-art technology are centers of excellence equipped with dynamic simulators (DIAS, C.; LANDRE, 2022), as exemplified in Figure 1.

Figure 1 – The *Centro de Excelência em Simulação Dinâmica e Segurança Ativa de Veículos* (SIM Center)

Source: Prepared by the author

These centers of excellence have elevated levels of technology and are increasingly present in the main research centers around the world (DELL'ANNUNZIATA *et al.*, 2022; VI-GRADE, 2021), e.g., the SIM Center. A partnership between the university and industry, this laboratory is located at the Pontifícia Universidade Católica de Minas Gerais (PUC Minas) as a project developed with the support of the Banco Nacional de Desenvolvimento Econômico e Social (BNDES), in 2016, standing out for currently being the only equipment of its magnitude in the southern hemisphere.

Two analyses are usually performed in simulators of this bulk: The objective and the subjective. While in the subjective analysis test drivers perform maneuvers with the virtual model, later reporting the sensations perceived regarding the behavior of the vehicle during driving and consequently suggesting changes for optimized results, through subjective

assessments (SA), the objective analysis is carried out comparatively with the telemetry data of the current model concerning the desired design behavior or to other reference vehicles, through objective metrics (AO; LI, 2022; KUMAR *et al.*, 2023; RAABE *et al.*, 2023).

Particularly in terms of subjective analysis, today there is no robust mechanism to quantify the dynamic behavior of virtual vehicle models without including the abstraction of distinct drivers (KIM, D. *et al.*, 2019a). Thus, the elaboration of a correlation method between subjective assessment and objective metrics has been a necessity of Automotive Engineering for years (DIAS, C. A. R.; LANDRE JÚNIOR, 2023; GIL GÓMEZ *et al.*, 2018; KIM, D. *et al.*, 2019b; ZHAO, J. *et al.*, 2018).

This context is corroborated by (ASH, 2002), in which the author was already exploring alternatives for establishing such correlations at the beginning of this century: Despite the limited use of artificial neural networks at that time, particularly due to the computational limitations back then. Notwithstanding over 20 years of technological advancement, recent research in this field indicates that a satisfactory correlation method is still required, especially concerning driver-in-the-loop (DIL) simulators, where findings remain particularly sparse. Notably, considerable advancements are still needed for the acceptance of this technology, especially when considering human factors (DE NALDA TÁRREGA *et al.*, 2022). Consequently, the present study distinguishes itself from previous works due to its focus on classifying the dynamic behavior of virtual vehicle models independently of the subjectivities associated with various drivers.

1.1 Aims

This topic will address the specific and general aims of the work.

1.1.1 General aim

The present work aims to classify vehicles' dynamic behaviors, in terms of subjective driving experiences, based on objective metrics, using artificial intelligence tools and data science techniques.

1.1.2 Specific aims

The above general aim will be achieved through the following specific goals.

a) Assess how the integration of data from virtual simulation improves understanding of the driver-vehicle interactions;
b) Analyze how powerful the influence of driver subjectivity is on the evaluation of vehicle systems in a simulation environment;
c) Evaluate the applicability of data science and artificial intelligence methods in assessing vehicle handling dynamics.

1.2 Motivation

Less than a decade ago, using centers of excellence in vehicle dynamics was restricted to high-performance vehicles and sometimes only with motorsport ones, e.g., Formula One. Since the first national road car project that carried out experiments at the SIM Center throughout its development was launched only in the last couple of years, the present work becomes important because it seeks to classify the quality of the dynamic behavior of virtual models in the center of excellence aforementioned, mainly because in these days this analysis is purely subjective and therefore can vary considerably according to the driver perception. Besides this, the time needed in simulations will be reduced with the developed solution. Consequently, the current costs using laboratories such as the SIM Center, estimated as one thousand euros per hour, will be reduced by about eighty percent.

1.3 Thesis structure

This text is arranged under the list presented below.

a) Chapter 1 seeks to justify the importance of the present work as well as to situate it in the development of the research field;
b) Chapter 2 investigates some fundamental theoretical topics to understand the methodology that will be proposed;
c) Chapter 3 scratches the methodology used during this research;
d) Chapter 4 explores the results;
e) Chapter 5 discusses some conclusions;

2 LITERATURE REVIEW

Before discussing the methodology of this work, it is necessary to review some topics in the bibliography. At the same time, to understand where this work is situated, the first section of this chapter seeks to present the state of the art in the related research field.

2.1 State of the art

Despite the first simulators dating back to the 1930s (PASZKIEL, 2020), the technology utilized in the current ones is considerably new. Yet, some works that explore the relationship between machine and human aspects are worth mentioning, as these methodologies can inspire both new and experienced researchers to make important developments (SERJE; ACUÑA, 2022).

Corroborating that the available literature does not include a comprehensive survey on the evaluation of the objective and subjective aspects, (GUASTADISEGNI *et al.*, 2023) develops a review to approach the objective metrics of vehicle rides and the approaches used to translate this data into subjective assessments. At the end of the work, the authors have achieved satisfactory procedures to perform ride quality analyses.

Meanwhile, (PAGLIARECCI *et al.*, 2020) performs similar work with the difference that now the aim is to develop a methodology for the tire handling performance evaluation. Reaching acceptable results in relating vehicle metrics and the drivers' assessments, the authors use a clustering method aiming to group, categorize, and differentiate specific tire performance. Also, in this process, the authors explain that vehicle responses have a big effect on the driver's steering input and, therefore, on the subjective rating.

This time, aiming for the handling analysis, (ZHANG, X. *et al.*, 2020) find a good consistency of subjective and objective evaluation by exploring an objective-index-mining method. Achieving up to eighty percent relation between OM and subjective assessments, the authors extract twelve core handling objective indexes with sample sizes over one hundred and twenty using the proposed method.

Another crucial area in vehicle development is related to its comfort. In (AO *et al.*, 2020), the authors delve into the relationship between objective metrics of whole-body vibration, hand-transmitted vibration, and SA to comprehend the connection between OM and subjective experiences. To achieve this, the authors employ linear and polynomial regression models, yielding compelling findings, e.g., identifying optimal positions and variables for

gathering objective data, as well as determining the most reliable variables for evaluation purposes.

In parallel, research on eco-driving strategies for electric vehicles has gained prominence due to the need to balance energy efficiency and passenger comfort. However, usually applied techniques can introduce acceleration variations that negatively impact passenger experience. In this context, (XUE *et al.*, 2025) try to determine driving profiles that minimize energy consumption without compromising comfort. To do so, a correlation between SA and OM is found, and the authors corroborate that this kind of methodology is essential for studies in dynamic DiL simulators.

On the other hand, (ZHOU, W. *et al.*, 2023) proposed a new evaluation method of drivability for passenger vehicles considering OM and SA. In this study, the authors use a mix of techniques, e.g., R-type clustering, ANN, and fuzzy logic. After judging the results, the evaluation tool developed had satisfactory results, achieving the maximum subjective and objective relative error of about five percent.

Nevertheless, particularly in works that use DiL simulators, before even approaching the relationship between objective metrics and SA, the correlation between physical vehicles and virtual models is sought (DIAS, C.; LANDRE, 2023). Since the credibility of the virtual data has been reached to the extent that such a model represents the physical vehicle as faithfully as necessary (DIAS, C. A. R. *et al.*, 2021), this is a key step in the development of the virtual models. In both works, the authors found satisfactory results and reached their aims.

Despite those studies primarily focusing on vehicle quality or, at most, the driver-vehicle relationship quality, modern research has also concentrated solely on the driver. This is exemplified by (LÖCKEL *et al.*, 2022) who, under the premise that understanding and modeling human driving behavior is crucial for vehicle development, addressed the complexities of objectively assessing and imitating professional race drivers. Their work highlights the influence of individual driving styles, intricate decision-making processes, and narrow stability margins. By employing a data-driven approach, the authors also achieved their aim at the end of the work.

2.2 Industry 4.0 and its main techniques

While (SONY; NAIK, 2019) define Industry 4.0 as the transformation of organizations to the digital landscape, (PICCAROZZI; AQUILANI; GATTI, 2018) argue that Industry 4.0 is based on the development of fully automated and intelligent production, also able to

communicate autonomously. More emphatically, (KAMBLE; GUNASEKARAN; GAWANKAR, 2018) state that the term discussed here presents a completely new perspective for the industry regarding how the integration of manufacturing processes and modern technologies can achieve maximum production with less use of resources.

Although (OZTEMEL; GURSEV, 2020) have reported that the term has several different interpretations, it is agreed in the literature that Industry 4.0 has a direct relationship with the technological evolution of recent years, where more and more tasks have been performed according to the evolution of computing devices (Figure 2).

Figure 2 – Stages of the Industrial Revolution

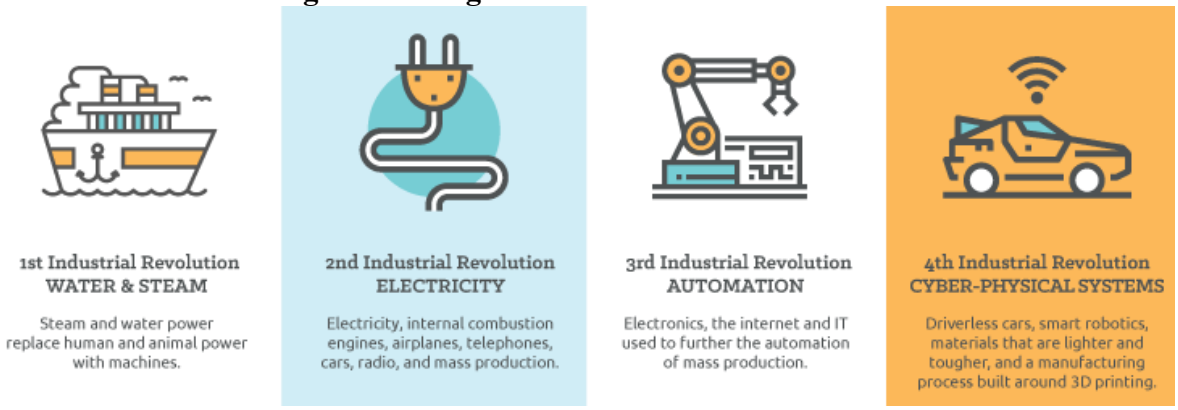

Source: (LEDWABA, 2020).

In short, the techniques developed in the fourth phase operate with substantial amounts of data, via mathematical modeling and systems connectivity, to obtain results that assist in decision-making (SPERINGER; SCHNELZER, 2019). Intuitively, the architecture of this relationship tends to become more complex as the interaction between humans and objects grows, as explained by Simota and Steiner (2017) *apud* (PINTO, 2019), and techniques such as DS are needed more than ever.

In this context, unfamiliar terms that are currently part of the routine of many areas of knowledge have been born, such as artificial intelligence, machine learning, internet of things (IoT), digital twin (DT), deep learning (DL), and big data (BD) (RAI *et al.*, 2021). However, some of these techniques are often confused. As a result, Figure 3 seeks to explain the difference between the terms.

Figure 3 – Artificial intelligence and some of its techniques

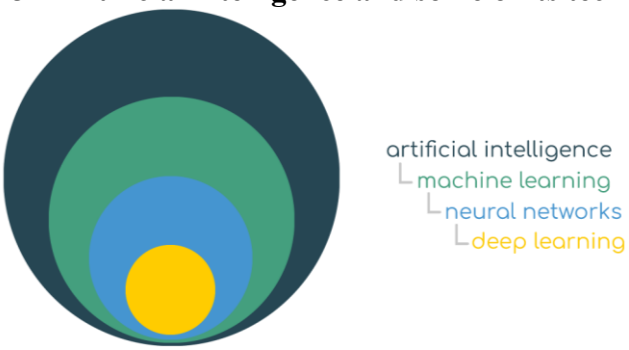

Source: Prepared by the author

According to the previous figure, artificial intelligence is a relatively broad set of techniques that aim to enable machines to reproduce certain human behaviors, e.g., machine learning. ML, consequently, is a set of techniques that allow the machine to learn without the need to be directly programmed.

Teaching a machine without the need to program it directly is initially equivalent to providing historical data composed of boundary conditions and their effects. From these data, the machine uses numerical models to seek the best correlation between the input and output information, thus predicting future solutions based on new input data. In this sense, (KHAYYAM *et al.*, 2020) list several ML techniques that can perform such prediction, such as reinforcement learning (RL), regression algorithms, Bayesian algorithm, k-means algorithm, and the already mentioned artificial neural networks.

Therefore, similarly to the flow developed above, neural networks are nothing more than one of the techniques that can be used to implement ML. On the other hand, deep learning is a technique that uses neural networks with multiple intermediate layers for deep analysis, as suggested by the technique's nomenclature (SONG; MONTENEGRO-MARIN; ENRIQUE, 2021), resulting in the deep neural networks. The concept of deep analysis arises from the principle that the investigation of the system occurs in several distinct stages, where each stage feeds the next with the information generated in the previous stage.

Still regarding the ML techniques, the better efficiency achieved by neural networks results in a greater prominence of this one over the other alternatives (DA LIO; BORTOLUZZI; ROSATI PAPINI, 2020a).

2.2.1 Artificial neural networks

According to (MARINKOVIĆ *et al.*, 2020), an artificial neural network is an established and powerful mathematical tool with the ability to learn and generalize results from

training. Working on this statement, (PINTO, 2019) explains that ANNs operate in a similar way to biological neural networks (Figure 4): Information is received, processed, and then passed on, which results in the identification and classification of patterns.

Figure 4 – Two neurons of a biological neural network and its main components

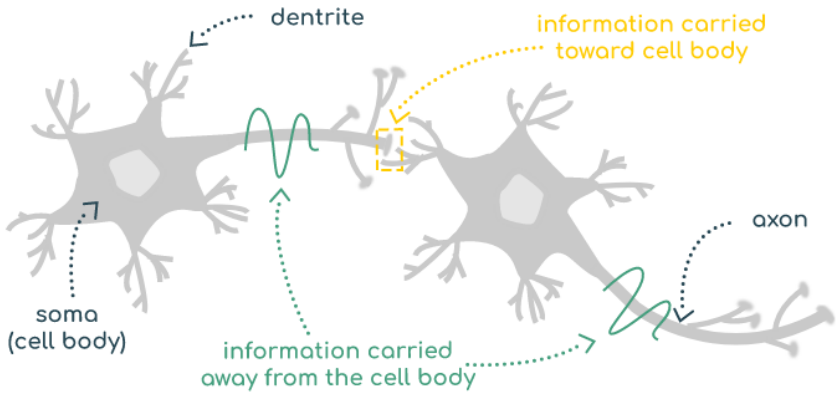

Source: Prepared by the author

As explained by (VAN DE BURGT; GKOUPIDENIS, 2020), a biological neuron consists of axons, dendrites, and a cell body. While the dendrites receive information, the cell body stores it until a certain activation signal is identified by the system. At that time, the stored information is transmitted to the next neuron via axons. Also, according to the authors referenced, the connection for transmission of information occurs via junctions in the order of nanometers, known as synapses.

Seeking to reproduce computationally a behavior like the above, ANNs appeared in 1943 (MCCULLOCH, 1943) and evolve in the following decades, along with the development of computational science (WANG, Y. *et al.*, 2020). Generally speaking, (FEIZIZADEH *et al.*, 2021) explains that an ANN is composed of three main levels: Input, hidden, and output layer. However, depending on the application, an ANN can have multiple hidden layers, as shown in Figure 5.

Figure 5 – Generic ANN with 3 inputs, 2 outputs, and n hidden layers with n neurons

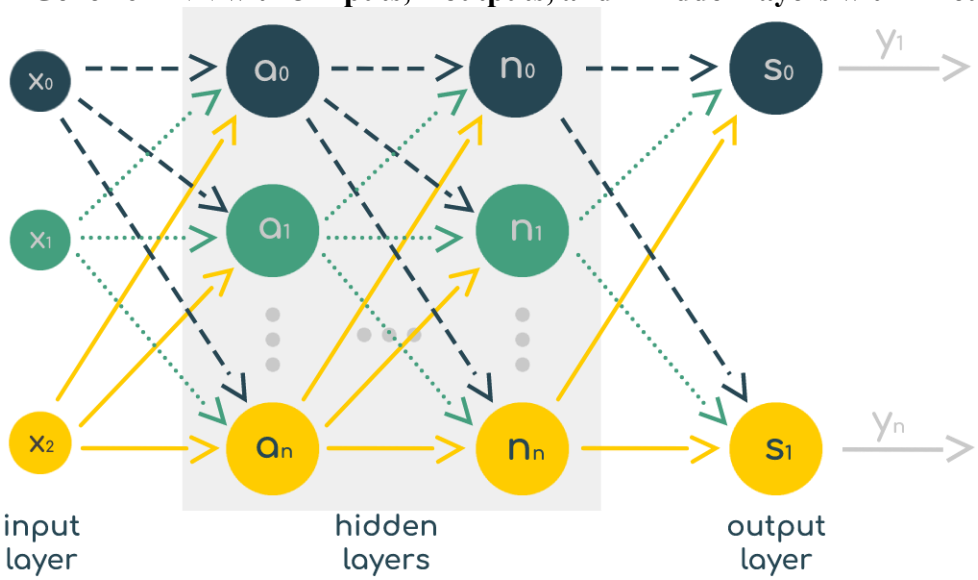

Source: Prepared by the author

This possibility corroborates what was previously discussed regarding the definition of deep learning, which is nothing more than a technique that uses ANNs with multiple hidden layers. Another definition derived from the figure above is that, as all neurons in one layer are connected to all neurons in the next layer, this is a fully connected ANN.

As explained by (NHU *et al.*, 2020), the number of hidden and output layers defines the depth of a neural network. Since in the network of Figure 5 the connection of neurons in all layers was performed from left to right, this architecture is called feedforward. On the other hand, there are recurrent neural networks (RNN) where one or more neurons receive feedback from other neurons in the same layer or from future layers. There is also the possibility of working with networks that have, simultaneously, feedforward layers and recurring layers (SHEAHAN *et al.*, 2021), all depending on the application goal.

However, in aiming for an ANN with multiple neurons to be able to perform classifications, it is necessary to train it from a pre-made database. While (BROWNLEE, 2016) explains that most of the data used for ML algorithms needs to be preprocessed, (DA LIO; BORTOLUZZI; ROSATI PAPINI, 2020b) says that ANNs are frequently used for these types of applications because it has outperformed most ML techniques. In this scenario, the next topics seek to address some of the main concepts and steps for the development and use of these networks.

2.2.1.1 Artificial neuron

According to Silva, Spatti and Flauzino (2010) *apud* (PINTO, 2019), an artificial neuron processes information in 10^{-9} s. In contrast to the 10^{-3} s required for processing the biological one, the artificial one is considerably superior, however, as shown generically in Figure 6, the artificial neuron typically works sequentially, unlike the biological neuron, which has high levels of parallelism.

Figure 6 – Main components of an artificial neuron

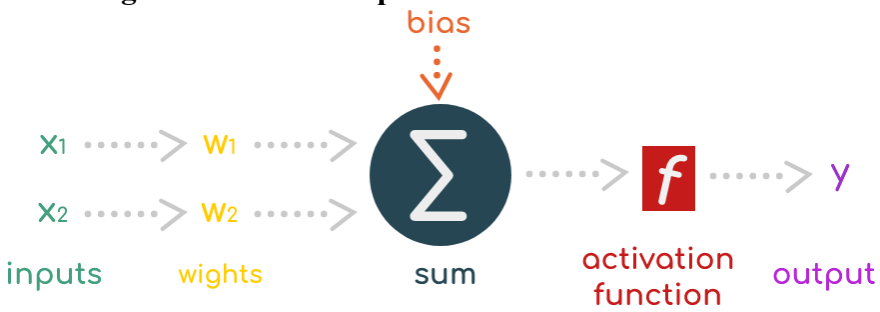

Source: Prepared by the author

As exposed in the figure above and discussed by (KOUTSOUKAS *et al.*, 2017), the artificial neuron is a component that follows the task list below:

a) Receive external signals as input ($x_0,\ x_1,\ x_2,\ \ldots,\ x_n$);
b) Multiply received signals by specific weights w for each of the inputs;
c) If necessary, add bias to adjust the activation threshold;
d) Add the values of each input and bias through a linear combiner (sum);
e) Return a non-linear y signal as output.

As for the third step, (GUE *et al.*, 2020) define activation potential as the difference between the linear combiner and the bias, where such potential is excitatory if the difference is positive, and inhibitory if it is negative (BAKER; ZHU; ROSENBAUM, 2020). On the other hand, as for the non-linearity of the output signal, (KOUTSOUKAS *et al.*, 2017) explains that it occurs after the signal has passed through the activation function, discussed in detail in the next section.

2.2.1.2 Activation functions

Activation functions are mechanisms that enable or disable neurons according to the characteristic conditions of the functions themselves (DA ROCHA, 2021). More boldly, (WANG, Y. *et al.*, 2020) say that it is the presence of activation functions that define ANNs as

AI engines. Having exposed the importance of these functions, (DATTA, 2020) says that the correct choice of the function to be used in the architecture of a network is fundamental, since it is through it that the definition of both availability and how the data is arranged for the next layer.

In this context, (DATTA, 2020) says that activation functions must have five properties:

a) Non-linearity: In this way, ANNs can work with linear and non-linear phenomena, the latter being a large part of the practical problems encountered in nature;
b) Differentiable (and, consequently, continuous): Necessary for the calculation of the loss function, which will still be worked on throughout this text;
c) Zero-centered: Although not strictly necessary, the use of zero-centered functions helps in training the network by considerably reducing processing time;
d) Maximum and minimum limits: Necessary to prevent calculated values from tending to infinite.

In this context, some of the main activation functions are described in Table 1 and presented in Figure 7, where u is the input signal of the functions and $y(u)$ the output.

Table 1 – The main activation functions

a) Heaviside:
   - According to (ALBERINI; CAPITANELLI; VITA, 2021), the Heaviside function is defined by Equation 1.

$$\mathbf{y(u)} = \begin{cases} \mathbf{0 \text{ if } u < 0} \\ \mathbf{1 \text{ if } u \geq 0} \end{cases} \quad \mathbf{(1)}$$

b) Bipolar step:
   - As discussed in (ALZUBI, 2021), the bipolar step differs from the unit step in its results being -1 when $y(u) < 0$, as follows in Equation 2.

$$y(u) = \begin{cases} -1 \text{ if } u < 0 \\ 0 \text{ if } u = 0 \\ 1 \text{ if } u > 0 \end{cases} \quad (2)$$

c) Symmetric ramp:
   - For activation in the symmetric ramp function, (PINTO, 2019) explains that a certain constant must be defined (Equation 3).

$$y(u) = \begin{cases} -1 \text{ if } u < \text{constant} \\ u \text{ if } -\text{constant} \leq u \leq \text{constant} \\ \text{constant if } u > \text{constant} \end{cases} \quad (3)$$

d) Sigmoid or logistic:

- According to Nwankpa et al. (2018) *apud* (DATTA, 2020), the sigmoid logistic function is one of the most used nowadays and is described by Equation 4.

$$y(u) = \frac{1}{1+e^{-u}} \quad (4)$$

e) Hyperbolic tangent:

- Similar to sigmoid logistics, the hyperbolic tangent function can rely on the use of linear coefficients that multiply the input signal to adjust the slope of the result before the inflection point (PINTO, 2019). However, this function differs from the first one once it assumes values between -1 and 1 (Equation 5).

$$y(u) = \frac{1-e^{-u}}{1+e^{-u}} \quad (5)$$

f) Gaussian

- This function uses concepts from Gaussian statistics for its definition. This feature results in equal results for activation potential values that are equidistant from the mean, explain (MURRAY; ABROL; TANNER, 2021) and (PINTO, 2019). So where c_g is the position of the center of the peak and σ_g the standard deviation, Equation 6 stands for the Gaussian activation function.

$$y(u) = e^{-\frac{(u-c_g)^2}{2\sigma g^2}} \quad (6)$$

Source: Prepared by the author

Figure 7 – The main activation functions

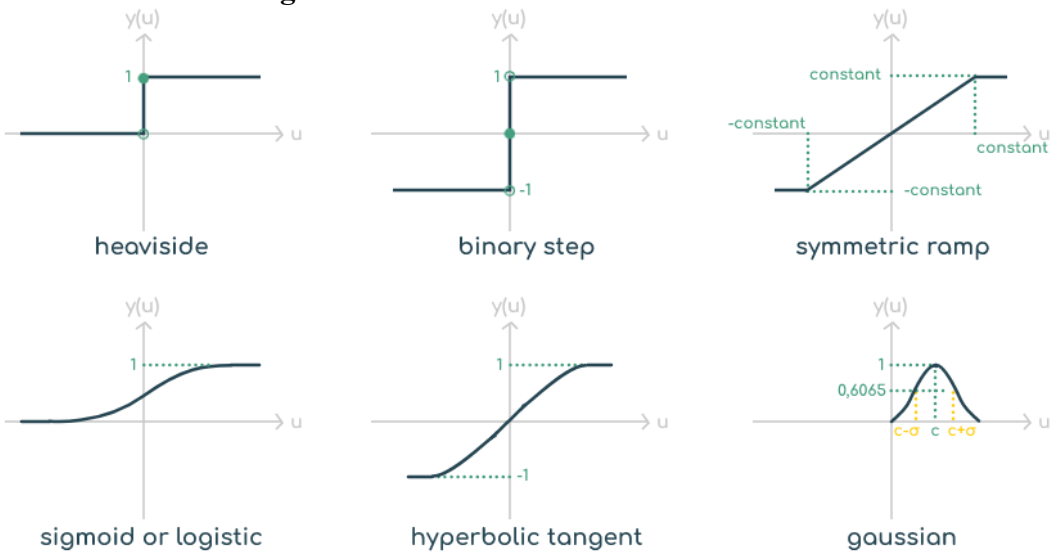

Source: Prepared by the author

2.2.2 Neural network training

There are two major groups of training techniques, named supervised and unsupervised training. In opposition to the latter, supervised training takes place when the class of label elements to be sorted is known (KHAYYAM et al., 2020). As these authors explain, while unsupervised training is commonly applied to the definition of patterns, supervised training is often used to target classifications and regressions.

Regardless of the technique or architecture chosen, (PULVERMÜLLER *et al.*, 2021; SCHWARZSCHILD *et al.*, 2021) explain that the supervised training principle of neural networks is invariant: From the error between the expected results and those found by the iteration, the weights and bias of each connection are adjusted while the boundary conditions provided for the algorithm are not satisfied (Figure 8).

Figure 8 – Schematic representation of the training process of an ANN

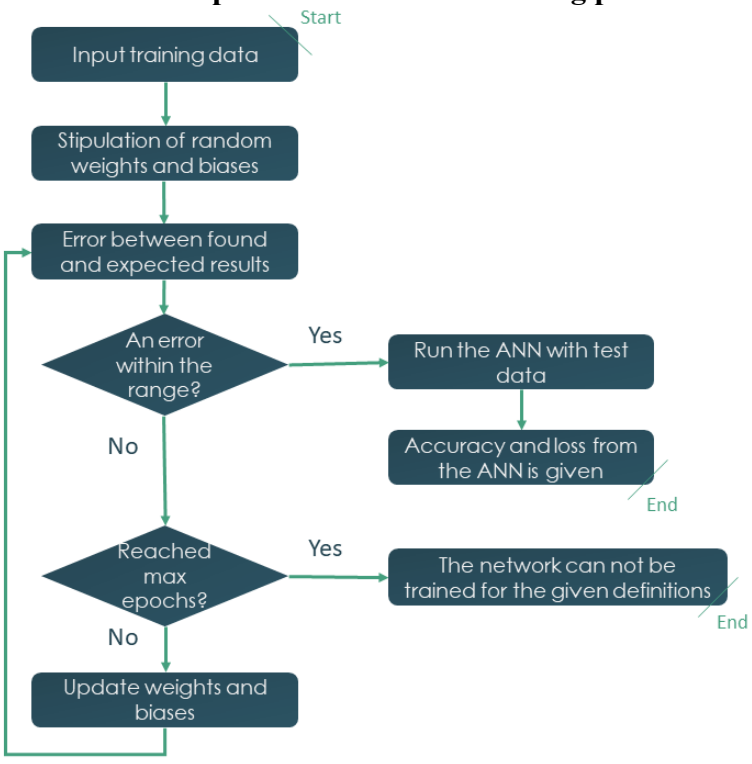

Source: Prepared by the author

Among the boundary conditions, one of the most important is model accuracy, once the iterative training process continues until the prediction error falls below a predefined threshold or the maximum number of epochs is reached. On the other hand, an epoch is the number of times the network receives all the training data and performs the weight and bias adjustments (PINTO, 2019). The simultaneous use of multiple boundary conditions is usually interesting

because it avoids situations in which the calculations do not converge, resulting in a non-interruption of the processing; or even aiming to avoid network overfitting.

Since the aim is usually to reduce the error during training, it is intuitive to assume that the smaller this error is, the better the network solution will be. However, exceedingly small errors can cause the phenomenon known as overfitting. Although some studies positively use this phenomenon (BARTLETT *et al.*, 2020), overfitting remains highly unwanted for most ANN applications. As explained by (BILBAO; BILBAO, 2017), overfitting occurs when the error found with training data is relatively small, however, for test data, this error is proportionately high.

In other words, this means that the network is addicted to training data, which are specific cases, but consequently has low generalization power for other scenarios. Still according to (BILBAO; BILBAO, 2017), this phenomenon usually occurs due to a variety of factors, among which stand out the inadequate number of layers and neurons in the network, the existence of noise in the input data, and an exaggerated amount of data for training.

Although the solutions for overfitting are still considerably empirical and therefore depend extraordinarily on the case studied, (YING, 2019) lists some highly effective strategies to avoid this behavior. Among them, the author argues that early stopping is one of the best solutions to avoid overfitting. This strategy consists of controlling the number of epochs as well as not working with extreme prediction errors.

2.2.2.1 The backpropagation technique

Among the most used techniques for the supervised training of ANNs, backpropagation (BP) stands out due to its robustness (SARKER, 2021). Also called the generalized delta rule, BP is the basis of other more complex techniques (ZHOU, C.; LIU; XU, 2021).

After the definition of random weights and bias, the backpropagation algorithm is performed through two major steps: While the first one is responsible for defining the output signals of each neuron until the final value of the network is found (functional signal), the second phase consists of updating the weights and bias of each connection, from right to left, from the error found in the iteration (error signal) (YANG *et al.*, 2021). On the other hand, Braga et al. 2017 *apud* (PINTO, 2019) defines the mean square error (E), a BP cost function to be minimized, according to Equation 7.

$$E = \frac{1}{2}\sum_{P}\sum_{i=1}^{k}(d_i^p - y_i^p)^2 \quad (7)$$

In the equation above, p corresponds to the number of training samples, k to the number of neurons present in the last layer, and d and y to the desired output and the last output of the neural network, respectively. According to (YU *et al.*, 2021), the return process in the ANN for parameter adjustment due to the error found (Figure 9) occurs continuously, being interrupted only when the convergence between the calculated and provided data is reached. Due to this characteristic, the technique was defined by the term backpropagation.

Figure 9 – Information flow during training with backpropagation

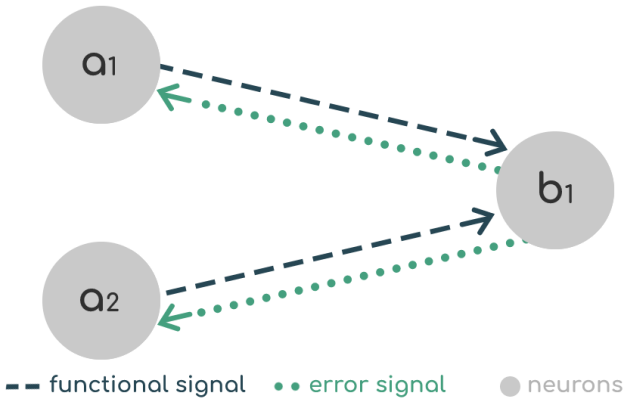

Source: Prepared by the author

2.2.3 Main models of neural networks

Given the complexity of biological systems, certain challenges in the development of ANNs faithfully reproduce biological behavior (JONES; KORDING, 2020). Along with this issue and the computational evolution in recent years, there are several artificial neural network solutions, and both Table 2 and Figure 10 seek to present some of the main ones.

Table 2 – Most used ANN models and their main characteristics

ANN	Architecture	Training process	Observations
Multilayer perceptron (MLP)	Feedforward; Fully connected	Supervised	Considered the basis of the algorithms of deep learning
Convolutional (CNN, ConvNet)	Feedforward; Fully connected	Supervised	Widely used in image recognition and computer vision; Learn directly from data
Long Short-Term Memory (LSTM)	Recurrent	Supervised	RNN type is widely used in natural language processing and chatbots
Self-organizing Map (SOM)	Multiple competing output layer neurons	Unsupervised	Learn via competition algorithms; Widely used for clustering and medical diagnostics

Source: Adapted from (SARKER, 2021)

Figure 10 – Some of the most used models of neural networks

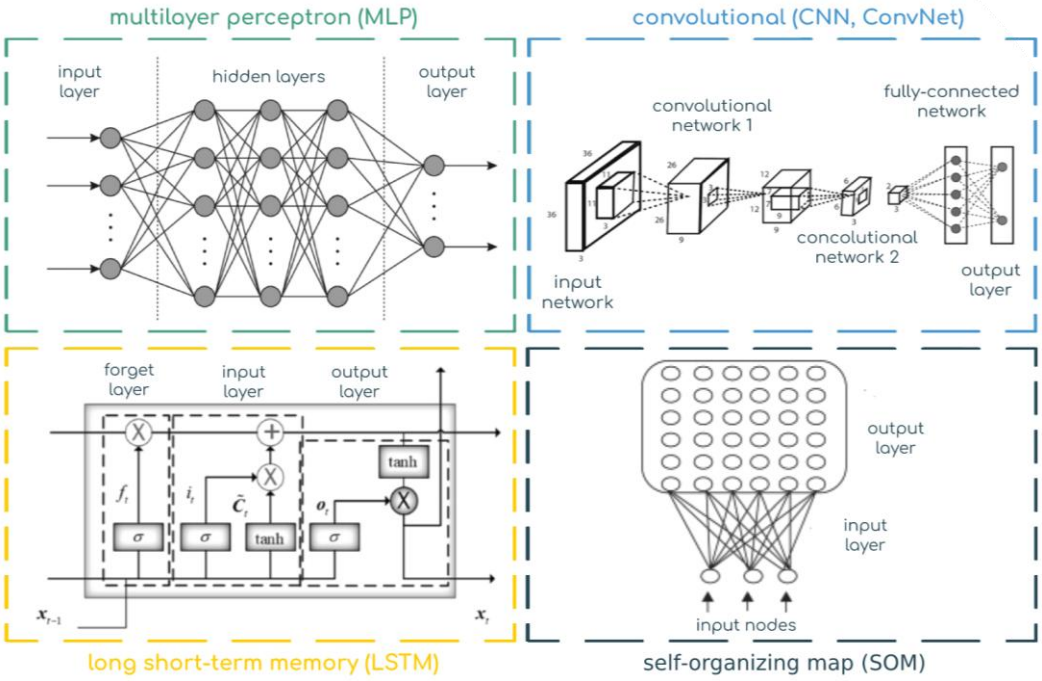

Source: Adapted from (SARKER, 2021)

More details about each type of network above as well as other types that were not mentioned in Table 2 can be found in the work of (SARKER, 2021), which consists of a review of the main types of ANNs.

2.3 Vehicle dynamics

Contrary to what is often idealized, vehicle dynamics do not only cover the behavior of cars on roadways. In fact, this study field is concerned with the movement of cars, buses, trucks, and other types of vehicles on the road surface (GILLESPIE, 1992). Still for the presented author, the dynamic topics are defined by the force that the vehicle suffers due to the presence of gravity, the aerodynamic variables, and the effort transferred by the tires. Corroborating the above, (ABE, 2015) also provides that road vehicles can be divided into two large groups: One that is free to move in any direction through tires, such as city buses, and another for vehicles with physically limited paths, such as locomotives.

The importance of vehicle dynamics is proved by the presence in the curriculum of engineering students for over a hundred years (JAZAR, 2017). As the author mentioned, this study emerged with the definition of methodologies on the behavior of the various systems linked to vehicles, and, currently, it tends to seek the modeling and optimization of systems through multibody analysis. According to (MARQUES *et al.*, 2019), a multibody system can

be defined as a set of bodies interconnected by joints and under the action of forces, interacting with each other and the rest of the system.

In the present work, the content of the vehicle dynamics in focus refers to the chassis design. Through the tires, the chassis interacts with the ground and, as (WEI; TAGHAVIFAR, 2017) explains, the road vehicles are prone to a series of oscillations due to uneven ground. Consequently, the vehicle may become unstable, and several other undesired effects may ensue. It is in this scenario that the design of vehicle chassis and their respective components becomes important in terms of guaranteeing stability, comfort, and safety to passengers.

According to (SUH; LEE; YOON, 2000), the chassis design is the step of a project that has the greatest influence on the performance of a vehicle in its initial stage, requiring too much attention when elaborated. In addition, (ELMADANY; DOKAINISH; ALLAN, 1979) comment that one of the main demands in a chassis design is the improvement in vehicle comfort during riding, which still is a reality nowadays (RAKHMATOV; BOKAREV; MARTYNOV, 2024; SKRICKIJ *et al.*, 2024; ZHANG, B.; LUO; TAN, 2024). Also, according to (ÖZCAN; SÖNMEZ; GÜVENÇ, 2013), the linear components responsible for several functions, including comfort, can be modeled and projected by solving a series of ordinary and linear differential equations.

2.3.1 Sprung and unsprung masses

Seeking to simplify the analyses, the vehicle mass and its respective inertia are commonly considered concentrated in the vehicle's center of gravity (CG). As explained by (GILLESPIE, 1992), the use of this definition in the analyses performed here is feasible because, during a turn, for example, all vehicle components also perform the maneuver. The same analysis is true if the vehicle is accelerating or braking since all components would be accelerating or decelerating, respectively.

This consideration is vital for the definition of two fundamental concepts: Sprung mass (M_s) and unsprung mass (M_{ns}), in which the latter is composed of tires, wheels, shock absorbers, and other adjacent components. Conversely, (STRUBLE; STRUBLE, 2020) states that the M_s is all the remaining mass of the vehicle which, consequently, is supported by the components that form the M_{ns} (Figure 11).

Figure 11 – Sprung and unsprung masses

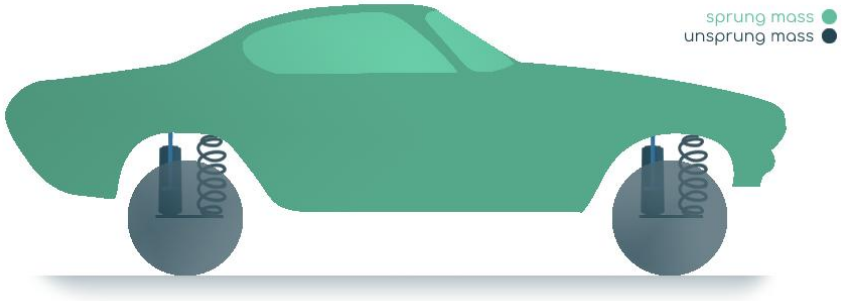

Source: Prepared by the author

As noted by (REIMPELL; STOLL; BETZLER, 2001), most suspension designs seek the maximum reduction of M_s. However, (MILLIKEN; MILLIKEN, 2002) emphasize that the higher the M_{ns}, the greater the problems felt by the driver regarding the oscillation frequency. Therefore, there is a fine line between the mass distribution in sprung and unsprung masses, so it must be done considering several factors during the project.

2.3.2 SAE coordinate system and Euler angles

Standardized by the Society of Automotive Engineers (SAE), Figure 12 shows one of the possible coordinate systems of a vehicle.

Figure 12 – SAE coordinate system

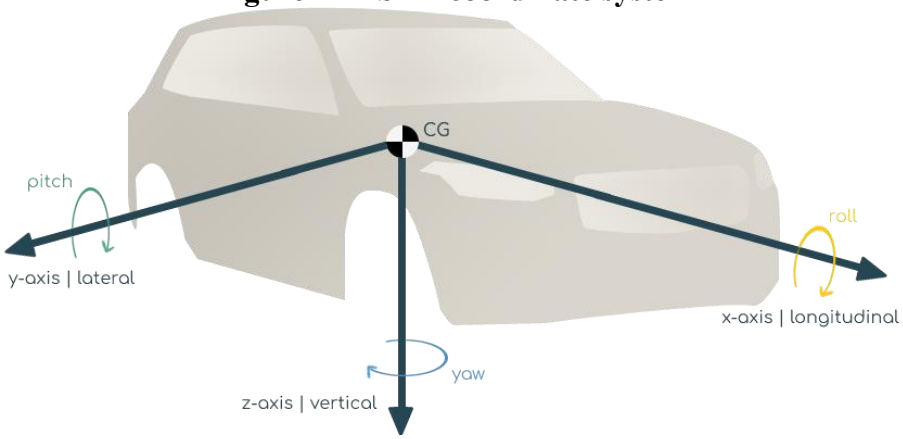

Source: Prepared by the author

The figure above states that the coordinate system is taken concerning the vehicle's center of gravity, that is, it is defined that the coordinate system is taken as fixed to the vehicle. In the same illustration, it is observed that the longitudinal axis (x-axis) is judged as positive when it moves from the CG to the front of the vehicle, while the positive vertical axis (z-axis) is given in the direction from the CG to the ground. Finally, the lateral axis (y-axis) is taken as positive when viewed from the left to the right of the vehicle.

Around the x, y, and z-axes, the Euler angles define the roll, pitch, and yaw angles, respectively, as highlighted by (MILLIKEN; MILLIKEN, 2002). Since these angles have a strong influence on the vehicle's dynamic behavior, they must be manipulated according to the interest of the project. According to (ZHANG, N.; DONG; DU, 2008), the effects caused by moments around the coordinate axes occur only on the sprung mass, which is corroborated by (ABE, 2015) when they explain that although the sprung mass responds to rolling, the unsprung mass can remain rigid without being directly influenced by the sprung mass.

According to (PENG; EISELE, 2000), yaw can cause a jackknifing folding effect in two-compartment vehicles, e.g., articulated buses or trucks with trailers. This phenomenon is the instability of the trailer concerning the vehicle's powertrain due to the formation of an unexpected angle between its two compartments, which induces the loss of vehicle control and, consequently, can cause the vehicle to tip over.

On the other hand, regarding the pitch effect, (KATZ; GARCIA, 2002) explains that this parameter is directly related to the mass transfer between the axles of a vehicle. For (AZMAN; KING; RAHNEJAT, 2007; GOBBI; MASTINU; PREVIATI, 2014), the pitch is diametrically linked to the dive and lift phenomena, illustrated respectively in Figure 13 and Figure 14. Adding to the importance of controlling this variable, (HEISSING; ERSOY, 2010) states that these effects have a strong influence on vehicle comfort.

Figure 13 – Dive

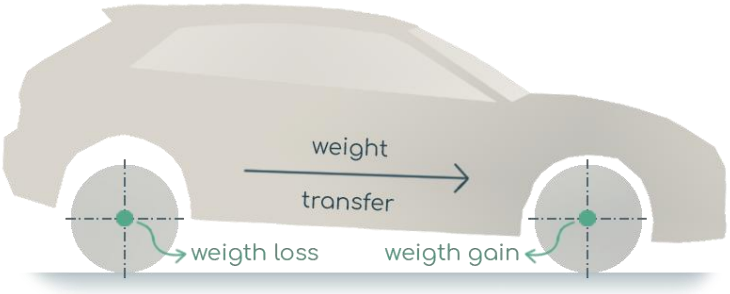

Source: Prepared by the author

Figure 14 – Lift

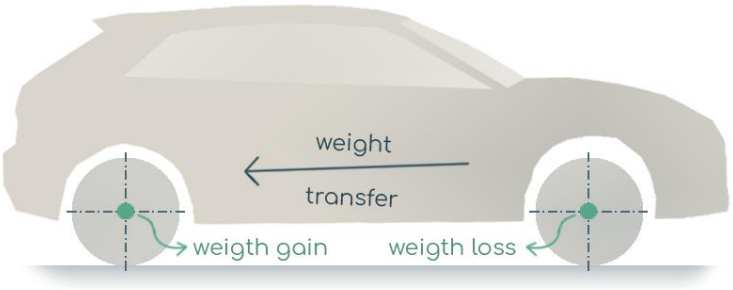

Source: Prepared by the author

According to the figure above, the dive occurs when dynamic effects induce the lowering of the front of the vehicle, raising the rear. Similarly, lift occurs when the front part moves negatively in the z-axis and, consequently, the rear descends. The last phenomenon is commonly called squat, as explained by (MILLIKEN; MILLIKEN, 2002), and occurs when a vehicle goes up an inclined road, for example, or in rear-wheel drive cars when they are suddenly accelerated. In dive, however, this tends to occur when a vehicle at high speed is ephemerally braked.

2.3.3 Suspension system

According to (BHOSALE *et al.*, 2019), it is through the suspension and steering systems that the driver feels vehicle responses as to what is necessary to keep it stable and under control. While (DHAMODHARAN; MOHAMED RAAFIQ; MADHU, 2015) confirm that vehicle suspensions are responsible for allowing the vehicle to roll and pitch, (GILLESPIE, 1992) explains that the designer must pay attention to factors such as system weight, cost, dimensioning, and production feasibility to design a suspension system capable of performing the following functions:

a) With the smallest possible load variation, keep the vehicle's tires in contact with the ground;
b) Through the wheels, smooth any transmission of disturbances between the chassis and the ground;
c) Promote efforts to balance and neutralize the susceptibility of the vehicle to transmit forces produced by the tires in contact with the ground: Whether longitudinally (due to acceleration and braking), laterally (due to turns), or to the torques induced by the engine and braking;
d) Around the longitudinal axis, provide resistance to the rolling moment in the chassis.

Suspension systems can be divided into two large sets: The first, here called an independent suspension system; and the second, defined as a dependent suspension system. As the name implies, an independent suspension system is one in which one side of the axle moves independently of the displacement of the opposite side of the same axle. In this case, when the wheel on one side of the axle is stressed by forces from irregularities in the track, for example, the wheel on the opposite side of the same axle is not influenced. On the other hand, if this

wheel is also displaced due to the load on the opposite side of the axle, there is a dependent suspension. Figure 15 performs this comparison.

Figure 15 – Depended and independent suspension systems

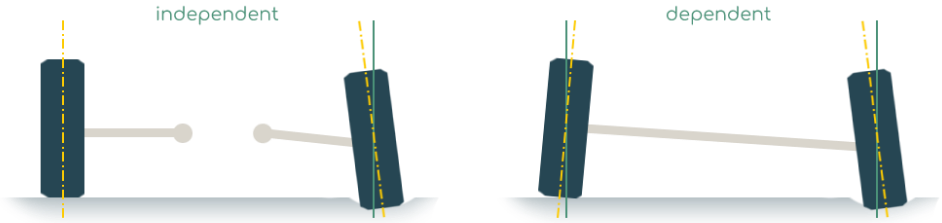

Source: Prepared by the author

Among the main advantages of the independent suspension system, (REIMPELL; STOLL; BETZLER, 2001) emphasize the reduced installation space, the low total weight, and the ease of steering the wheels, in addition to the lower level of vibrations and the greater space for positioning the engine (GILLESPIE, 1992). At the same time, dependent suspensions are often found on heavy vehicle axles due to their greater capacity to support loads and due to their relatively low cost. Once this characteristic is directly related to the permissible loads, vehicles with such a configuration also have a smaller influence on body rollovers. Despite the lower tire wear, this type of suspension has as its main disadvantage the greater susceptibility to vibrations.

Most of today's urban cars have independent front suspension, McPherson structure, and twist beam-dependent suspension at the rear. On the other hand, light commercial vehicles tend to have leaf spring-dependent suspension on the rear axle while sport utility vehicles (SUV) have multilink independent suspension in both front and rear.

2.3.3.1 McPherson strut

According to (REDDY *et al.*, 2016), the McPherson structure (Figure 16) is one of the most used by the automotive industry today.

Figure 16 – Schematic front view of McPherson's main components

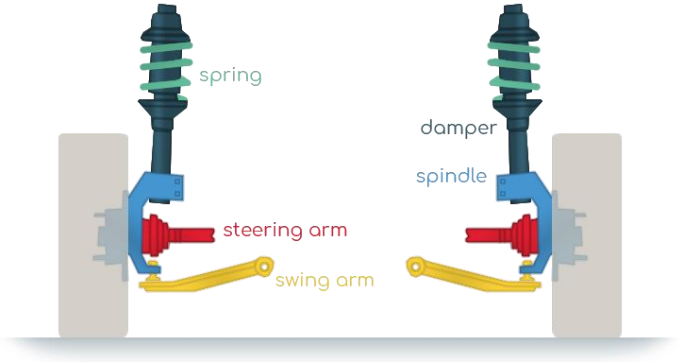

Source: Prepared by the author

Common in front-wheel drive cars, the McPherson structure is the most used in light vehicles currently, as explained by (DUTTA; CHOI; CHOI, 2016). Also, the McPherson structure presents a relatively great quality in the reduction of the occupied space and, as stated by (KLOCKE *et al.*, 2014), the automotive industry seeks compact cars to adapt to the current urban and mobility context. In this scenario, (GILLESPIE, 1992) comments that the advantages of this structure are even greater when the engine is mounted transversally. (KIM, G. *et al.*, 2012; PURUSHOTHAM, 2013) embody, still, reporting that another positive point of this type of structure is the proportionally low cost of manufacture and assembly.

Despite the many applications at the front-end of cars, (FALLAH; BHAT; XIE, 2010) states that there are also McPherson structure solutions for the rear suspension. In addition, the authors address that, despite the various advantages (e.g., the distribution of loads received from the ground over a larger area of the bodywork), there are some downsides to this structure. Among them, the greater need for steering, less isolation to vibrations between bodywork and track, and greater tire wear are highlighted.

In their studies, (KIM, G. *et al.*, 2012) presented a survey where 69% of complaints about McPherson were noise related. (DUTTA; CHOI; CHOI, 2016) also comment that a lateral load is generated on the shock absorber when the wheel moves vertically, which increases friction and consequently reduces the ride comfort. For (MARQUES *et al.*, 2019), this friction results in the energy dissipation that was previously produced to perform work, so it is an undesirable situation in most cases. Intuitively, these advantages and disadvantages are taken into consideration concerning the other equivalent suspension types.

2.3.3.1.1 Spring

Considered as the main elastic component of the suspension, the spring is a fundamental item for this system and the model most used today in automotive projects is the helical type. As (DUTTA; CHOI; CHOI, 2016) explains, the main parameters that affect the stiffness (k) of the spring are the free length, that is, the length of the spring when there is no load applied to it; the number of turns, the nominal and cross-sectional diameters, and, finally, the pitch of the turns. Equation 8 describes the behavior of a spring in a linear regime where F is the applied force and Δ the resultant linear displacement.

$$F = k\Delta \tag{8}$$

In the McPherson structure, the springs are inclined concerning the damping tower axis. According to (RYU *et al.*, 2010), this inclination is used aiming to optimize vehicle comfort once the suspension friction is reduced. The authors in question also complement by reporting that the magnitude of this inclination is defined according to the concept that the reaction force is relative to the geometric axis of the spring.

According to (BITENCOURT, 2016), the springs have a direct influence on the dynamic load of the wheel and, consequently, on the quality of the ride comfort. Also, according to the author in question, the component studied in this topic plays a vital role in the occurrence of rollover and the pitch of the vehicle as well as in its drivability.

2.3.3.1.2 Damper

Connecting sprung and unsprung masses, the dampers are responsible for generating damping force (F_a), which is directly related to the velocities of the respective masses ($\dot{\Delta}$) according to the damping factor c (Equation 9). Currently, most vehicle shock absorbers are hydraulic, which according to (SUNG; SEONG; CHOI, 2013) is an interesting alternative due to the cost.

$$F_a = c_a \dot{\Delta}_a \tag{9}$$

The damping tower is attached to the bodywork at its upper end (JR; LOSEKANN, 2003). Although this is negative since it transmits forces to bodywork, there is the positive circumstance of greater dissipation of the same reactions due to the greater contact area at the junction (GILLESPIE, 1992). Figure 17 presents one of the distinct types of car shock absorbers, and their main components, in a simplified way.

Figure 17 – Cutaway view of a car shock absorber

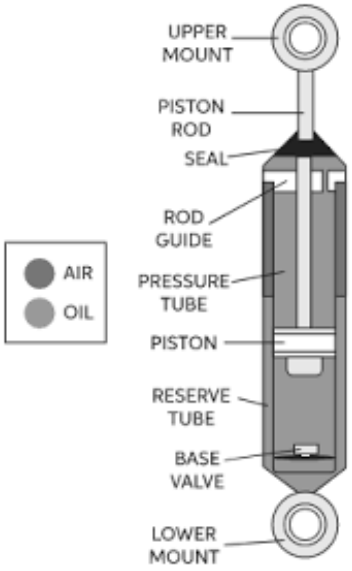

Source: (CHEGG, 2023).

In the McPherson strut, the behavior of the dampers is influenced by lateral loads, as previously stated. According to (DUTTA; CHOI; CHOI, 2016), helical springs have the characteristic of canceling this unwanted effect on the damper, which consequently causes a reduction in friction in it. If this did not happen, the life of the shock absorber would be considerably reduced, in addition to the presence of greater noise and the reduction of vehicle comfort.

2.3.3.1.3 Bump stop and rebound stop

Figure 17 presented two fundamental components in terms of comfort and durability of the suspension system: The upper and lower mounts. These two components are best explained when the way the suspension system works is understood.

According to (DINIZ, 2014), the suspension system has two movement limits: Jounce and rebound. While the jounce happens when the suspension system has an upward movement, which causes its force elements to be compressed, the rebound happens when the suspension movement is downward, that is, the opposite of the jounce. The two phenomena presented are illustrated in Figure 18.

Figure 18 – Jounce and rebound

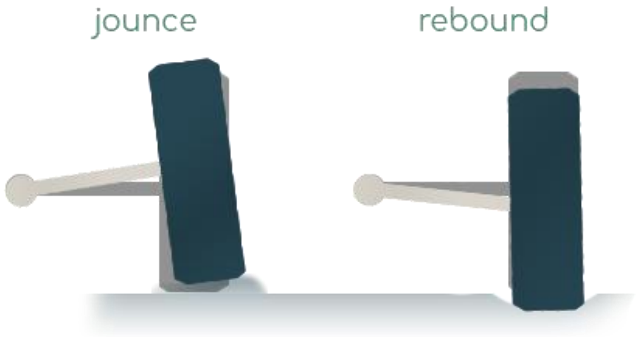

Source: Prepared by the author

Corroborating this idea, (VARGAS, 2011) says that the jounce is the movement that approximates the sprung and unsprung masses, while the rebound increases this distance. Another way to define these concepts is given by (STRUBLE; STRUBLE, 2020), since they say that rebound is a phenomenon that happens when the springs are fully stretched.

Due to physical assembly issues, the contact between metallic components is accentuated in the maximum jounce and rebound. As a result, the life of the shock absorber would be drastically reduced. Therefore, as (STRUBLE; STRUBLE, 2020) comment, the purpose of the bump and rebound stop is exactly to reduce this impact to minimize excessive wear on the shock absorber, which can even cause this component to burst.

Returning to the diving and lifting examples, (HEISSING; ERSOY, 2010) explains that when the bump stop releases the received energy, the unwanted phenomenon of diving on the vehicle body can occur. As a result, the vehicle comfort would be reduced as well.

2.3.3.1.4 Control arm

According to (HEISSING; ERSOY, 2010), the control arms have characteristics such that they react to longitudinal forces applied to the suspension. Aiding in the kinematic control of the suspension and in the absorption of loads arising from the contact between the tire and the ground, as presented by (LEAL, 2007), the control arms have other auxiliary components in the region of connection with the chassis, the so-called cushions. The function of these components is to absorb and reduce the amplitude of oscillation frequencies generated on the road to increase the vehicle's driving comfort.

2.3.3.1.5 Steering arm

The steering arm steers the wheel according to the vehicle driver's request, as presented by (MACFARLANE, 2016). In this context, the steering arm is connected, in addition to the

bearing, to the steering system. Once the driver turns the steering wheel, a rack-and-pinion system transforms rotational to translational motion, and the wheels are steered through the steering arm connected to the bearing.

2.3.3.1.6 Knuckle

The knuckle is responsible for connecting several components of the suspension and steering systems such as the steering rod, the wheel and tire assembly, and the swingarm, as explained by (CARVALHO; FARIA, 2010). As it supports the axle responsible for transmitting movement to the wheels, (D BASTOW G HOWARD, 2004) comment that this component requires extra care during its dimensioning.

2.3.3.1.7 Anti-roll bar

Present on some vehicle models, the anti-roll bar is fixed to the chassis and connected directly to the suspension system. Also, known as a sway bar, its function is very intuitive according to its name: Reduce vehicle body roll.

Depending on the vehicle's suspension characteristics, the vehicle may or may not need the anti-roll bar on the front suspension, rear suspension, or both. In addition to these characteristics, the vehicle segment and consequently its application is fundamental to define the need to implement this bar. In passenger vehicles, the presence of a stabilizer bar in the front suspension with diameters of less than 20mm is currently used, while all-terrain vehicles usually have bars on both axles with diameters of less than 30mm.

2.3.3.2 Rigid Axle Suspension

Presented in Figure 19, (JANARTHANAM; GHODEKAR; APTE, 2007) emphasize that the main characteristic of the Rigid Axle Suspension is the presence of a solid axle, as induced by the name. Corroborating, (LEAL, 2007) explains that this component results in greater stability for the vehicle during running-in and makes the system more robust, justifying the fact that it is used in most small and medium-sized car projects these days. In addition, (COSTA, 2020) presented a negative point of this system by saying that the presence of a torsion bar increases the weight of the project.

Figure 19 – Rigid Axle Suspension

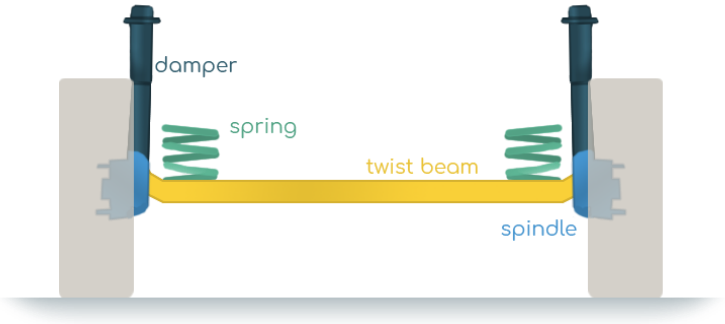

Source: Prepared by the author

According to (GILLESPIE, 1992), a major disadvantage of this system is that in case of sharp curves at remarkably high speeds, the wheel inside the curve can come off the ground and, consequently, cause the vehicle to roll over. Despite this, (HEISSING; ERSOY, 2010) presents good resistance to lifting and diving effects as other advantages of the system.

As (LEAL, 2007) explains, that this type of dependent suspension has a limited number of components. The author also comments that, in general, this type of suspension is composed of a pair of oscillating arms and the torsion axis, also known as a crossbar or torsion bar. Complementing, (FANG; TAN, 2015) says that the arms have high resistance to bending and torsion.

The torsion axle suspension contains several elements present in the McPherson strut that have already been detailed previously, such as the damping tower and springs, in addition to the bump and rebound stop – but of course, with different specifications such as its geometry. Despite some structural differences and consequently in their properties, these elements will not be discussed again since the operating principle is the same. However, the torsion axis will be detailed below.

2.3.3.2.1 Solid axle

As mentioned earlier, the torsion shaft is commonly called a crossmember or torsion bar. Naming the system, the cross member assumes the role of one of the main integral parts of the torsion axle suspension since its profile has a direct influence on parameters such as the inclination and vertical response of the wheels in addition to the suspension's roll center. Going further, (SUGIURA *et al.*, 2000) claims that the torsion bar design defines the behavior of the suspension. Therefore, due to the complexity of the variables it involves, conducting this system design can involve considerable difficulty in some cases and require powerful computational resources.

According to (FANG; TAN, 2015), modern torsion axle suspension designs seek to connect the swingarms and cross members at the same geometric point, which results in relatively high stresses. In principle, large deformations are caused when there are high stresses and, due to the high values of rotation at which the cross member (Figure 20) is stressed, the fatigue in it must be dimensioned with certain attention.

Figure 20 – Solid axle

Source: Adapted from (REIMPELL; STOLL; BETZLER, 2001)**.**

As an alternative to combat fatigue, a resource widely used in the automotive industry is the application of reinforcements at strategic points. Most of the time, these points boil down to the connection between the crossmember and the swingarms, since there is a cross-section variation in them and, therefore, the stress build-up values are higher. Still according to (FANG; TAN, 2015), these reinforcements significantly increase the stiffness value of the system.

2.3.4 Steering system

(GILLESPIE, 1992) reports that the vehicle's steering system (Figure 21) aims to generate a translational response in the wheels according to the rotational movement of the steering wheel caused by the driver and, consequently, to control the direction of the vehicle. However, as direct as this relationship may seem, some observations are necessary regarding the transmission of the request made by the driver with the vehicle's response. According to (MILLIKEN; MILLIKEN, 2002), there is a certain delay between what is imputed by the driver and what is received by the wheels. During this period, the authors also comment that to generate the yaw speed necessary for the vehicle to be able to rotate around its Z axis, there is an excess of lateral force on the front wheels compared to in the back.

Figure 21 – Generic steering system

Source: Day (2013) ***apud*** (DA SILVA, 2017).

Solidifying what was presented by the authors of the previous paragraph, (REIMPELL; STOLL; BETZLER, 2001) comment that there is no direct relationship between the rotation angle of the steering wheel and the direction in which the vehicle is headed. Also, according to the author, this does not occur because of the development of lateral forces, the change in the steering angle of the front wheels, the rotation of the steering wheel, and the change in the direction in which the vehicle heads are not linear parameters. This nonlinearity is because the chassis components show a certain complacency when they are requested and, therefore, factors such as body roll have a direct influence on this relationship.

Regarding the composition of the steering system, this system usually has three main components: The steering wheel, the column, and the steering gear. Between the steering box and the wheels, there is also the steering arm and the tie rod. In addition to the steering wheel, present from the beginning of vehicles and commonly seen in a circular shape, the other components will be discussed below.

2.3.4.1 Steering column

According to (SHAIKH; PARVEZ; SHAKEBUDDIN, 2015), the primary function of the steering column is to connect the steering wheel with the steering gear, allowing the steering to take place. The authors also add that there are rigid type columns and those that can dissipate energy, providing more safety to the driver in case of impact. In this case, during a collision, the column is retracted towards the vehicle's front-end, seeking to provide greater safety for the driver in eventual crashes. In some new vehicles, the steering column has height and position adjustments, for example, improving driving comfort.

2.3.4.2 Steering gearbox

As (GILLESPIE, 1992) explains, the primary function of the steering gearbox is to transform the rotation movement of the steering wheel, transmitted by the steering column, into a translation movement, thus taking place the steering of the wheels. To this end, it is conventional that this system has a rack and pinion set, where it is based on a gear, called pinion, which rotates on its axis and, due to its positioning in space, translates over a gear of infinite radius, called a rack. The rack, in turn, can be connected to the crossbar or even directly to the chassis in some cases. As well as variations on the rack's joint point, mechanisms other than the pinion rack are found to perform the main function of this component.

2.3.4.3 Steering arm

The steering arm is a mechanical component that ends the transmission of the rotation signal assigned to the driver until the final response of the vehicle's wheel steering. Connected to the output of the headset, the steering arm is connected to the knuckle, finally turning the wheels. An important detail about the steering arm is that it is capable of withstanding only tensile loads since its length is greater than its cross-section. If the component is subjected to compressive stress, this relationship between length and cross-section can lead to fatigue failure.

2.3.4.4 Electronic powered steering

Most vehicles produced in recent years have an electric steering system (EPS) in their composition, which as (CHABAAN; WANG, 2001) points out is an evolution of steering systems. The acronym EPS is derived from the English term electric power system.

Before electric steering, however, a mechanism that was widely used and is still found in a considerable number of models today is hydraulic steering. While this one has a fluid pump to reduce the torque to be provided by the driver to turn the wheels, the electric steering has an electric motor, as presented by (DA SILVA, 2017). Also, according to this author, electric steering is a technique that supplies energy from an auxiliary engine to the car's steering system, becoming a superior technique than the hydraulic assistance.

The electrical system has many advantages over traditional systems, and these positive points can even address issues related to engine efficiency. Despite the several advantages presented by (KIM, J.-H.; SONG, 2002), (SAIFIA *et al.*, 2015) comment that the controllers of

an EPS must be designed in such a way as to pay attention to friction and irregularities in the roadway, since these variables are the main sources of noise and non-linearities in the operation of the electrical system.

2.3.5 Kinematics parameters

Among the many parameters that a vehicle chassis system has, this topic will address some of the main ones. Directly influencing the dynamic behavior of the vehicle, if the kinematics and compliance (K&C) parameters are not well designed, several undesirable effects will occur during riding (JACKSON; GLICKMAN; DALE JR, 2003). Among them, the authors highlight excessive and non-linear tire wear, in addition to driving performance and stability. The importance of this observation is stressed by (SHAO *et al.*, 2018), where the authors say that drivability is one of the most important parameters for the safety and stability of a vehicle.

2.3.5.1 Toe angle

The toe angle (Figure 22) is defined by the DIN 70000 standard as the angle between the central plane of a vehicle, in the longitudinal direction, with the line of intersection of the central plane of one of the wheels with the ground plane.

Figure 22 – Toe angle orientation

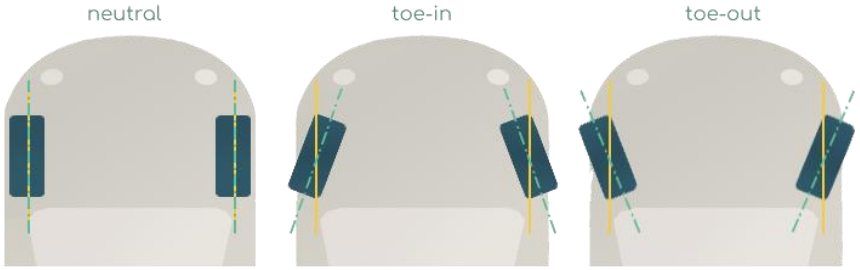

Source: Prepared by the author

Also, according to this standard, the toe angle is considered negative (convergence -) when the planes parallel to the wheels intersect in front of the vehicle. On the other hand, the opposite is true for the intersection of planes in the case of a positive angle (convergence +). Convergence is neutral if the planes are parallel.

Seeking to understand the influence of the toe angle on the vehicle's dynamic behavior, (GILLESPIE, 1992) comments that at the point of contact between the tire and the ground, there is an effort in the same direction and the opposite direction to the movement. Intuitively, a vehicle moving with a neutral toe faces lower rolling resistance, which results in less tire wear.

Because of the load distribution, the convergence values vary according to the weight that the vehicle is subjected to, and, due to this, (LEAL, 2007) points out that the convergence angle must be evaluated in several situations. Also, according to the author, the rear wheels of a passenger vehicle, for example, tend to diverge due to the rolling resistance presented above. Due to this effect, the definition of toe in a static situation must provide for such divergence. In other words, the toe angle must be defined so that, when the vehicle starts moving in a longitudinal direction, the wheels are as close as possible to being aligned with the longitudinal axis of the vehicle. For this corrective effect to be achieved, static convergence is usually set to a slightly positive condition.

2.3.5.2 Camber angle

As presented in the previous topic, toe angle is defined when the vehicle is analyzed by the XY plane. Analyzing the YZ plane, (KRÖNK, 2017) defines the vertical inclination of the wheel as the camber angle, which according to the DIN 70000 standard is the angle formed between a line that vertically intersects the center of the wheel and another parallel to the axis vehicle vertical is the camber angle.

According to (LEAL, 2007), the camber angle has a direct influence on tire wear in the same way as the toe angle. In his study, the author also emphasizes that when the angle is different between the two wheels of the same axle, there will be a strong influence on the vehicle alignment.

In his study, (LELEDAKIS, 2014) comments that a camber value is defined in the early stages of a vehicle suspension project looking for certain driving characteristics. However, as shown for the toe angle, this value changes due to factors such as steering, irregularities in a roadway and the body roll itself when the vehicle is in motion. According to (BHOSALE *et al.*, 2019), although the camber value does not considerably affect the behavior of a vehicle when traveling in a straight line, this parameter plays a fundamental role in turns.

The camber angle is defined with negative values (camber -) when the symmetry axis of the tires in the front view of the vehicle converges to the center of the vehicle above the road surface. Similarly, this angle is positive (camber +) if the same axis converges at the center of the vehicle below the road surface. As shown in Figure 23, there is a neutral camber if the symmetry axes of the tires on both sides of the same axis are parallel to each other.

Figure 23 – Camber angle orientation

Source: Prepared by the author

(REIMPELL; STOLL; BETZLER, 2001) explain that usually slightly positive camber values were previously targeted since the vehicle tends to present vertical alignment of the wheels when it is loaded. However, as pointed out by (LEAL, 2007), the projects of the last decades have opted for negative camber since this configuration allows greater grip of the outer wheel in curves, which consequently improves the behavior of the vehicle during the realization of the contour of the turn.

Presented in the next topics, (JAMBUKAR; CHANDRAMOHAN, 2019) add that the camber angle value varies depending on the kingpin and caster angles according to the steering angle.

2.3.5.3 Caster angle

According to (JAZAR, 2017), the camber angle varies with another angle known as the caster. The study of these authors corroborates the previously exposed concept that the suspension system of a vehicle is completely interconnected and, therefore, changing one parameter directly interferes with others.

In the XZ plane, the axis that intersects the center of the damping tower is defined as the steering axis. According to (ALMEIDA, 2012) and (JAZAR, 2017), the caster corresponds to the angle formed between the steering axis and the plane perpendicular to the ground, as shown in Figure 24.

Figure 24 – Caster angle orientation

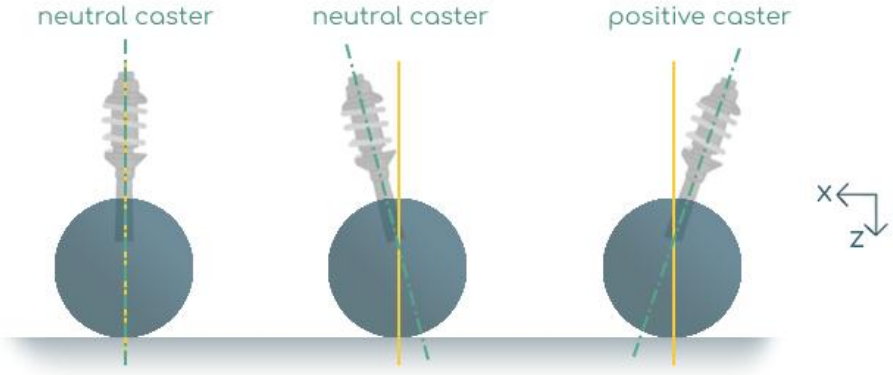

Source: Prepared by the author

Also, according to DIN 70000 and DIN 70020, the caster angle is considered positive (caster +) when the intersection of the steering axis with the ground line occurs ahead of the projection of the wheel center on the ground. Intuitively, the caster is negative (caster -) when the intersection of the steering axis occurs after this projection, while it will be neutral if the two axes are aligned (neutral caster).

According to (JAZAR, 2017), positive caster is better for the vehicle's performance in turns. However, according to (REIMPELL; STOLL; BETZLER, 2001), some front-wheel drive vehicles rely on a negative caster angle to increase the self-aligning torque caused by the traction forces. In addition to the camber variation, (ALMEIDA, 2012) comments that the caster angle also influences the steering wheel self-alignment and the vehicle response received by the driver. The angle discussed in this topic also defines a parameter known as mechanical trail or caster arm, often found in classic pieces of literature under the definition of caster trail.

2.3.5.4 Caster trail

Regardless of the positive or negative orientation of the caster angle, it is observed that there is an offset between the points where the steering axis intersects the ground line. Therefore, a triangle is formed and, considering the side opposite the caster angle, there is a parameter known as caster trail, shown in Figure 25.

Figure 25 – Caster trail

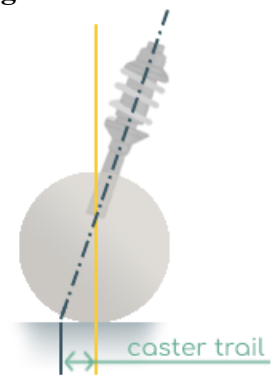

Source: Prepared by the author

According to the figure above, the caster arm can be defined as the respective anterior or posterior distance to the steering axis and the projection of the center wheel on the ground (JACKSON; GLICKMAN; DALE JR, 2003).

Regarding the influences of the caster arm in a suspension system, (REIMPELL; STOLL; BETZLER, 2001) comment that this parameter changes the point at which vertical and lateral forces are applied. As a result, the tire undergoes a moment that leads to its self-alignment. Since its value is related to the caster angle, (LELEDAKIS, 2014) says that the caster arm produces a response from the vehicle regarding its steering to the driver, in addition to the wheel alignment effect after steering.

2.3.5.5 Steering ratio and understeer gradient

(BISWAL, 2016) defines the steering ratio (τ) as the relationship between the steering wheel rotation angle (SWA) and wheel steer angle (λ), according to Equation 10.

$$\tau = \frac{SWA}{\lambda} \tag{10}$$

Corroborating with this author, (LELEDAKIS, 2014) comments that the higher the value of the steering ratio, the more the steering wheel must be rotated to steer the wheels in the same value. Along with what was presented, the same author also comments that the torque required to rotate the steering wheel is also reduced with a decrease in the steering ratio. Being a dimensionless factor since it is a ratio between two angles, the values of this parameter vary around 5:1 in competition vehicles, 10:1 in passenger vehicles, and 30:1 in heavy vehicles such as buses and trucks, as provided by (JAZAR, 2017). Nevertheless, some electric vehicles already have steering ratios of less than 10:1 for low-speed maneuvers such as parking maneuvers.

According to (REIMPELL; STOLL; BETZLER, 2001), the fact that the steering ratio decreases with the increase of the steering angle of the wheels is purely kinematic and the decrease of this value can be an advantage in steering systems that rely on hydraulic or electric assists. Improving handling properties, this advantage is because turns and other maneuvers are performed with less effort from the vehicle driver, the lower the steering ratios are.

As previously mentioned, the slip angle is defined as the angle between the velocity vector and the longitudinal axis of the tire (JAZAR, 2017). From the relationship between the vehicle tire slip angles, (GILLESPIE, 1992) defines the understeer gradient (K) and comments that a vehicle can be classified as neutral, understeer, or oversteer (Figure 26) according to this gradient.

Figure 26 – Vehicle behavior cornering according to the understeer gradient

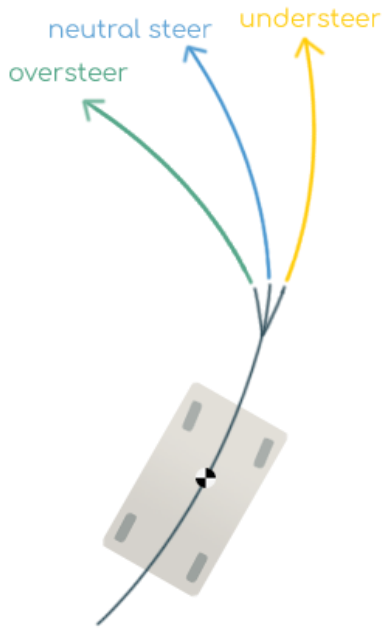

Source: Prepared by the author

Corroborating this, (BITENCOURT, 2016) says that the understeer gradient is responsible for determining the direction and magnitude in which the vehicle's steering wheel must be steered to make a turn. Another definition presented by the author is that this gradient can still be described as the value of the steering angle that has to be imposed, according to a given lateral acceleration, to fulfill the direction desired by a driver in any given turn.

The understeer gradient is given by Equation 11, in $\mathrm{degree/g}$, where a_y is the lateral acceleration, L is the distance between the vehicle's axles and R is the radius of the turn.

$$\delta = \frac{180}{\pi}\frac{L}{R} + Ka_y \tag{11}$$

According to (SCHWARK *et al.*, 2015), what classifies the behavior of the vehicle as oversteering is the need to decrease the steering angle proportionally to the increase in speed during a turn. To contour this turn, the driver must decrease the steering angle, therefore, since the rear tire slip angle increases due to the lateral force applied to the vehicle's center of gravity. As a result, the front axle tends to be steered toward the inside direction of the curve, causing an effect to be corrected with less steering of the axle toward the inside direction of the curve. (GILLESPIE, 1992).

When the opposite of what is presented in the above paragraph occurs, (VILELA; BARBOSA, 2011) says that the vehicle has understeer behavior. On the other hand, (ALI; MAJEED, 2018) comment that a neutral vehicle is one in which the slip angle is the same in all its tires. (GILLESPIE, 1992) complements by saying that vehicles classified as neutral do not need to vary the steering angle according to the variation in speed during the performance of a given curve. Table 3 summarizes the main characteristics of the three behaviors described above.

Table 3 – Understeer gradient and its main characteristics

Understeer gradient	K	Slip angle	Notes
Understeering	> 0	front $>$ rear	Greater front slip compared to rear-end;
Neutral	$= 0$	front $=$ rear	Ackermann and slip angle are equivalent
Oversteering	< 0	front $<$ rear	Greater rear slip angle compared to the front-end;

Source: Prepared by the author based on (GILLESPIE, 1992; JAZAR, 2017)**.**

2.3.6 Vehicle dynamics models

If all the variables present in the physical system are considered, modeling a vehicle becomes a really difficult task. However, to make possible the study of these systems, some simplified models allow the study of vehicle dynamics that can present significant results. In the present topic, some of these models will be discussed.

As explained by (SHIM; GHIKE, 2007), the complexity of the model used in the analysis of a vehicle depends on what kind of result is desired and how accurate it needs to be. In addition, (HAPPIAN-SMITH, 2001) corroborate the idea presented by saying that different models can provide results involving the influence of different physical phenomena. Still emphasizing the importance of the development of models for the study of running a vehicle, the last author presents three models of vertical dynamics that will be discussed below: A

quarter vehicle, a half vehicle, and a complete vehicle. In addition to these, two models of lateral and longitudinal dynamics will also be presented in this topic.

2.3.6.1 Quarter-car model

A traditional and commonly used vehicle suspension model for simplified vertical analysis is the quarter-car model (Figure 27). Despite not considering the dynamics of the wheels, (SANDU; ANDERSEN; SOUTHWARD, 2011) confirm the quality of the results obtained with this model when they use it for the analysis of a McPherson strut.

Figure 27 – Quarter-car model

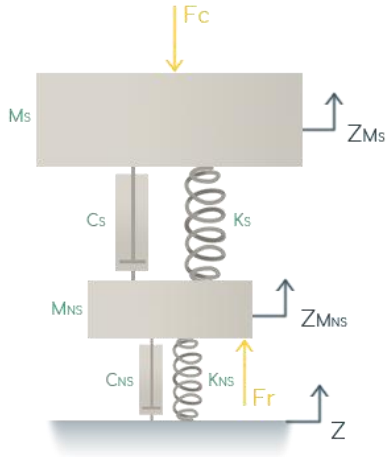

Source: Prepared by the author

Considering a mass corresponding to approximately a quarter of a vehicle, since the weight of the vehicle is not evenly distributed due to factors such as the pitch, for example, (GILLESPIE, 1992) states that the sprung mass has properties related to damping (C_s) and the stiffness (K_s), as well as unsprung mass also has stiffness components (K_{ns}) and damping (C_{ns}). According to Jazar (2017), the last two components presented are related to the unsprung mass, highlighted through the unsprung mass subscript ns.

Also, according to Figure 27, two vertical forces are applied to the model: The force of the body F_c and the power of the wheel F_r, in opposite directions. Due to this, there is a vertical displacement that is directly influenced by the mentioned force parameters as well as by the sprung and unsprung masses, stiffness, and damping factors. Differential Equations 12 and 13 define the displacement of the sprung and unsprung masses where Z_{M_s}, $Z_{M_{ns}}$, and Z are M_s, M_{ns} and road displacements, respectively.

$$M_s\ddot{Z}_{M_s} + C_s(\dot{Z}_{M_s} - \dot{Z}_{M_{ns}}) + K_s(Z_{M_s} - Z_{M_{ns}}) = F_c \quad (12)$$

$$M_{ns}\ddot{Z}_{M_{ns}} + C_s(\dot{Z}_{M_{ns}} - \dot{Z}_{M_s}) + K_s(Z_{M_{ns}} - Z_{M_s}) + C_{ns}(\dot{Z}_{M_{ns}} - \dot{Z}) + K_{ns}(Z_{M_{ns}} - Z) = F_r \quad (13)$$

Through the generalized form of Equation 14, the equations above can also be written in a matrix form, as follows in Equation 15. In this representation, [m] refers to the mass matrix, [c] to the damping matrix, [k] to the stiffness matrix, and {z} and {F} to the displacement and force unidimensional matrices, respectively.

$$[m]\{\ddot{z}\} + [c]\{\dot{z}\} + [k]\{z\} = \{F\} \quad (14)$$

$$\begin{bmatrix} M_s & 0 \\ 0 & M_{ns} \end{bmatrix}\begin{bmatrix} \ddot{Z}_{M_s} \\ \ddot{Z}_{M_{ns}} \end{bmatrix} + \begin{bmatrix} c_s & -c_s \\ -c_s & c_s + c_{ns} \end{bmatrix}\begin{bmatrix} \dot{Z}_{M_s} \\ \dot{Z}_{M_{ns}} \end{bmatrix} + \begin{bmatrix} k_s & -k_s \\ -k_s & k_s + k_{ns} \end{bmatrix}\begin{bmatrix} Z_{M_s} \\ Z_{M_{ns}} \end{bmatrix} = \begin{bmatrix} F_c \\ F_r - (c_{ns}\dot{Z} + k_{ns}Z) \end{bmatrix} \quad (15)$$

As it involves too much simplification when compared to a vehicle, the quarter vehicle model does not allow the analysis of some parameters such as roll and pitch, for example. In the presented scenario, some other models are presented below.

2.3.6.2 Half-car model

While the quarter-car model involved only two degrees of freedom (vertical translation of the sprung and unsprung masses), (HAPPIAN-SMITH, 2001) shows that the half-vehicle model is more complete than the first one because it involves four degrees of freedom: While each unsprung mass has the freedom to move vertically, the other two degrees of freedom are related to the vertical displacement and the pitch of the body, as shown in Figure 28.

Figure 28 – Half-car model

Source: Prepared by the author

Compared to the quarter-car model, the half-car model is more complete and, consequently, allows analysis regarding pitch movements. However, the body roll movement is still not possible to obtain with this model despite the complexity of studying it being greater

when compared to the quarter-car model. Aiming at a model that allows an analysis of greater fidelity to a physical vehicle, there is also the full-car model.

Considering that there is a gap between the roll center and the CG, a model like the half-car is derived for roll analysis. In this case, however, the vehicle is observed by the YZ plane, and more details can be found in the work of (ZHOU, C.; LIU; XU, 2021). While the former is usually defined as the vehicle's pitch model, the latter is called the rollover model. The equations that describe the behavior of both models can be found in (JAZAR, 2017).

2.3.6.3 Full-vehicle model

The third and final vertical model to be presented is the full-car model (Figure 29). Following the analysis made for the quarter-car and half-car models, (HAPPIAN-SMITH, 2001) emphasizes that the premises are the same: With greater complexity, the model is more complete and allows the analysis of more phenomena, in addition to obtaining results closer to those seen in physical vehicles.

Figure 29 – Full-car model

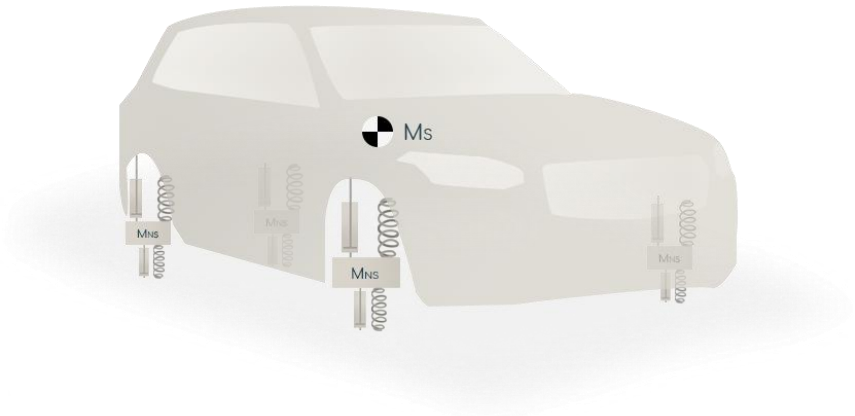

Source: Prepared by the author

Also, according to the figure above, this model has seven degrees of freedom, one for the vertical displacement of each unsprung mass, one for the vertical displacement of the body, one for the pitching moment and the last one for the rolling moment. As performed for the half-car model, the equation of the full-car model can be found in detail in (JAZAR, 2017).

As observed in the models presented, the tire has been represented by an elastic and damping component. Discussed in (HAPPIAN-SMITH, 2001), several models to represent the dynamic behavior of tires, fundamental components in the study of suspensions, have been developed over the years. However, the model used in the representations discussed above is the simplest, involving only an elastic component and a damping component.

2.3.6.4 Longitudinal model

As explained by (JAMES; ANDERSON; DA LIO, 2020), the longitudinal dynamics is commonly defined considering only the longitudinal forces that are generated and that are imposed on the vehicle. Simultaneously, seeking to address electronic units such as cruise control, (SUN *et al.*, 2022) say that the purpose of longitudinal controllers is to regulate vehicle speed.

During the design of a vehicle, a fundamental parameter to be analyzed is the weight distribution by the suspension axles. Equally, understanding the tensile forces for acceleration and braking as well as the influence of aerodynamic drag on these is of paramount importance. In this context, the longitudinal model (Figure 30) helps in the study of these properties.

Figure 30 – Longitudinal model

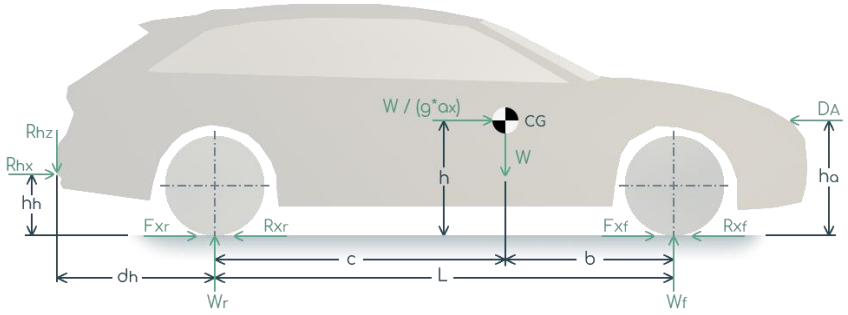

Source: Prepared by the author

The relationship of the static weight distribution per axle is given according to the longitudinal distances from the center of gravity to the front and rear-end axles of the vehicle (Equations 16 and 17, respectively). On the other hand, considering the vehicle in motion, the longitudinal acceleration component can be considered applied to the CG of the vehicle.

$$W_{fs} = \frac{W_c}{L} \tag{16}$$

$$W_{rs} = \frac{W_b}{L} \tag{17}$$

In this context, (GILLESPIE, 1992) uses the summation of moments to define the dynamic distribution of weights per axle (Equations 18 and 19), where θ is the slope of the track concerning the XY plane of the vehicle. At the same time, Table 4 describes the parameters present in the Equations 16-19.

$$W_f = \frac{cW\cos\theta - R_{hx}h_h - R_{hz}d_h - \frac{W}{g}a_x h - D_A h_a - hW\sin\theta}{L} \tag{18}$$

$$W_r = \frac{bW\cos\theta + R_{hx}h_h + R_{hz}(d_h + L) + \frac{W}{g}a_x h + D_A h_a + hW\sin\theta}{L} \quad (19)$$

Table 4 – Longitudinal model parameters

Symbol	Details
a_x	Longitudinal acceleration
b	Distance between the center of gravity and the front axle
c	Distance between the center of gravity and the rear axle
DA	Horizontal component of drag force
d_h	Distance between rear axle and towing point
F_{xf}	Front tractive force
F_{xr}	Rear tractive force
g	Gravity acceleration
h_a	Height of the point where the drag force is considered
h_h	Trailer hitch height
L	Distance between axles (pitch)
R_{hx}	Horizontal component of towing force
R_{hz}	Vertical component of towing force
R_{xf}	Front rolling resistance
R_{xr}	Rear rolling resistance
W	Total weight
W_{fs}	Weight supported by front axle
W_{rs}	Weight supported by rear axle
W_f	Weight supported by front axle
W_r	Weight supported by rear axle
eθ	Road slope

Source: (GILLESPIE, 1992).

The aerodynamic drag influences the longitudinal dynamics, as shown in the table above, and varies according to the profile of the body and vehicle peripherals, such as mirrors. In the case of formula-type cars, where the tires are exposed, the wheels function as a kind of barrier, considerably reducing the vehicle's performance (DIAS, C. A. R.; JÚNIOR, 2022).

2.3.6.5 Bicycle model

Aiming to study the behavior of a vehicle in turns, especially as a function of the longitudinal position of the CG and the lateral stiffness of the tires (PACEJKA, 2006), a model consolidated in the literature and commonly used is the bicycle model (Figure 31). Using this model is possible because the turn radius at high speeds is greater than the vehicle's pitch, which results in a negligible difference, on the same axle, between the steering angles of the wheels inside and outside the curve (GILLESPIE, 1992).

Figure 31 – Bicycle model

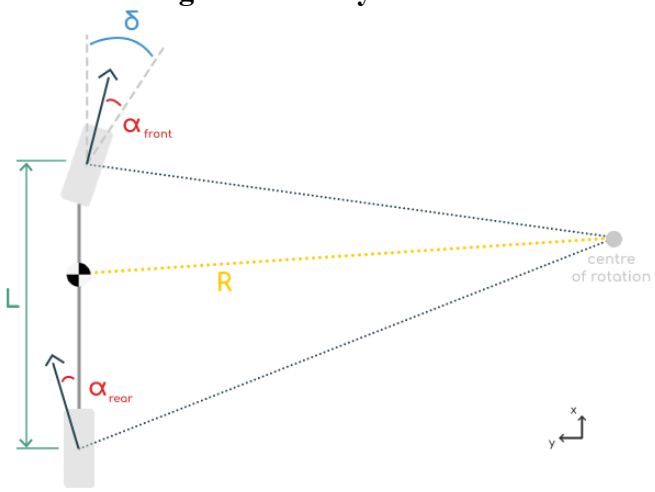

Source: Prepared by the author

According to (LANEVE, 2020), the model in the figure above allows the analysis of both kinematic and dynamic steering. While the kinematics happen at low speeds, that is, the lateral acceleration is disregarded and consequently the slip angle (α) tends to zero; dynamic steering takes place in the opposite situation and the wheels are under the action of lateral forces in addition to the rolling forces.

Working with the forces and kinematics of the model shown in Figure 31, (GILLESPIE, 1992) defines Equations 20 and 21 to describe the lateral forces acting on the front (F_{yf}) and rear (F_{yr}) suspensions, respectively, of a vehicle of mass m riding through a turn of radius R and at a longitudinal speed V_x.

$$F_{yf} = M\frac{b}{L}\frac{V^2}{R} = \frac{W_r}{g}\frac{V^2}{R} \tag{20}$$

$$F_{yr} = M\frac{c}{L}\frac{V^2}{R} = \frac{W_f}{g}\frac{V^2}{R} \tag{21}$$

The bicycle model is also frequently used in the development of electronic stability control (ESC), and this functionality is increasing in new vehicle projects. Detailed in (RIBEIRO, 2019), this model has 7 degrees of freedom: Three for the lateral, longitudinal, and angular velocities of the center of gravity and four for the longitudinal velocities of each of the four wheels. Details regarding its equation can be found in the last two works mentioned above.

According to (ABE, 2015), most vehicles can be modeled by a simplified mathematical representation. In some practical cases where the results found via simulation need relatively high accuracy, the models presented in this section may not be sufficient. In these cases, it becomes necessary to use more elaborate resources such as multibody systems.

2.3.7 ADAMS/Car and VI-CarRealTime

Similar to vehicle simulation software such as ADAMS/Car, VI-CarRealTime allows for vehicle analysis within the scope of vehicle dynamics. To this end, in the VI-CRT a virtual model is created by specifying certain vehicle parameters and then a sequence of tests is performed, as shown in Figure 32.

Figure 32 – Vehicle during simulation in VI-Grade package

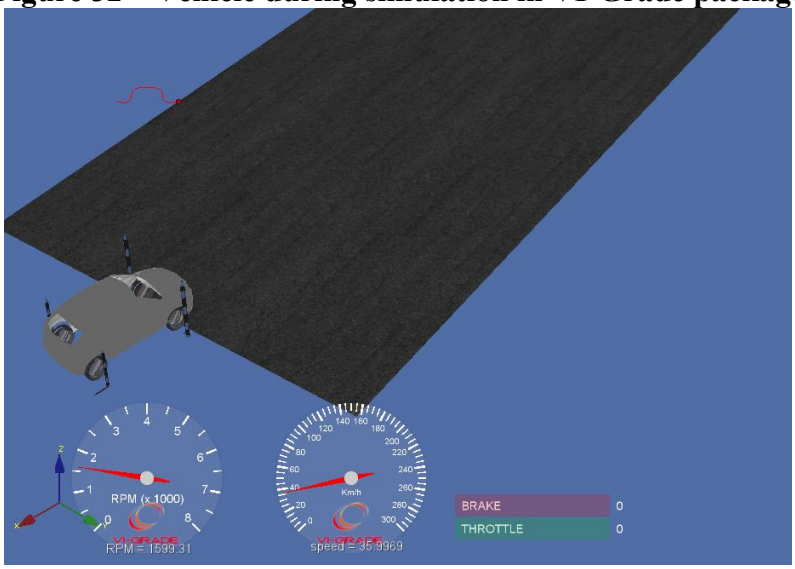

Source: Prepared by the author

VI-CRT is a virtual simulation environment focused on four-wheel vehicles, and, among its features, there is the possibility of running simulations independently or in partnership with MATLAB/Simulink (SORRENTINO, 2020). As a result, the VI-CRT models are, by nature, simpler than the ADAMS/Car models, which facilitates their use in DIL simulators.

Tests in VI-CarRealTime are performed by creating events and, among the most used, MaxPerformance stands out. In this event, the dynamic speed profile limit for a route is defined and the vehicle is subjected to running in the best possible condition to complete the proposed route with the highest possible speed. With dynamic vehicle simulators, VI-CRT partners with a software package like VI-DriveSim (Figure 33). In this, tests are carried out to certify that the maximum displacements of the simulation DIL are compatible with the admissible strokes of the simulator robots (NEVES, 2018).

Figure 33 – Virtual simulation of the movement of a DIL simulator

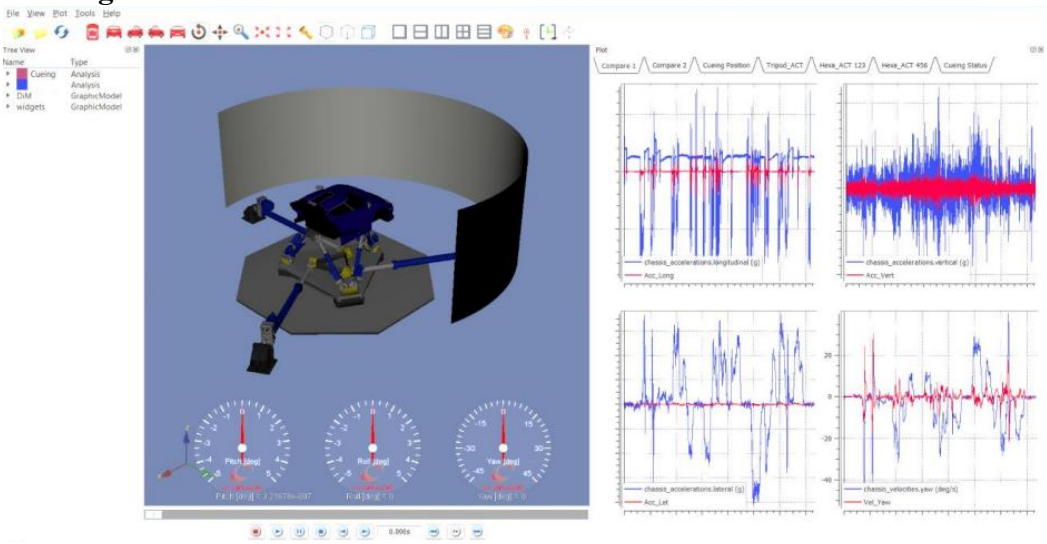

Source: (NEVES, 2018).

The next section will discuss, in detail, the use of dynamic vehicle simulators.

2.3.8 Vehicle Dynamic Simulators and the SIM Center

According to (JAMSON, 2010), a vehicle dynamics simulator can be divided into three main components: The vehicle cabin, the robots, and the tooling responsible for the construction of the graphic scenario and the sound system (Figure 34). Relating these three groups and finally allowing the simulation to be conducted, there is the virtual multibody model in which outputs are used to produce the loads and the displacement of the cabin to generate dynamic behavior.

Figure 34 – DiM 150 Simulator

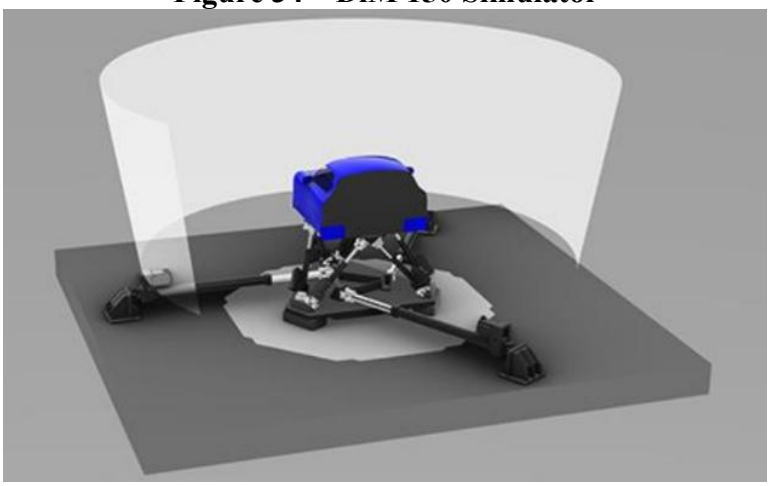

Source: (BRUSCHETTA; MINEN, 2019).

Previously discussed in this text and corroborated by (VEPA, 2015) studies, a virtual model is fundamental in simulators since they are fed with the information provided by the models. The importance of this information being consistent with a physical vehicle is as great as the movements of the platforms and the graphic creation of the roadway are correctly reproduced since the last author cited also comments that these systems are responsible for reducing the difference between the physical vehicle and the virtual simulation.

In recent years, simulation has been presented as one of the main and most fundamental steps of an engineering project. In this context, vehicle dynamics development in academia and the automotive industry has used simulators that usually present between six and nine degrees of freedom, where the more degrees of freedom the equipment presents, the more realistic the simulation of a vehicle can be. The present research was conducted with a simulator of nine degrees of freedom, the SIM Center (Figure 1).

As presented by the portal (VI-GRADE, 2021), the SIM Center is a center of excellence in vehicle dynamics that consists of a partnership between industry and academia, through PUC Minas, in addition to the financial support of the BNDES. Currently, standing out for being the only dynamic simulator of this robustness in the southern hemisphere of the planet, the equipment is produced by VI-Grade and is a driver-in-the-loop simulator, that is, the driver interacts in real-time with the simulation.

The vehicle simulators use, in general, three types of simulation: Model-in-the-loop (MIL), hardware-in-the-loop (HIL), and driver-in-the-loop (DIL) (Figure 35). Used in centers of excellence in vehicle dynamics, the latter is the most elaborated of the three presented (VEPA, 2015) because it includes drivers actively participating in the tests (the so-called real-time simulation).

Figure 35 – Driver-in-the-loop simulation

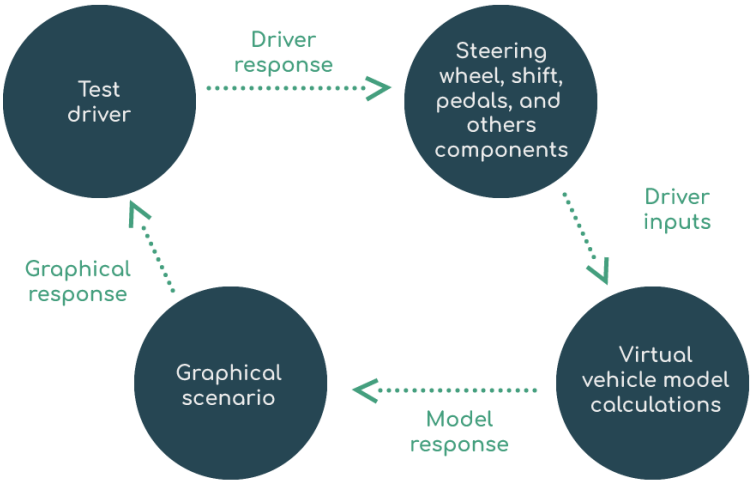

Source: Prepared by the author

Parallel to the DIL simulation, there is the model-in-the-loop simulation, where only the model is present in the simulation loop; and hardware-in-the-loop, which in addition to the model also involves some type of physical equipment, which increases the complexity of the simulation, but on the other hand can increase the accuracy of the results obtained.

The center of excellence pictured here also has a curved screen that increases driver immersion by providing the sensation of being on a physical roadway. Likewise, the vehicle's cabin mirrors are screens that represent the scene that would be seen in the mirrors if the vehicle were on a track; and also, the interior of the simulator's cockpit is faithful to a physical car, optimizing the driver's immersion during the simulation due to this set of details.

As (NEVES, 2018) explains, the SIM Center robot structure has a hexapod and a tripod (Figure 36). Respectively, these two mechanisms have six and three degrees of freedom, totaling nine in the system.

Figure 36 – SIM Center's platform robots: The longer arms belong to the tripod, while the shorter ones, fixed on the red platform, belong to the hexapod

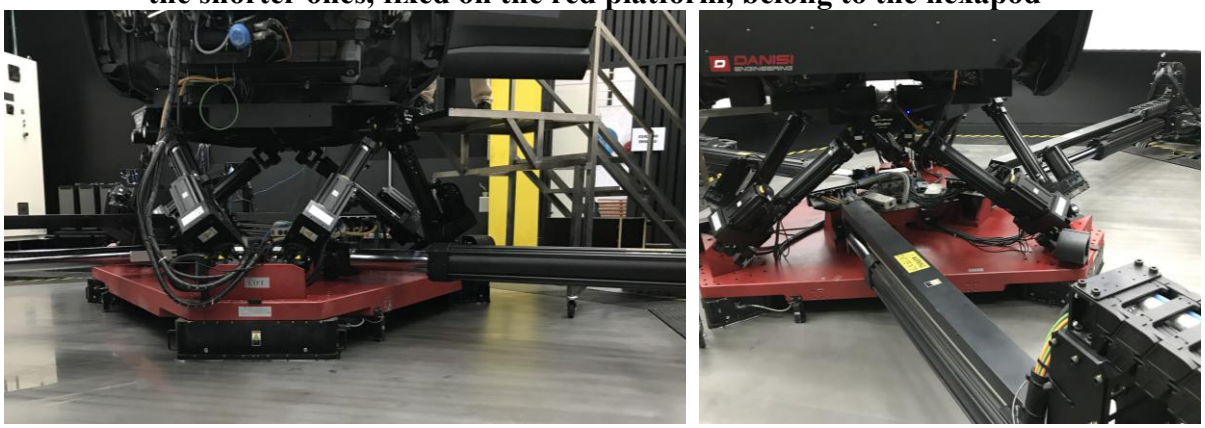

Source: Prepared by the author

In this system, the tripod moves, through airbag actuators, on a platform with a smooth and rigid surface. While the hexapod is responsible for roll, pitch, and vertical translation movements, the tripod is responsible for yaw movements and ground plane translations (BRUSCHETTA; MINEN, 2019).

3 METHODOLOGY

Aiming to achieve the tender goals, the methodology proposed for this research is presented in a flowchart by Figure 37.

Figure 37 – Methodology flowchart

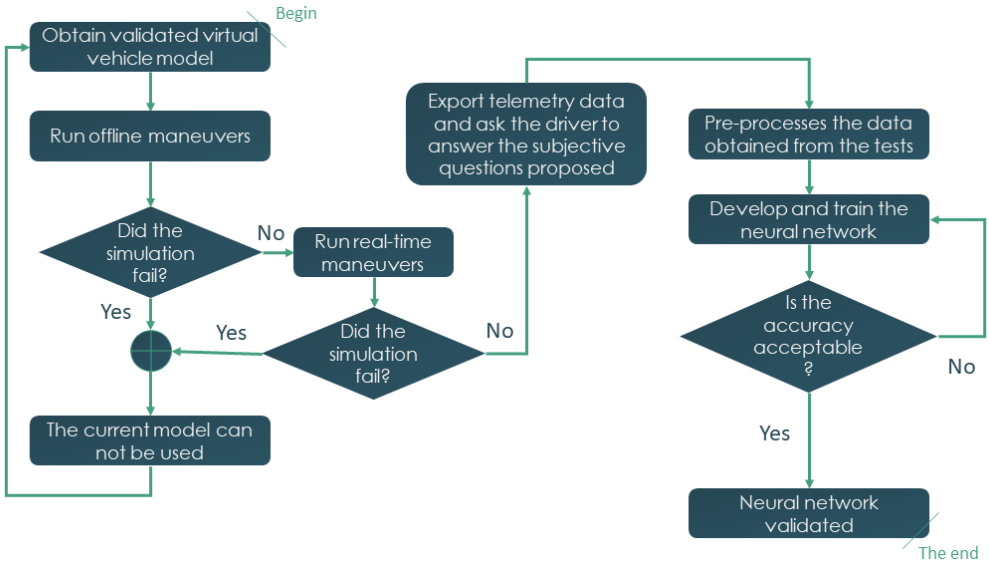

Source: Prepared by the author

After the theoretical discussion, the methodology proposed in the figure above is divided into three large groups: The first, related to the manipulation of virtual vehicle dynamics models; the second, associated with processing the data obtained via telemetry and according to the perceptions of human drivers; and the third, related to the adjustment of the DNN. Each of these groups, with their sub-steps, is covered in more detail in the following topics. In these, the parameters used for definitions, such as what would be a validated virtual vehicle model, a failure in the simulation, or even the accuracy of the acceptable network, are also worked on.

3.1 Definition of virtual vehicle models

Aiming for a robust artificial neural network to be used across a wider range of vehicles, ideally, automobiles from diverse categories should be utilized during data collection. In this context, tests with vehicles such as mini hatchbacks, hatchbacks, sedans, SUVs, and light commercial vehicles like pickup trucks and vans have been planned. However, two key points limit this model gathering.

First, a more important premise was the use only of models whose KnC and handling parameters were previously correlated to the physical test vehicles, as discussed in (DIAS, C., 2021; DIAS, C.; LANDRE, 2022). This choice is primarily due to the intention of training the

network so that the results obtained by the dynamic simulator also encompass the variations achieved with virtual models of physical vehicles. Consequently, this ensures that numerical variations of virtual models minimally influence the trained data. Concurrently, as will be discussed in detail in the real-time tests section, the need to include a relatively high number of human drivers to blend their subjectivities results in considerable simulation sessions, which constitutes a limitation.

With that, the availability of virtual models under the imposed conditions currently limits the scope of the DNN. Nevertheless, with the inclusion of more virtual vehicle models from other categories, the same methodology used here should be valid for developing other neural networks, one group for each vehicle category.

In the presented context, tests were planned to include four distinct models, as listed in Table 5. It is noteworthy that the base vehicle chosen was a sports model, where this choice is based on the expectation that changes made to the car's parameters are more easily perceived in its dynamic behavior, given that these cars typically have more refined tuning.

Table 5 – Parameters modified in the models

Model	Variation	Details
V00	Reference model	-
V01	Brake pad friction	-20.0%
V02	Vehicle weight	+23.67% (considering passengers' weight)
V03	Spring preload	-5.92% (rear) and -5.76% (front)

Source: Prepared by the author

Considering a context where volunteers with varying levels of driving experience would drive the models, selecting the above parameters and their variations was related to the presumed ease of perception of vehicle drivability quality. Some guidance regarding the intensity of parameter adjustments can be found in works such as (DIAS, C. *et al.*, 2024), where the authors suggest tests with specific variations from the base parameter values and achieve satisfactory results.

Once the models are adjusted, tests with virtual driver models are performed. Consequently, denominated as offline, these tests are described in the following topic.

3.2 Offline tests

In addition to obtaining parameters about vehicle behavior, offline tests are a fundamental step in centers of excellence in vehicle dynamics to guarantee the safety of the simulator, since inconsistencies regarding the construction or conversion of the model from software such as ADAMS/Car to VI-CRT, for example, are detected without placing the endangered robots. (DIAS, C.; LANDRE, 2023).

Concurrently, it became necessary to validate that the changes imposed on each model influenced the vehicles' behavior. Therefore, a set of maneuvers consolidated in the literature and commonly used for vehicle suspension and steering analysis was performed. While some of these maneuvers have performance parameters defined by a standard, such as the double-lane change (DLC), described by ISO 3888-2:2018, and the constant radius change, described by SAE J266-199601 and ISO 4138:2012; some have varying parameters according to the purpose of those who perform them (ISO 3888-2, 2011; ISO 4138, 2012; and SAE J266, 1996). Table 6 presents the chosen maneuvers and some details about them.

Table 6 – Offline tests

Maneuver	Description
Fishhook	Safety maneuver where the vehicle undergoes a sudden change in trajectory, resulting in a fishhook-like path (ZALEWSKI, 2017)
J-turn	Safety maneuver that induces the vehicle to extreme stability conditions (ARAB; YI, 2021)
Slow ramp steer	Maneuver where the steering wheel angle varies linearly and slowly so that this input angle forms a ramp. Often used for lateral vehicle analysis (FARRONI; SAKHNEVYCH, 2022)
Step steer	Maneuver where the steering wheel angle suddenly varies from one value to another, stabilizing in this final value (ESMAEILI; KAZEMI; TABATABAEI OREH, 2019)
Sweep Steer	Maneuver where the steering wheel angle oscillates between defined and increasing frequencies (TALARICO *et al.*, 2022)
Straight acceleration	A maneuver where the vehicle is accelerated from a standstill to a predefined longitudinal speed within a specified time interval
Straight breaking	A maneuver where the vehicle starts at a predefined longitudinal speed and is braked to a stop within a specified time interval
Lap in Hockenheim	Using the Max Performance event, the virtual driver completes a fired lap through the aiming circuit to complete it at the minimum time possible

Source: Prepared by the author

Choosing these maneuvers and their parameters for open-loop tests for simulation was based on related works (BONERA *et al.*, 2020; DE CARVALHO PINHEIRO *et al.*, 2019; FERRARIS *et al.*, 2019; NI; HU; XIANG, 2019; PARRA *et al.*, 2019; STERTHOFF; HENZE; KÜÇÜKAY, 2021; WANG, Q. *et al.*, 2020; ZHANG, X. *et al.*, 2022; ZHAO, L. *et al.*, 2020).

In addition, the fishhook and J-turn maneuvers were chosen because they are emergency maneuvers, pushing the vehicle to its limits (NHTSA, 2002). Additionally, slow, step, and sweep steer maneuvers were selected to assess stability and steering. Similarly, acceleration and braking maneuvers were included as consolidated tests to examine a vehicle's acceleration and braking capabilities (GRABA *et al.*, 2021; ILIE; CRISTESCU, 2023). Lastly, the Hockenheim track was selected due to its interesting characteristics: A sequence of straight lines and low- and high-speed corners demand both longitudinal and lateral vehicle performance in distinct scenarios. Figure 38 shows the generic vehicle path in each of those maneuvers.

Figure 38 – Vehicle displacement during a generic j-turn (a), fishhook (b), sweep steer (c), slow steer (d), and sweep steer (e) maneuvers, besides during a lap in the Hockenheim track (f)

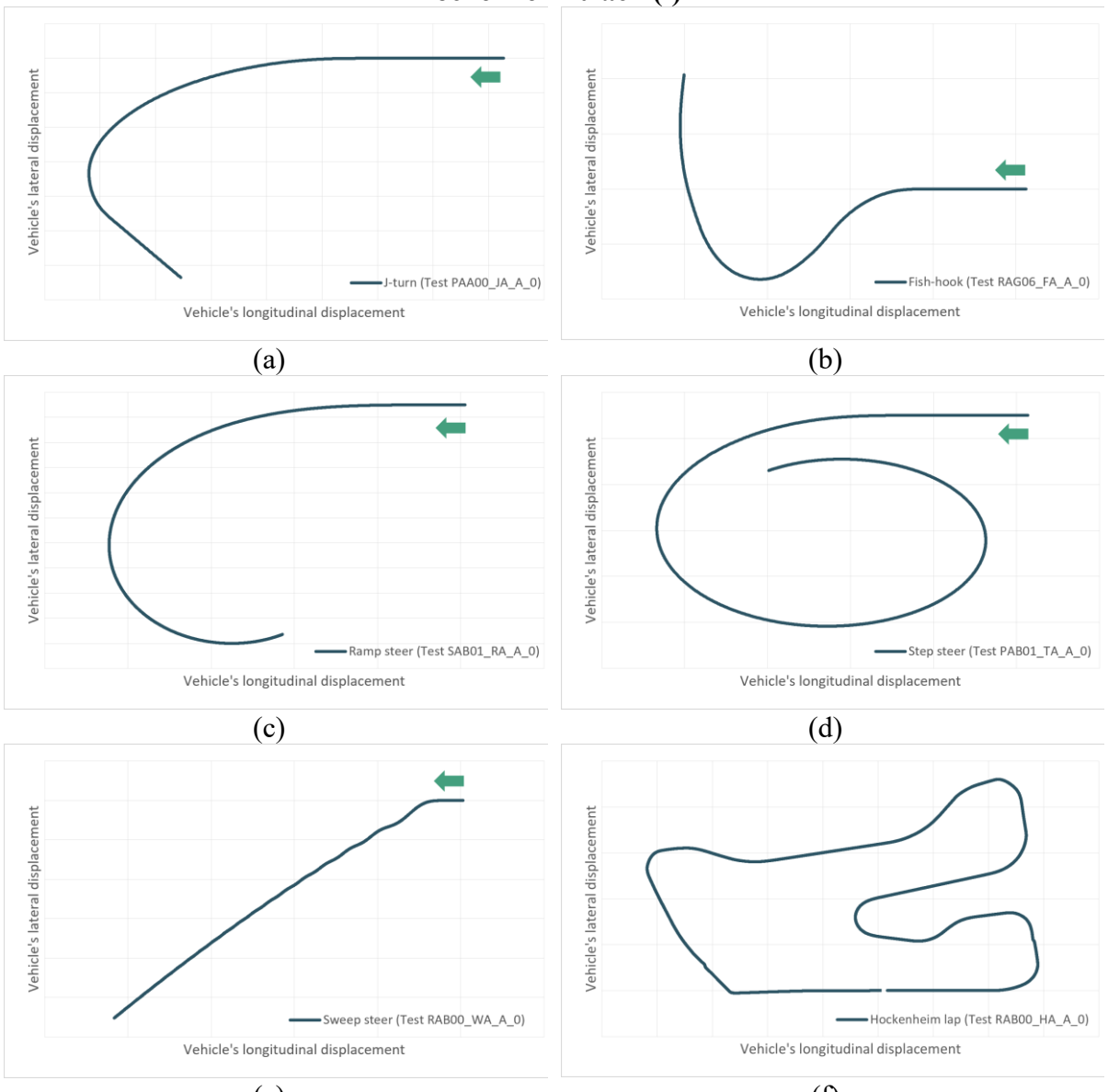

Source: Prepared by the author

As will be covered in detail in the data pre-processing topic, the telemetry of the tests above results in serial temporal data, however, some key parameters are chosen at specific times for using the network.

Finally, it should also be noted that after conducting the tests mentioned here, two models showed inconsistency and were discarded. During the real-time tests, described in the following topic, the same happened for a third model, resulting in the four vehicle models available and previously shown in Table 5.

3.3 Real-time tests

While the offline runs, e.g., safety maneuvers, depend only on the definition of some parameters for simulating with a virtual driver, the execution of these same maneuvers in real-time tests requires a human driver who also maintains certain regularity during the simulation of different vehicles.

Due to this consideration and aiming to achieve a final solution that is relatively simple yet satisfactory for use, the metrics derived from the real-time tests involve completing a lap on the Hockenheim circuit, a renowned track in the world of motorsport and various testing endeavors due to its characteristics of long straights and distinct curves ranging from high to low speeds (MANCA, 2020; MASSARO; LIMEBEER, 2021; NOVI *et al.*, 2020). Consequently, some sections along the circuit were considered to obtain the metrics needed.

Alongside the acquisition of OM, some SA regarding the vehicle's behavior were posed to the drivers during the test runs, as outlined in
Table 7.

Table 7 – Subjective assessments

Code	Assessment
Q0	Steering wheel response
Q1	Difficulty in maintaining the vehicle in curves
Q2	Braking response
Q3	Acceleration response
Q4	Overall experience

Source: Prepared by the author

These questions were subsequently evaluated according to the criteria outlined in the SAE J1441 standard, which is widely used for classifying vehicle handling quality (SAE J 1441, 2016). In this standard, it is defined a rating scale from one to ten that reflects perceptions that

both more and less experienced drivers would have regarding the dynamic behavior of the vehicle, according to Table 8.

Table 8 – Subjective grades according to SAE J1441 standard

		Unacceptable				Acceptable					
Customer perception of parameter	Detected by	All custom	Avarage			Critical	Trained				
	Noticeability	High			Moderate			Small		Very small	None
	Sensation	*Intolerable*	*Extreme annoyance*	*Annoyance*	*Slight annoyance*	*Small disturbance*		*Minor Disturbance*	*No disturbance*		
	Reaction	*Refusal*	*Protest*		*Complaint*	*Acceptance*		*Appreciation*			*Enthusiasm*
Rating scale	Assessment	*Very bad*	*Bad*	*Poor*	*Marginal*	*Barely acceptable*	*Acceptable*	*Fair*	*Good*	*Very good*	*Excellent*
	Number	*1*	*2*	*3*	*4*	*5*	*6*	*7*	*8*	*9*	*10*

Source: Adapted from SAE International (2016).

Once again, considering that less experienced drivers should participate in the tests, the application of these rating scales was conducted only for models V01, V02, and V03. To do so, the drivers regarded the base model V00 with a rating of five in all aspects. After driving a few laps in the V00 model to become acquainted with the simulator and the vehicle's responses, the volunteers drove the other vehicles and evaluated the model they had just driven in comparison to the base model.

It is worth noting that this testing phase allowed drivers not only to complete laps on the Hockenheim circuit but also to evaluate the virtual model with more abrupt accelerations or while carrying higher speeds into curves, for example, to truly feel the difference in the vehicle's dynamic behavior. After completing this evaluation and answering the SAs, the volunteers completed a full lap on the circuit so that metrics could be monitored and recorded with the assistance of the WinTax software.

Regarding the number of drivers (n), the minimum required to obtain satisfactory results was determined based on a review of the literature available in (DIAS, C. A. R.; LANDRE JR, 2024). According to this review, after an initial screening of results from PubMed and ScienceDirect, fifty-nine studies were analyzed where the authors employed distinct numbers of volunteers for tests involving driver-in-the-loop simulators. After applying several considerations and filters, the remaining relevant studies were listed, and Figure 39 presents the n used in each study.

Figure 39 – Number of drivers used in studies with DiL simulators where subjectivity and objectivity played a crucial role

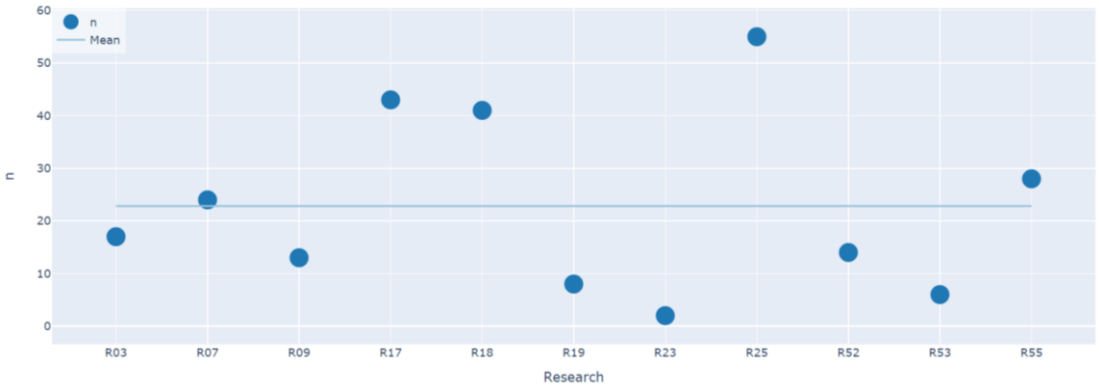

Source: Prepared by the author

As a result, a minimum of twenty-three drivers was determined for the experiments. Further details regarding this review can be found in (DIAS, C. A. R.; LANDRE JR, 2024), where the filtering criteria and boundary conditions are discussed in greater depth.

3.4 Data pre-processing

Pre-processing input data to an artificial neural network is usually the most laborious step in the process. Mainly, this is due to two characteristics: While the first is related to the relatively large amount of data obtained from the experiments, the second is related to the requirements of the ML technique used for proper functioning. In addition to these points, the challenge is greater for the present work due to the need to correctly select telemetry data that are linked to the proposed subjective assessments.

Based on previous works in the literature and research on what is currently used by the automotive industry, the parameters presented in Table 9 were defined as the DNN input (BÎNDAC *et al.*, 2022; DERRIX; PROKOP, 2022; PAUCA; CARUNTU, 2024; TOTA *et al.*, 2022; WANG, M. *et al.*, 2020).

Table 9 – Parameters analyzed in each track sector of the Hockenheim track runs

Sector type	Parameter	When
Straights	Longitudinal velocity, pitch acceleration	After dividing each straight line in half, the variation between the beginning and the end of each of these halves was identified.
Turns	Lateral acceleration, roll acceleration, and steering wheel demand	The turn is divided into three sectors: entry, apex, and exit. In each of these three sectors, the parameters presented were obtained at the point of greatest lateral acceleration

Source: Prepared by the author

In this sense, the telemetry data is divided into sectors defined as interesting on the track. In other words, two big groups were taken: Straight lines and turns. While in the first two

segments of the sector are taken, the first and the second half of the straight; in the latter, a subdivision into three segments is also conducted: Entry, apex, and exit; each region being distinct and with its specific data. To this end, a sequence of algorithms in Python programming language, with the support of libraries for DS such as NumPy and Pandas, were written.

After executing the pre-processing, a spreadsheet is generated where each column corresponds to one of the parameters previously listed in Table 9. Along with these, the subjective assessments of the parameters asked of the driver, also previously displayed during this work (Table **7**), are attributed to each test run.

3.5 Artificial neural network development and training

In a simplified manner, Figure 40 presents the general idea of the DNN developed in this study. It is noteworthy, however, that the SA data is utilized solely during the training and testing phases of the DNN, once the goal of this work is for the neural network to accurately predict these SA and consequently the vehicle's dynamic behavior.

Figure 40 – Inputs and outputs for training the DNN

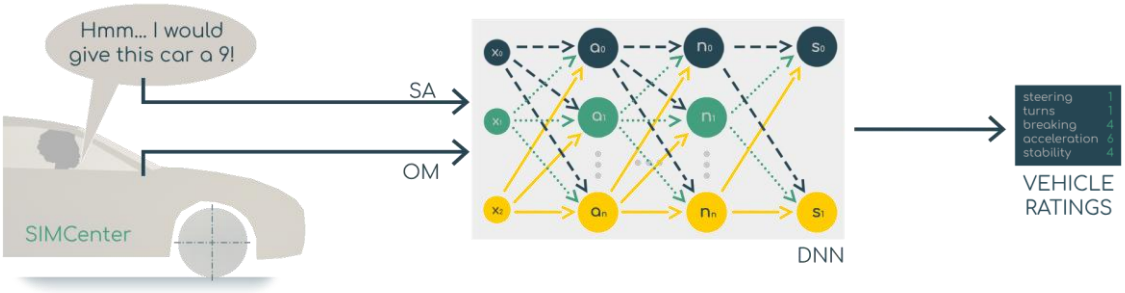

Source: Prepared by the author

However, some previous steps must be taken for the above proposal to be implemented. At this point in the text, it is important to highlight that two distinct pre-processing steps are performed within the data obtained after the offline and real-time simulations. While the first is related to the course of action done on the simulations' telemetry data, a second part of pre-processing must be conducted on top of the worksheet generated by the first step.

Some tests of this second pre-processing step are carried out only by the good practice of using ANNs, as is the case of checking empty or non-numeric values, for example, since these checks had already been made in the algorithms that read the telemetry data. However, other steps such as normalizing the input values are essential. Known as scaling, this normalization is necessary when the units of input values are on different scales, e.g., lateral

acceleration and pitch angle, so that the network does not neglect smaller values compared to larger ones (ASSEGIE *et al.*, 2023).

Still regarding the data, in every ANN the variables must be divided into labels and features. While the labels are the data that must be predicted, the features are the data used to predict the labels. To do so, functions from Scikit-learn, a free machine learning library also in the Python programming language, were used. In the same way, functions from this library were used to divide the registers in a proportion of 75% to train and 25% to test the network. Currently, there is no unanimity regarding which proportion is ideal, but most research recommends using values near the ratio of 80/20 (GÉRON, 2017).

Since five subjective questions are expected as system outputs, five distinct neural networks were trained to better adapt to each question. Besides this, the algorithm was developed in such a way as to guarantee that each of the DNNs has its specific execution parameters, i.e., the definition of the best activation function, batch size, and solver, known as hyperparameters (GÉRON, 2017; KOUTSOUKAS *et al.*, 2017). To do so, a Scikit-learn network classifier function, called GridSearchCV, was used to find the best possible hyperparameters.

The GridSearchCV is a cross-validation technique. With this function, it is easier to find the optimal parameter values from a given set of suggested parameters to use in an artificial neural network (SCIKIT, 2023). In the present work, the activation functions tested were logistic, tanh, and ReLU; while the batch size ranged from ten to fifty, and the solvers were Adam and SGD. While the difference between the other parameters was previously presented, the variation between solvers is how the calculation of the network weights is carried out, influencing the accuracy and execution time of the processing. Once the methodology developed here works with some brand-new features, there are not so many past similar works to serve as references. Consequently, the choice for these parameters was at some point empirical, but always checking the programming library documentation to use resources with characteristics compatible with the physical system approached (SCIKIT, 2023).

With the definition of ideal parameters for each network, the training can then be started. As stopping conditions, five hundred was defined as the maximum number of interactions, as well as a tolerance of 10^{-3}. Here, it is highlighted that for all networks, the ideal hyperparameters found were the use of ReLU for the activation function, the Adam model as the solver, and ten as the batch size. Based on the results obtained, the artificial neural network model chosen in this work was the multilayer perceptron, which is the basis of several other more complex and elaborate networks (CHOLLET, 2018).

Additionally, following an empirical approach due to the lack of close references, three hidden layers were defined, each comprising fifty neurons. Consequently, the network developed here was classified as a deep neural network because it possesses more than one hidden layer (MENG; DASGUPTA, 2016; USTEBAY; TURGUT; AYDIN, 2019). It is worth highlighting that the execution of tests to determine the number of hidden layers and neurons in each of these layers was guided by the complexity of the system under study, where higher intricacy tends to require more hidden layers and neurons (BAU *et al.*, 2020).

4 RESULTS

With almost fifty hours of real-time running in the driver-in-motion simulator and conducting the offline tests, the results section will present the findings in distinct subsections for each phase of the tests, similar to what was done in the methodology section.

4.1 Offline tests

One of the most effective analyses for validating the brake system modification in a vehicle, due to its highly visual nature, is the braking time analysis (Figure 41). According to this figure, the braking distance required by V01, the model with the lowest brake friction, is significantly greater than all the others. Additionally, V02, the heaviest vehicle, also requires a longer braking distance compared to models V00 and V03. On the other hand, V00 and V03 should exhibit the same braking distance since the modified spring preload in V03 is not expected to influence the braking distance, which is also confirmed by this figure.

Figure 41 – Braking distance required for the virtual models during the braking test

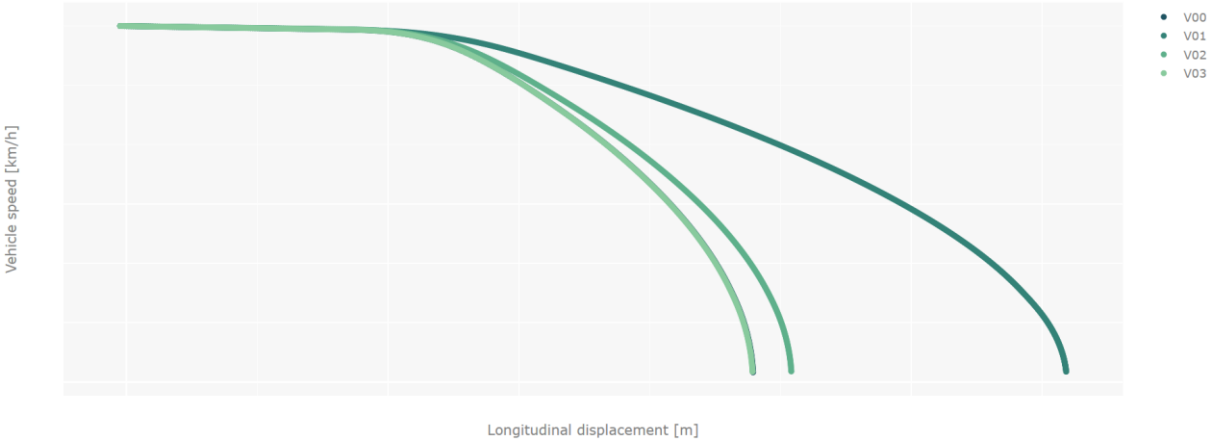

Source: Prepared by the author

Similarly, the acceleration test provided valuable insights into the dynamic behavior of the different models. According to Figure 42, which also presents the vehicle speed curve over displacement, all vehicles reached the same final speed: However, V02, being considerably heavier, takes longer to respond to throttle input, resulting in slower gear shifts and, consequently, taking more time to reach the final test speed. As expected, the behavior of the other models is similar, as parameters directly related to speed were not varied.

Figure 42 - Acceleration test: The heavier vehicle requires more time to reach the final speed

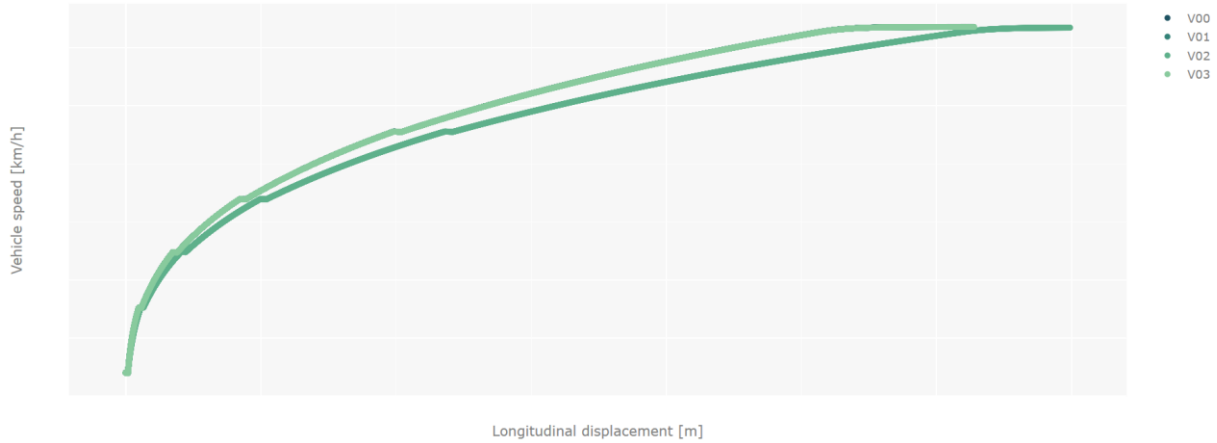

Source: Prepared by the author

Finally, to validate the third and final model, vehicle V03, the step steer maneuver indicated, through the roll center height, how this model is noticeably taller than the others, as shown in Figure 43. It is also worth noting that the initial section, where V03 shows a higher roll center height compared to the others, is a stabilization period in the simulation given the behavior for the remainder of the maneuver. As expected, there is no variation between the base model, V00, and the V01 model.

Figure 43 – Variation of roll center height during the step steer maneuver

Source: Prepared by the author

Among the maneuvers performed, one that shows a clear relationship between the modified variables and the dynamic behavior of these variations in the vehicle is the sweep steer. According to Figure 44, model V02 exhibits constant oscillations. However, although V00 and V01 have overlapping points during this maneuver, vehicle V03 confirms its looser behavior by displaying higher pitch angle values than the base model for most of this test.

Figure 44 – Sweep steer: Variations in V02 and V03 are observed, while V01 maintains the behavior of V00

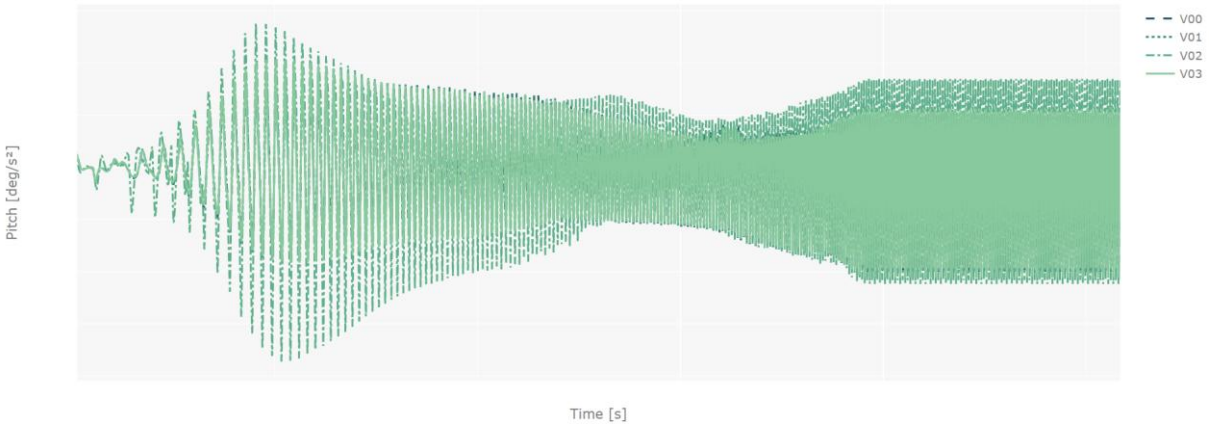

Source: Prepared by the author

Before discussing the results of the other maneuvers, several crucial points should be noted regarding the traces in the figure above. Concerning the test boundary conditions, the final frequency specified is consistently achieved by the virtual driver beginning in the last third of the maneuver, where the pitch angle oscillates with constant maximum and minimum values within the corresponding period (P_1). By zooming in on this region (Figure 45), this behavior becomes evident, and another well-defined period is observed (P_2).

Figure 45 – Pitch acceleration during sweep maneuvers reveals well-defined periods: P_1 and P_2

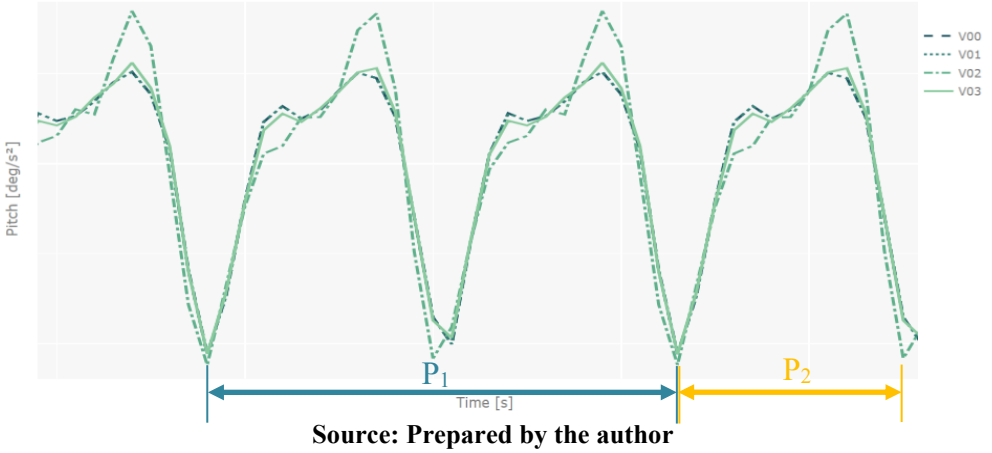

Source: Prepared by the author

To understand the impact of this behavior, a Fast Fourier Transform (FFT) is applied to the curves, and Figure 46 displays the frequency domain for the pitch signal of the vehicles. While F_{P1} is the frequency corresponding to period P_1, F_{P2} is the frequency corresponding to period P_2.

Figure 46 - Pitch acceleration during sweep maneuvers: Frequency domain

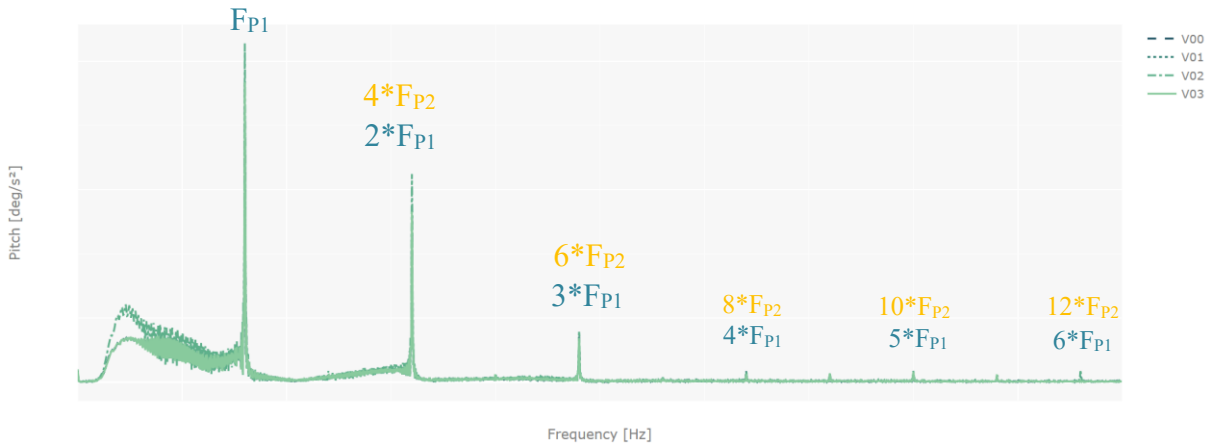

Source: Prepared by the author

A first notable comparison is that V02, the heavier vehicle, exhibits higher amplitude values across the entire spectrum, reinforcing the discussion in the time domain. However, an even more intriguing aspect of the plot above is the well-defined nature of the fundamental frequencies and their respective harmonics. This behavior is believed to be due to the non-linearity of various suspension components, e.g., bushings, as such well-defined peaks in the FFT are characteristic of systems with non-linear behaviors.

In parallel, model V03 shows increased amplitudes, particularly below P_1, raising the possibility that, in this case, the vehicle is being excited at a rigid body frequency. Consequently, further analysis of these offline maneuver data is conducted to investigate system behavior, focusing on identifying the excitation source at this frequency. Based on initial intuition, phenomena related to engine rotation are the first variable examined, with Figure 47 displaying these variable curves in both the time and the frequency domains.

Figure 47 - Engine rotation over time (a), zoomed-in view after curve stabilization versus time (b), and in the frequency domain (c)

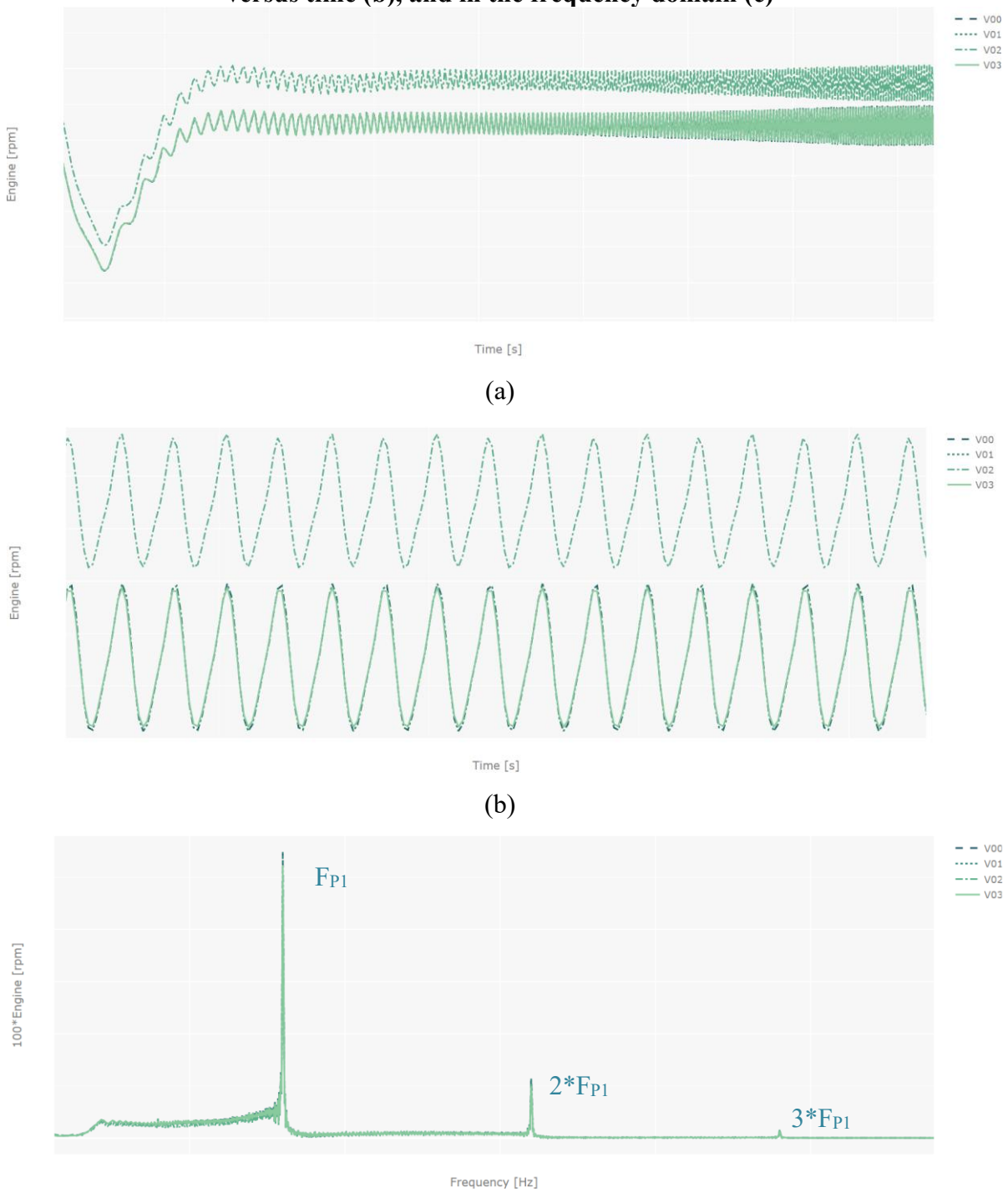

Source: Prepared by the author

Having identified the excitation sources for P_1 and P_2, several interesting analyses can still be conducted based on these data. For the observed behavior to occur, an exceptionally trained driver would be necessary to operate the vehicle, and even so, typical human-induced oscillations would be present.

On the other hand, as shown in Figure 48, the vehicle's steering angle matches precisely the angle input by the virtual driver. While this may be seen as a limitation when analyzing vehicle behavior influenced by human driver steerability, it is ideal for this part of the study, as these results confirm that all telemetered vehicle behavior stems purely from modifications made to the model parameters. Consequently, any feedback or subjective evaluation given by the driver in real-time tests will reflect only their perceptions.

Figure 48 – Steering angle over time during the sweep maneuver

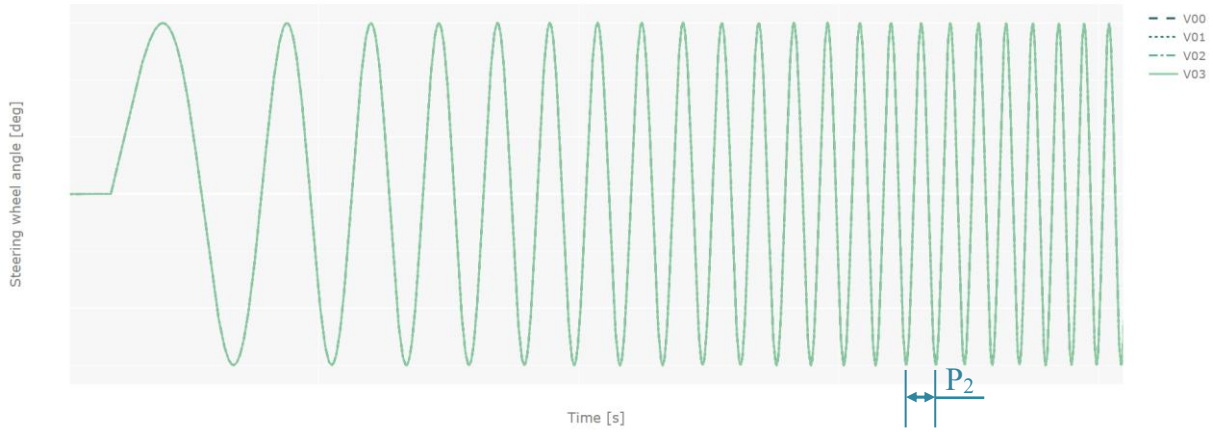

Source: Prepared by the author

It is also noteworthy that, as shown in the figure above, the same frequency corresponding to period P_2 is identified.

Moving on to other maneuvers, another interesting observation regarding V03, and perhaps even more evident, comes from the analysis of steering wheel torque versus time during the J-turn safety maneuver (Figure 49). According to the figure below, the responsiveness of model V03 is reflected in the larger amplitudes in steering input, particularly in the initial phase of the maneuver, to correct the vehicle's behavior.

Figure 49 – Vehicles' dynamic behavior during the J-turn maneuver

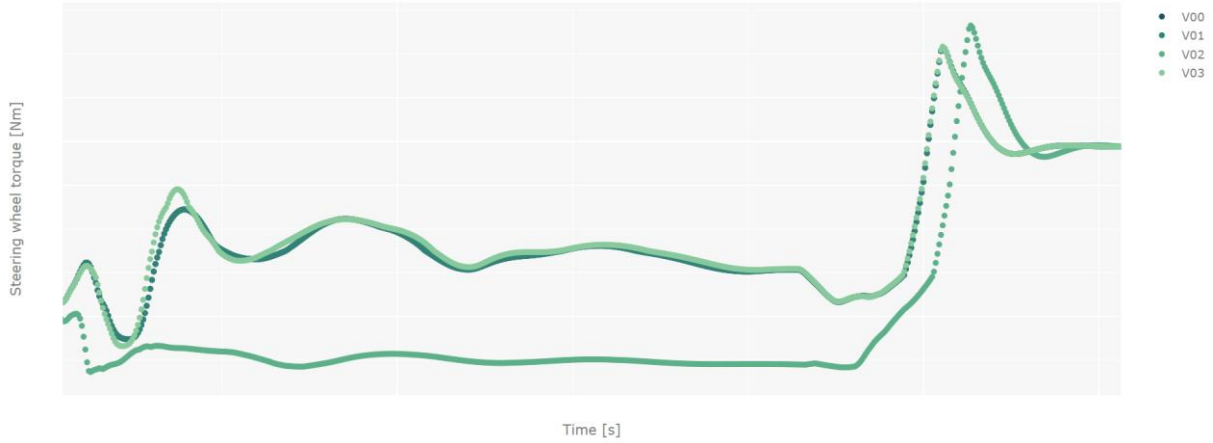

Source: Prepared by the author

Therefore, the developed virtual models are validated in terms of responding dynamically as expected so that the driver can perceive the differences during driving. Consequently, the real-time tests were conducted and are discussed in the following section.

4.2 Real-time tests

The real-time tests were conducted with twenty-five drivers, exceeding the minimum number of volunteers determined from the literature, with twelve females and thirteen males. While Figure 50 presents the mean and standard deviation of the SA given by the drivers, another crucial piece of information about these drivers for understanding the results is population statistics: The average driving experience is 51.330±77.032 months. Besides the high standard deviation being alarming at first sight, it can be of skillful use for this study as it involves very distinct driving experiences.

Figure 50 – Standard deviation and mean of the five questions assessed by the drivers

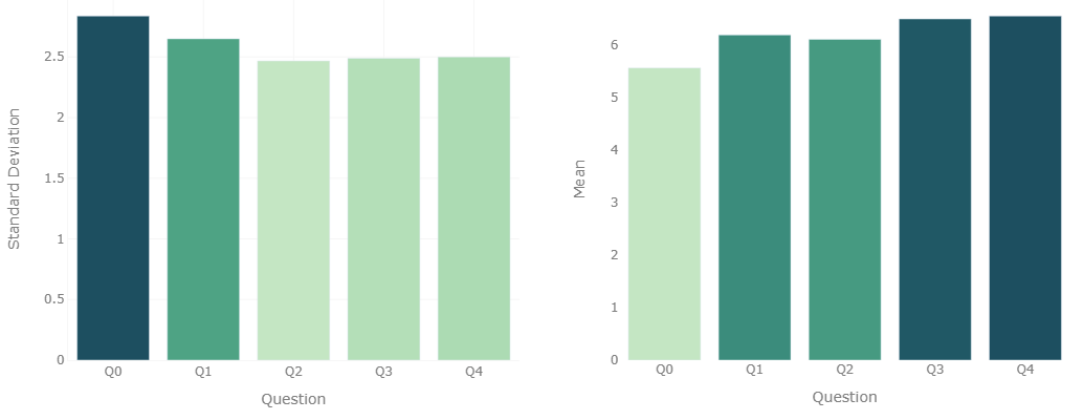

Source: Prepared by the author

It is noteworthy that during the tests, about seven drivers did not feel well during the simulation. Known as motion sickness (QUEZADA; NICOLAS, 2024; XIANG *et al.*, 2024), this is a common occurrence, although it still opens the door for various issues to explore the root cause (LIU-HENKE *et al.*, 2020; LUCAS *et al.*, 2020). Nevertheless, this factor did not influence the results obtained, as additional volunteers were sought to ensure at least the twenty-three drivers needed.

Additionally, the telemetry gathered from the runs served to validate the software developed for defining the track sectors. With just over five hundred lines of code, this algorithm divides the different sections of a run on the Hockenheim track (Figure 51) and retrieves the parameters proposed in Table 9.

Figure 51 – Hockenheim sectors. Which sector combines the suffix "S" and a sequential number

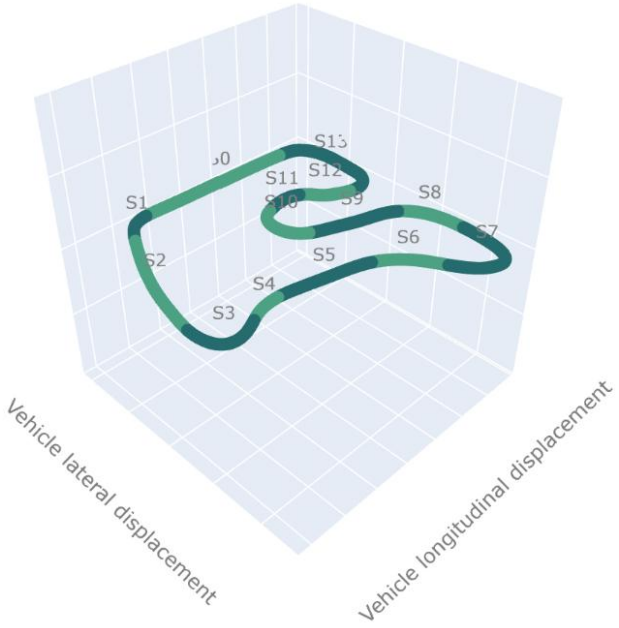

Source: Prepared by the author

Besides, in this case, the results shown were obtained by processing a spreadsheet from a real-time simulation, this software can do the same for the offline simulation that uses a virtual driver model. From this point, considering the sectors identified above for each simulation, some analyses are performed to understand the behavior and eventually a correlation between the studied variables before addressing the DNN results. Aiming to certify the quality of what is being used as a feed for the networks, Figure 52 shows an example of these analyses.

Figure 52 – Scatter plot for pitch angle in three different track sectors (S2, S5, and S9) and assessment Q2

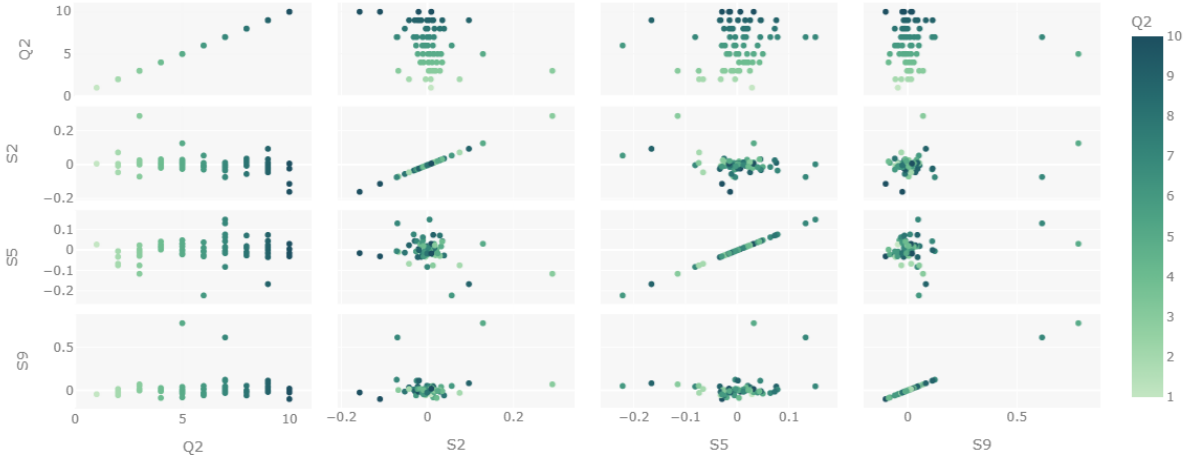

Source: Prepared by the author

The above scatter matrix could be displayed for all collected data. However, due to the substantial number of variables, these figures will not be shown. In any case, Figure 53 presents one of the cases in which some values were distant from the average. While they are still considered acceptable, it is expected that some difficulties will arise during the ANN processing to correlate this data.

Figure 53 – Scatter plot for steering wheel torque demand (S3, S6, and S11) and assessment Q0

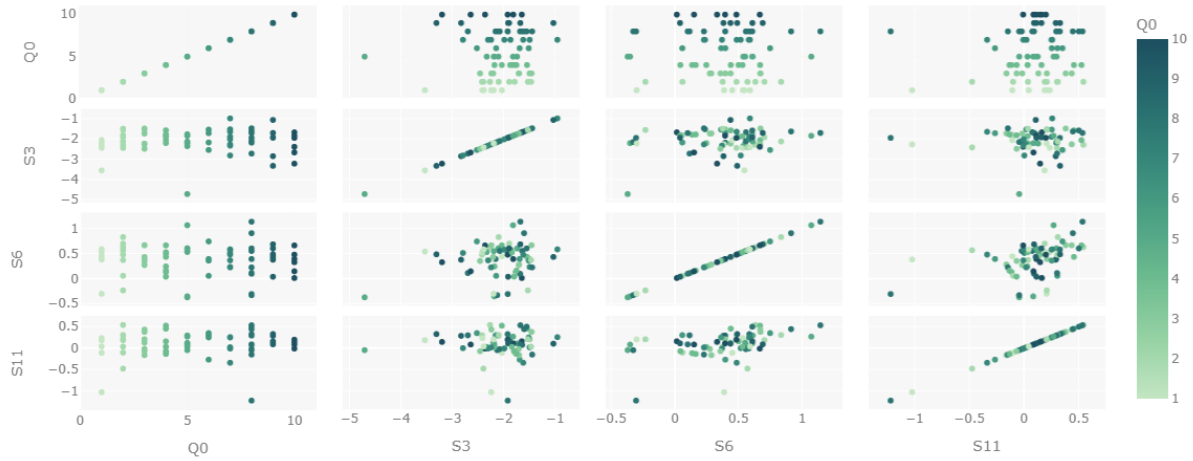

Source: Prepared by the author

Although the occurrence shown in the above figure repeats in some situations, most of the analyses revealed an interesting correlation between the variables. As an example, a third and final scatter plot is presented in Figure 54, this time relating the vehicle's acceleration response in the initial straight sections to the pitch angle.

Figure 54 – Scatter plot for delta pitch at the beginning of straight sections S2, S5, and S9, and assessment Q3

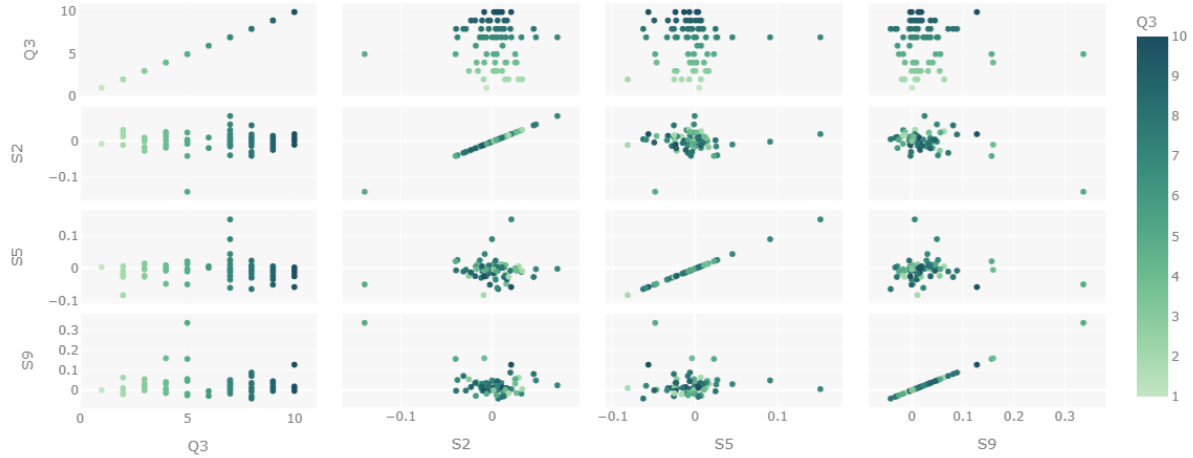

Source: Prepared by the author

After analyzing the relationship between some metrics and subjective assessments, the data could finally be processed through the DNNs, and the following section discusses the results obtained.

4.3 Neural networks

In this section, the results related to the deep neural networks training and testing will be presented. Although the initially proposed networks did not yield satisfactory results, adjustments in the methodology were made to optimize the outcomes, as will be discussed below.

4.3.1 Networks in the initially proposed configurations

A technique commonly used to verify the results obtained by an ANN after training or testing is called the confusion matrix. Intuitively, these matrices display how many times the network correctly estimated the expected result, which is represented in the main diagonal. Conversely, the squares above and below the main diagonal indicate the instances where the network's estimate was incorrect and the corresponding error amount. In this context, **Figure 55** presents the confusion matrices for the trained networks.

Figure 55 – Confusion matrices for the initial configuration of the networks: Training

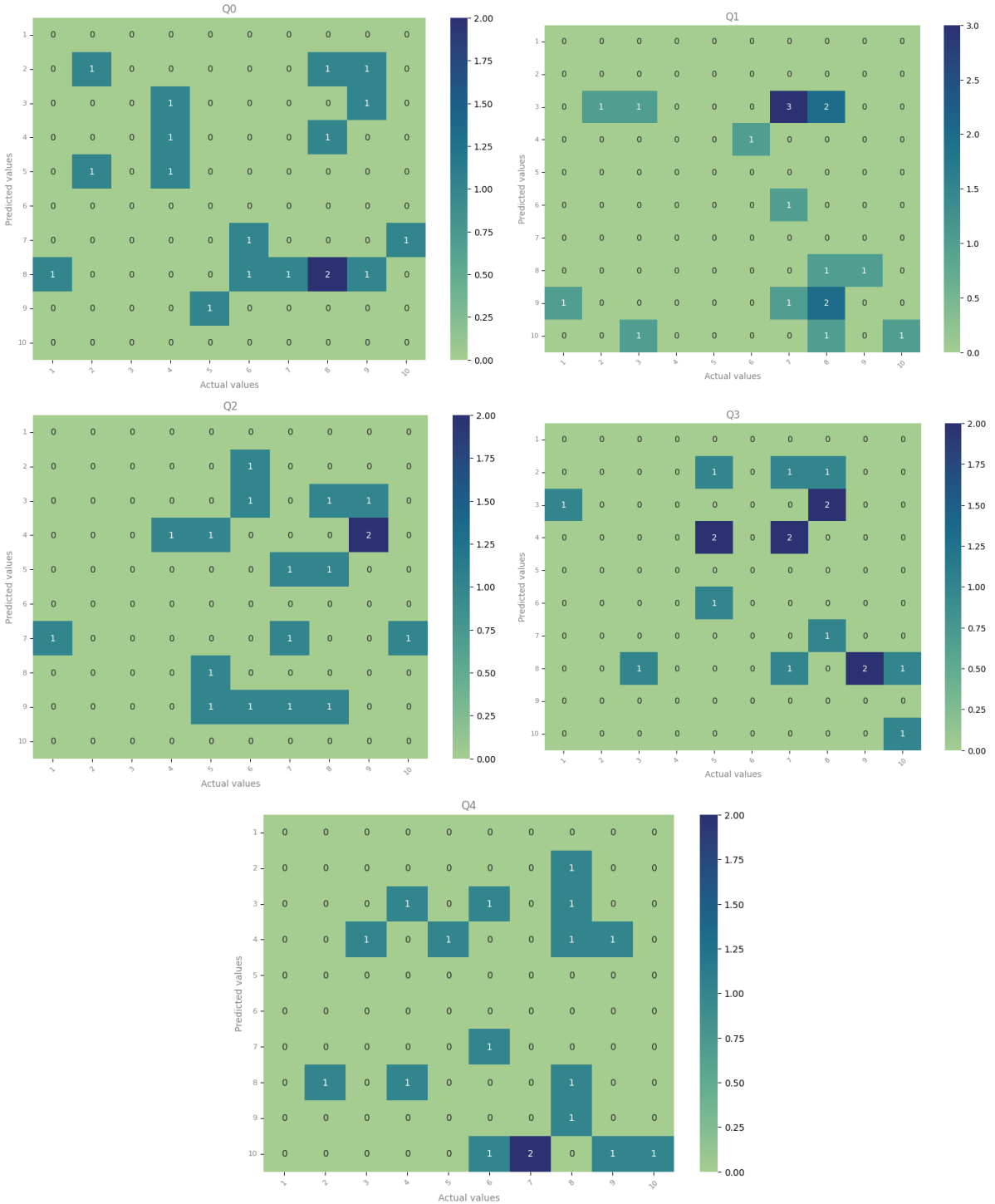

Source: Prepared by the author

As stated, the trained networks faced considerable difficulty in estimating the expected values, as the main diagonals of the confusion matrices are significantly underpopulated. In numerical terms, this is expressed by the defined accuracies: 22.22% for Q0, 16.67% for Q1, 11.11% for Q2, 5.56% for Q3, and 11.11% for Q4. Aiming to optimize the networks' accuracy, a sequence of adjustments to the hyperparameters is proposed.

Initially, the first proposal was to increase the number of iterations while decreasing the learning rate, followed by reducing the error tolerance. Without improvements, the next step was to alter not only the number of neurons per layer but also the number of hidden layers present in the networks. However, even after mixing these alternatives, the accuracies did not exceed 25%, necessitating an adjustment in the methodology.

4.3.2 Generation of additional data

Since the DNN presented accuracies below 25% with only the data obtained during the runs of the twenty-five drivers, despite extensive exploration of different hyperparameters and varying numbers of neurons and layers, a sequence of procedures is suggested to increase the sampling. Literature provides several methods and recommendations for performing this procedure according to specific cases and boundary conditions, such as interpolation, transfer learning with pre-trained networks using larger datasets, and perturbation of the standard deviation (IWANA; UCHIDA, 2021; MAHARANA; MONDAL; NEMADE, 2022).

Following the recommendations outlined in (BENGIO, 2012) and adapting certain steps experimentally to fit the problem at hand, efforts were made to ensure that the newly generated data possess the same nature as the original data according to the technique developed below:

a) Identify the standard deviation of each parameter;

b) Apply an arbitrary factor to maintain the standard deviation between 0.01 and 0.1, which is acceptable in the literature for increasing training data in ANN;

c) Concatenate the original data with the original data subtracted from the values obtained in step (b) and with the original data added to the values obtained in step (b), aiming to maintain the mean for the processed data;

d) Apply the Kolmogorov-Smirnov test (KS) to ensure that the generated data aligns with the original sampling and is therefore significant.

At the end of the data generation process, all KS tests indicated that the generated values fell within the statistical standard of the original data and could not be refuted. Consequently, a new loop of DNNs training was initiated.

4.3.3 Improved neural networks

Revising the definition of hyperparameters according to the proposed methodology, there was no change in the activation function, which continued to yield the best results with ReLU. However, the newly defined optimal batch size was set to five, while the solver

employed was SGD. Following a series of tests, a satisfactory balance between accuracy and the prevention of overfitting was achieved by utilizing a DNN consisting of three layers, each containing ten neurons, along with the tolerance set at 10^{-3} and a limit of fifty iterations. In this scenario, the resulting accuracies were 92.59%, 87.04%, 85.19%, 77.78%, and 81.48% for the networks corresponding to questions Q0, Q1, Q2, Q3, and Q4, respectively. This significant improvement compared to the original DNNs is further highlighted by the confusion matrices plotted for the new networks in Figure 56.

Figure 56 - Confusion matrices for the final DNNs: Training

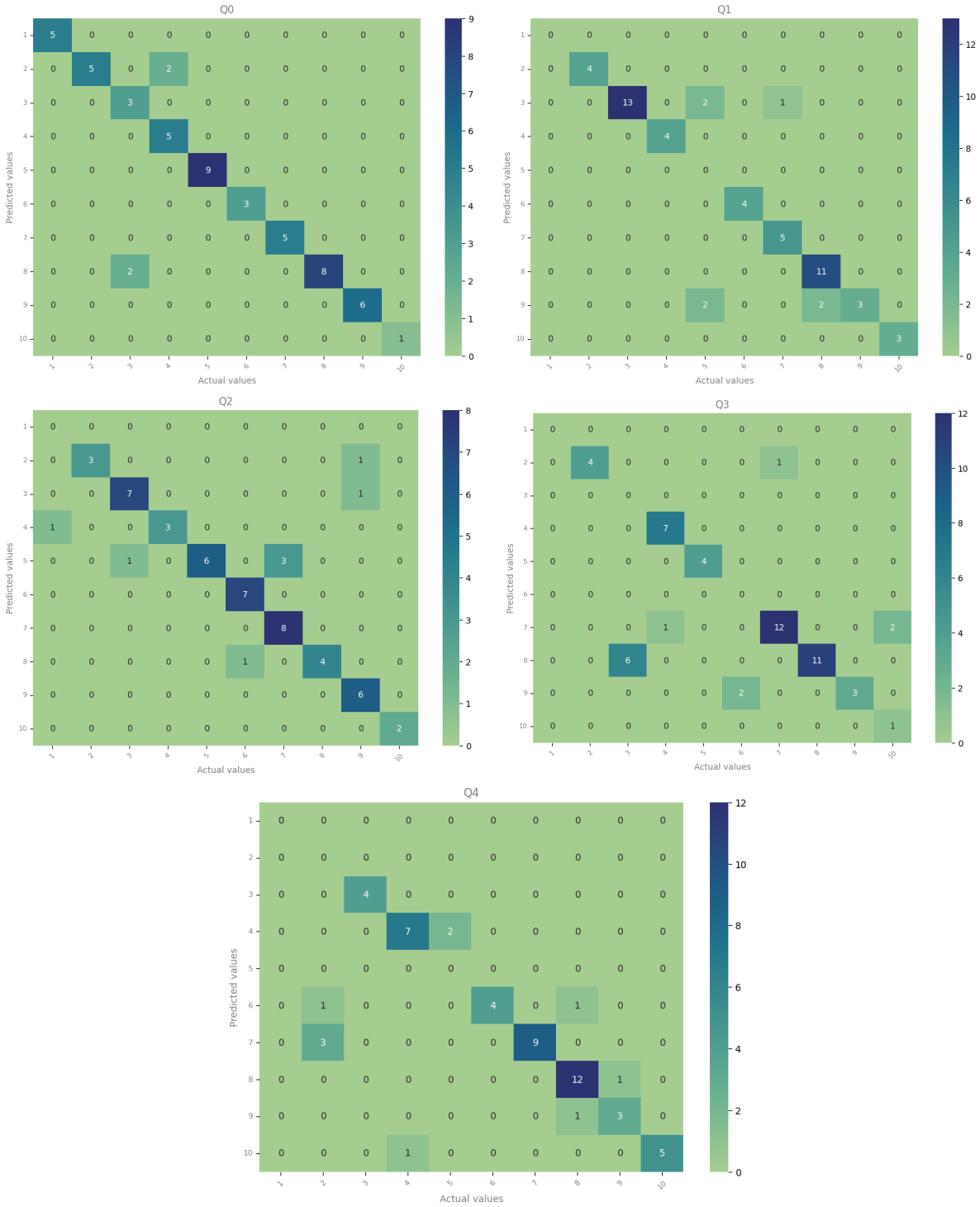

Source: Prepared by the author

According to the figure above, most of the results are located along the main diagonals of the matrices, albeit with some points falling outside of them. While this may initially seem negative, as the network failed to estimate these values, controlling for this effect is important to avoid training a network that is overly constrained to only predict the values present in the training dataset: An overfitted one.

Finally, to conduct the last validation, the final trained networks were used to predict the values from the test data package. The results are presented in Figure 57, where a sizable portion of the results align with the main diagonals, as anticipated.

Figure 57 – Confusion matrices for the final DNNs: Testing

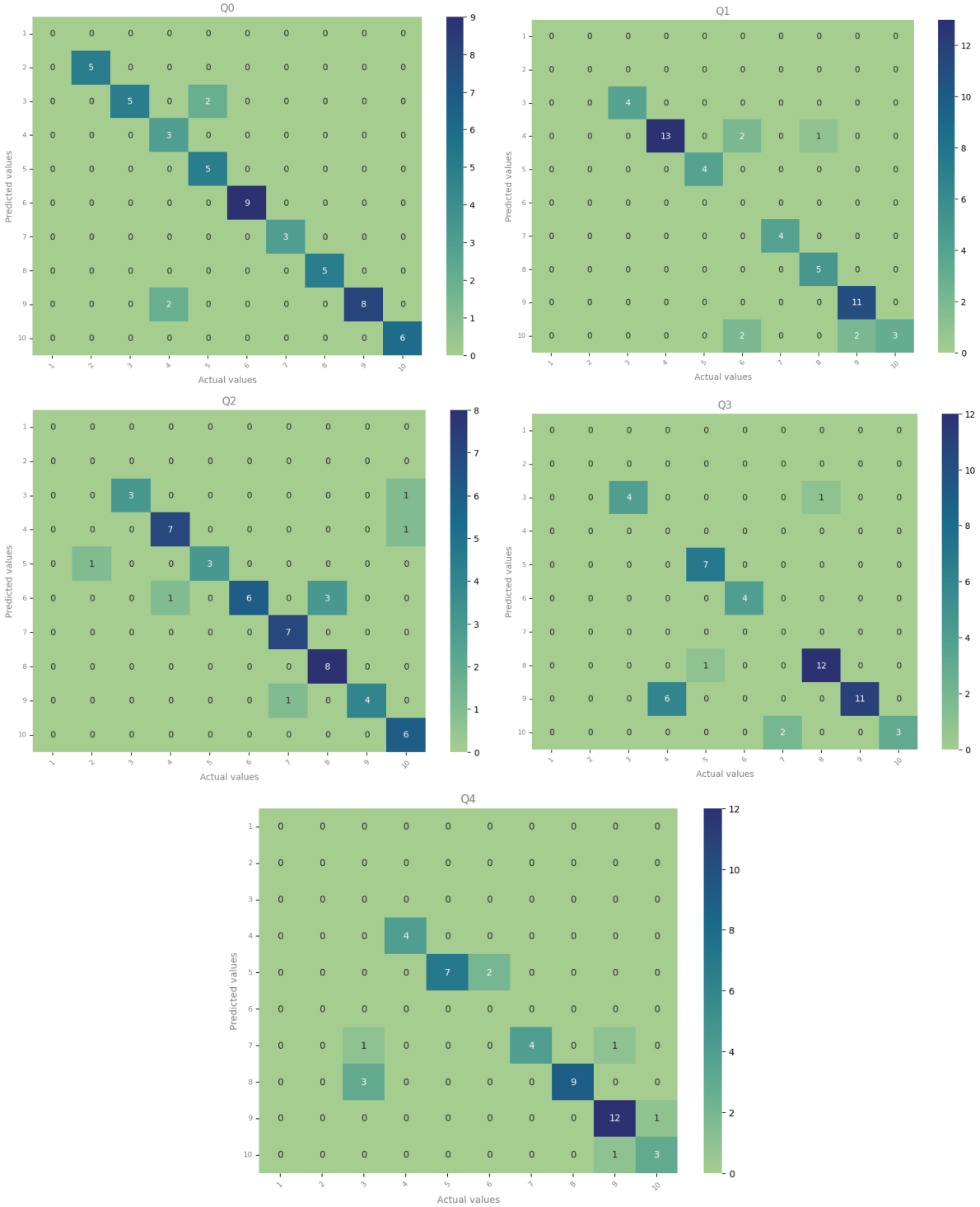

Source: Prepared by the author

Summarizing, after the data augmentation process, this work's methodology can be updated with the steps in Figure 58.

Figure 58 – Sequential process of data generation and neural network training

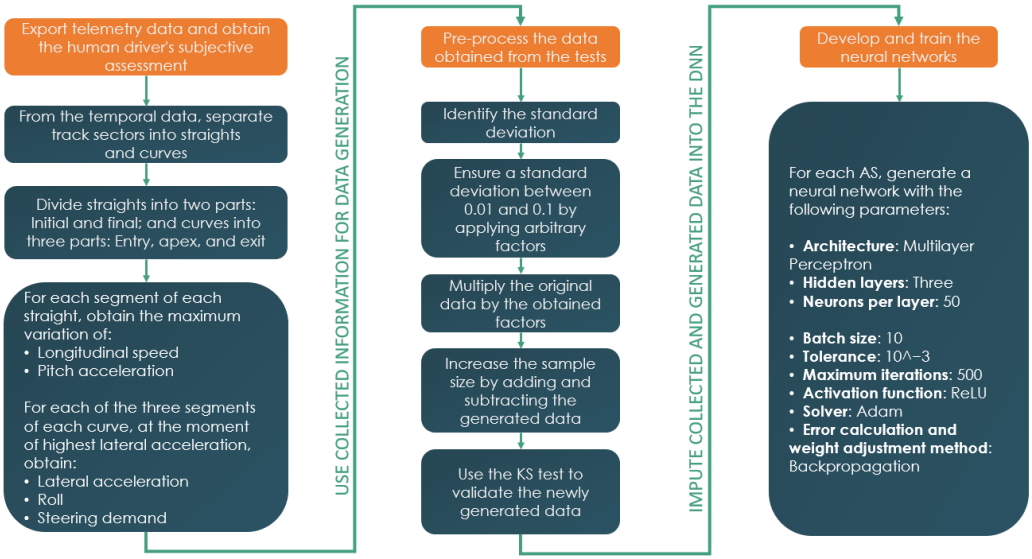

Source: Prepared by the author

As outlined at the beginning of this text, the assessment of a vehicle's dynamic behavior in virtual simulators traditionally requires the involvement of an experienced driver. However, with the implementation of the workflow presented in the figure above, this requirement is effectively eliminated. Moreover, evaluations conducted under such conditions tend to be significantly influenced by the driver's subjectivity: Nevertheless, this methodology herein addresses this limitation by mitigating individual driver preferences within the evaluation system.

Given the increasing adoption of driving simulators within the automotive industry, the proposed methodology enhances the accuracy of vehicle model classification while simultaneously reducing simulation time and costs; thereby streamlining the overall vehicle development process.

5 CONCLUSIONS

Under the aim of evaluating vehicle dynamic behaviors in subjective driver experiences based on objective metrics, the present work successfully achieves its goal by a methodology capable of directing the expected results. By leveraging deep neural networks within a dynamic driver-in-the-loop vehicle simulator, this system bridges the gap between driver perceptions and measurable data.

The DNNs developed in this work have shown a remarkable ability to standardize vehicle ratings across drivers with varying levels of experience, which is a critical achievement as it minimizes the inherent subjectivity that different drivers bring to vehicle evaluations. By focusing on objective metrics such as vehicle stability during turns, the network consistently assigned scores from one to ten to vehicles, in five distinct categories, regardless of individual driver perceptions or preferences.

Moreover, a significant contribution of this study is the possibility of combining a data generation algorithm with DNN configurations capable of upgrading the mean accuracy of the results from less than 25% to almost 90%. Consequently, this broadens the range of evaluators and increases the efficiency of vehicle assessments without compromising the quality of results.

As a result, the reduction in both development time and project costs is another key benefit demonstrated by this research: Through the automation of subjective evaluations, the time required to fine-tune vehicle models can be significantly reduced. Quantifying this advantage, the estimated operation cost for this kind of simulator is currently about one thousand euros per hour.

Simultaneously, the discussion presented here was only made possible by the ability to work with specific parameters to understand driver-vehicle interactions. In other words, meaningful results were achieved by adjusting vehicle parameters directly correlated with what drivers were expected to perceive regarding the vehicle's dynamic behavior. While tests conducted with a virtual driver validated the expected behaviors, the relationship was not as straightforward when the subjective perspectives of human drivers came into play.

The influence of driver subjectivity became evident during the scoring of the models. At this stage, volunteers with differing vehicle driving style preferences assigned widely varying scores within the same category. Additionally, a systematic review of studies utilizing driver perceptions in simulated environments underscored the significant impact of human behavior on testing outcomes and provided insights on how to address this challenge.

In this context, the application of data science and artificial intelligence tools proved essential for the success of the proposed methodology. While the most intuitive conclusion was the feasibility of evaluating vehicle behavior in a satisfactory manner using deep neural networks, the methods employed to preprocess and optimize the data significantly enhanced the networks’ accuracy.

Summarizing, this research presents a robust and scalable approach to vehicle evaluation by correlating subjective experiences with objective data. In other words, the developed system has the potential to make vehicle handling assessments more efficient, cost-effective, and consistent, fostering innovation in Automotive Engineering.

For future research, it is suggested to define new evaluation classes for vehicles, focusing on parameters not only related to the vehicles' handling but also comfort. In parallel, exploring the combination of DNN with other AI techniques, such as reinforcement learning, could open new possibilities for automating and optimizing vehicle evaluation processes.

REFERENCES

ABE, M. *Vehicle handling dynamics: theory and application*. [S.l.]: Butterworth-Heinemann, 2015.

ALBERINI, C.; CAPITANELLI, R.; VITA, S. F. A numerical study of a degenerate diffusion equation driven by a Heaviside function. *Computers & Mathematics with Applications*, v. 89, p. 139–149, 2021.

ALI, K. H.; MAJEED, F. A. A. Investigation of Vertical and Pitch Road Vehicle Dynamic Responses to Improve the Critical Speed Using Controllable Semi-Active PID Suspensions. *Association of Arab Universities Journal of Engineering Sciences*, v. 25, n. 2, p. 103–112, 2018.

ALMEIDA, D. *Dimensionamento cinemático e dinâmico de suspensão duplo A*. 2012. 1–83 f. BSc – Universidade de Brasília, Brasília, 2012.

ALZUBI, J. A. Bipolar fully recurrent deep structured neural learning based attack detection for securing industrial sensor networks. *Transactions on Emerging Telecommunications Technologies*, v. 32, n. 7, p. e4069, 2021.

AO, D. *et al.* Analysis of Co-Relation Between Objective Measurement and Subjective Assessment for Dynamic Comfort of Vehicles. *International Journal of Automotive Technology*, v. 21, n. 6, p. 1553–1567, 12 dez. 2020.

AO, D.; LI, J. Subjective assessment for an advanced driver assistance system: a case study in China. *Journal of Intelligent and Connected Vehicles*, v. 5, n. 2, p. 112–122, 17 maio 2022.

ARAB, A.; YI, J. Instructed Reinforcement Learning Control of Safe Autonomous J-Turn Vehicle Maneuvers. 12 jul. 2021, [S.l.]: IEEE, 12 jul. 2021. p. 1058–1063.

ASH, H. *Correlation of Subjective and Objective Handling of Vehicle Behaviour*. 2002. 1–207 f. PhD – University of Leeds, Leeds, 2002.

ASSEGIE, T. A. *et al.* Evaluation of feature scaling for improving the performance of supervised learning methods. *Bulletin of Electrical Engineering and Informatics*, v. 12, n. 3, p. 1833–1838, 1 jun. 2023.

AZMAN, M.; KING, P. D.; RAHNEJAT, H. Combined bounce, pitch, and roll dynamics of vehicles negotiating single speed bump events. *Proceedings of the Institution of Mechanical Engineers, Part K: Journal of Multi-body Dynamics*, v. 221, n. 1, p. 33–40, 2007.

BAKER, C.; ZHU, V.; ROSENBAUM, R. Nonlinear stimulus representations in neural circuits with approximate excitatory-inhibitory balance. *PLoS computational biology*, v. 16, n. 9, p. e1008192, 2020.

BARTLETT, P. L. *et al.* Benign overfitting in linear regression. *Proceedings of the National Academy of Sciences*, v. 117, n. 48, p. 30063–30070, 2020.

BAU, D. *et al.* Understanding the role of individual units in a deep neural network. *Proceedings of the National Academy of Sciences*, v. 117, n. 48, p. 30071–30078, dez. 2020.

BENGIO, Y. Practical recommendations for gradient-based training of deep architectures. *Computer Science: Machine Learning.10.48550/arXiv.1206.5533*, 2012.

BHOSALE, D. *et al.* To Study the Influence of Variation in Camber and Toe on Handling of Passenger Vehicle during Cornering. 2019, Warrendale: Society of Automotive Engineers, 2019.

BILBAO, I.; BILBAO, J. Overfitting problem and the over-training in the era of data: Particularly for Artificial Neural Networks. 2017, [S.l: s.n.], 2017. p. 173–177.

BÎNDAC, I.-M. *et al.* Theoretical and experimental research on the double lane change maneuver. *MATEC Web of Conferences*, v. 373, p. 00054, 20 dez. 2022.

BISWAL, A. S. Design and Optimization of the Steering System of a Formula SAE Car Using Solidworks and Lotus Shark. 2016, [S.l: s.n.], 2016.

BITENCOURT, R. *Simulação em tempo real e correlação da dinâmica automotiva em manobras livres em pista de teste*. 2016. Programa de Pós-Graduação em Engenharia Mecânica, Pontifícia Universidade Católica de Minas Gerais, Belo Horizonte, 2016.

BONERA, E. *et al.* On the Influence of Suspension Geometry on Steering Feedback. *Applied Sciences*, v. 10, n. 12, p. 4297, 23 jun. 2020.

BROWNLEE, J. *Machine learning mastery with python*. [S.l.]: Machine Learning Mastery Pty Ltd, 2016.

BRUSCHETTA, M.; MINEN, D. Advanced features to make Dynamic Driving Simulators suitable for studies on Assisted and Autonomous Driving. *Assisted and autonomous driving on driving simulators*. [S.l.]: Springer, 2019. .

CARVALHO, M.; FARIA, M. Análise por elementos finitos de mangas de eixo de suspensão automotiva sob carregamento cíclico. 2010, Rio de Janeiro: ABCM, 2010.

CHABAAN, R. C.; WANG. Control of electrical power assist systems: H-infinity design, torque estimation and structural stability. *JSAE review*, v. 22, n. 4, p. 435–444, 2001.

CHOLLET, F. *Deep Learning with Python*. Shelter Island: Manning Publications Co., 2018.

COSTA, G. *Autopédia: os vários tipos de suspensões*. . [S.l: s.n.]. Disponível em: <http://performancetrends.com/Definitions/Wheel-Rate.htm>. , 2020

D BASTOW G HOWARD, J. P. W. *Car Suspension and Handling*. Londres: Pentech Press Limited, 2004. v. 2.

DA LIO, M.; BORTOLUZZI, D.; ROSATI PAPINI, G. PIETRO. Modelling longitudinal vehicle dynamics with neural networks. *Vehicle System Dynamics*, v. 58, n. 11, p. 1675–1693, 2020a.

DA LIO, M.; BORTOLUZZI, D.; ROSATI PAPINI, G. PIETRO. Modelling longitudinal vehicle dynamics with neural networks. *Vehicle System Dynamics*, v. 58, n. 11, p. 1675–1693, 1 nov. 2020b.

DA ROCHA, D. A. *Classificação do grau de retinopatia diabética e segmentação de lesões em imagens de retina usando Redes Neurais convolucionais* . 2021. 1–66 f. Master – Pontifícia Universidade Católica de Minas Gerais, 2021.

DA SILVA, R. R. *Projeto de controladores para um sistema de direção elétrica utilizando a metodologia de projeto baseado em modelos*. 2017. Faculdade de Tecnologia, Universidade de Brasília, Brasilia, 2017.

DATTA, L. A survey on activation functions and their relation with xavier and he normal initialization. *arXiv preprint arXiv:2004.06632*, 2020.

DE CARVALHO PINHEIRO, H. *et al.* Torque Vectoring in Electric Vehicles with In-wheel Motors. [S.l: s.n.], 2019. p. 3127–3136.

DE NALDA TÁRREGA, V. *et al.* Human Autonomous Vehicle (HAV): From sickness prevention to emotional response. 2022, [S.l: s.n.], 2022.

DELL'ANNUNZIATA, G. N. *et al.* Estimation of Vehicle Longitudinal Velocity with Artificial Neural Network. *Sensors*, v. 22, n. 23, p. 9516, 6 dez. 2022.

DERRIX, D.; PROKOP, G. Experimental Analysis of the Influence of Body Stiffness on Drivability and Dynamic Body Behavior with On-Road Experiments. *SAE International Journal of Vehicle Dynamics, Stability, and NVH*, v. 6, n. 3, p. 10- 06- 03–0019, 3 jun. 2022.

DHAMODHARAN, P.; MOHAMED RAAFIQ, N.; MADHU, S. A review paper on multilink suspension mechanism with compliant joints. *Int. J. Appl. Eng. Res*, v. 10, n. 33, p. 25491–25493, 2015.

DIAS, C. *Análise da taxa de esterçamento de um modelo automotivo correlacionado em K&C em um simulador driver-in-the-loop*. 2021. 1–135 f. MSc – Pontifícia Universidade Católica de Minas Gerais, Belo Horizonte, 2021.

DIAS, C. *et al.* Braking system analysis with the aid of a dynamic vehicle simulator with nine degrees of freedom. *Australian Journal of Mechanical Engineering*, p. 1–10, 17 abr. 2024.

DIAS, C. A. R. *et al.* Steering ratio analysis in a vehicle dynamics simulator using a kinematics and compliance correlated model. 26 mar. 2021, [S.l: s.n.], 26 mar. 2021.

DIAS, C. A. R.; JÚNIOR, J. L. *Review of the dual-axis steering system used by Mercedes-AMG in Formula One*. . [S.l: s.n.], 2022.

DIAS, C. A. R.; LANDRE JR, J. Practical recommendations for gradient-based training of deep architectures. p. 1–14, 2024.

DIAS, C. A. R.; LANDRE JÚNIOR, J. The use of artificial intelligence in driver-in-the-loop simulation: a literature review (2023). *Australian Journal of Mechanical Engineering*, p. 1–9, 21 set. 2023.

DIAS, C.; LANDRE, J. Vehicle dynamics response due to the adjustment of K&C parameters with the aid of a dynamic simulator with 9 DOF and a correlated virtual model. *Proceedings of the Institution of Mechanical Engineers, Part D: Journal of Automobile Engineering*, p. 095440702211100, 12 jul. 2022.

DIAS, C.; LANDRE, J. Vehicle dynamics response due to the adjustment of K&C parameters with the aid of a dynamic simulator with 9 DOF and a correlated virtual model. *Proceedings of the Institution of Mechanical Engineers, Part D: Journal of Automobile Engineering*, v. 237, n. 10–11, p. 2616–2631, 12 set. 2023.

DINIZ, D. *Estudo da dinâmica vertical em suspensão duplo a de um veículo off-road tipo baja*. 2014. 1–134 f. MSc – Universidade Federal de Campina Grande, Campina Grande, 2014.

DUTTA, S.; CHOI, S.-M.; CHOI, S.-B. A new adaptive sliding mode control for Macpherson strut suspension system with magneto-rheological damper. *Journal of Intelligent Material Systems and Structures*, v. 27, n. 20, 28 dez. 2016.

ELMADANY, M. M.; DOKAINISH, M. A.; ALLAN, A. B. Ride dynamics of articulated vehicles–a literature survey. *Vehicle system dynamics*, v. 8, n. 4, p. 287–316, 1979.

ESMAEILI, N.; KAZEMI, R.; TABATABAEI OREH, S. H. An adaptive sliding mode controller for the lateral control of articulated long vehicles. *Proceedings of the Institution of Mechanical Engineers, Part K: Journal of Multi-body Dynamics*, v. 233, n. 3, p. 487–515, 4 set. 2019.

FALLAH, M. S.; BHAT, R.; XIE, W.-F. H-infinity robust control of semi-active Macpherson suspension system: new applied design. *Vehicle System Dynamics*, v. 48, n. 3, p. 339–360, 2010.

FANG, X.; TAN, K. Efficient concept design of twist beam rear axles. *ATZ worldwide*, v. 117, n. 1, p. 24–29, 2015.

FARRONI, F.; SAKHNEVYCH, A. Tire multiphysical modeling for the analysis of thermal and wear sensitivity on vehicle objective dynamics and racing performances. *Simulation Modelling Practice and Theory*, v. 117, p. 102517, maio 2022.

FCA PRESS. *FCA inaugurates first Latin American vehicle dynamics simulation center*.

FEIZIZADEH, B. *et al.* A deep learning convolutional neural network algorithm for detecting saline flow sources and mapping the environmental impacts of the Urmia Lake drought in Iran. *Catena*, v. 207, p. 105585, 2021.

FERRARIS, A. *et al.* All-Wheel Drive Electric Vehicle Performance Optimization: From Modelling to Subjective Evaluation on a Static Simulator. out. 2019, [S.l.]: IEEE, out. 2019. p. 1–6.

GÉRON, A. *Hands-On Machine Learning with Scikit-Learn and TensorFlow*. Sebastopol: O'Reilly Media, Inc., 2017.

GIL GÓMEZ, G. L. *et al.* Machine learning to classify and predict objective and subjective assessments of vehicle dynamics: the case of steering feel. *Vehicle System Dynamics*, v. 56, n. 1, p. 150–171, 2 jan. 2018.

GILLESPIE, T. D. *Fundamentals of Vehicle Dynamics*. Warrendale, PA: SAE International, 1992.

GOBBI, M.; MASTINU, G.; PREVIATI, G. Farm tractors with suspended front axle: Anti-dive and anti-lift characteristics. *Journal of Terramechanics*, v. 56, p. 157–172, 2014.

GRABA, M. *et al.* Impact of the acceleration intensity of a passenger car in a road test on energy consumption. *Energy*, v. 226, p. 120429, jul. 2021.

GUASTADISEGNI, G. *et al.* Ride analysis tools for passenger cars: objective and subjective evaluation techniques and correlation processes – a review. *Vehicle System Dynamics*, p. 1–27, 13 out. 2023.

GUE, I. H. V *et al.* Artificial neural networks for sustainable development: a critical review. *Clean Technologies and Environmental Policy*, p. 1–17, 2020.

HAPPIAN-SMITH, J. *An introduction to modern vehicle design*. [S.l.]: Elsevier, 2001.

HEISSING, B.; ERSOY, M. *Chassis handbook: fundamentals, driving dynamics, components, mechatronics, perspectives*. [S.l.]: Springer Science & Business Media, 2010.

ILIE, F.; CRISTESCU, A.-C. Experimental Study of the Correlation between the Wear and the Braking System Efficiency of a Vehicle. *Applied Sciences*, v. 13, n. 14, p. 8139, 13 jul. 2023.

INTERNATIONAL ORGANIZATION FOR STANDARDIZATION. *ISO 3888-2: Passenger cars - Test track for a severe lane-change manoeuvre - Part 2: Obstacle avoidance*. . [S.l: s.n.]. , 2011

INTERNATIONAL ORGANIZATION FOR STANDARDIZATION. *ISO 4138/2012: Passenger cars — Steady-state circular driving behaviour — Open-loop test methods*. *International Organization for Standardization*. [S.l: s.n.]. , 2012

IWANA, B. K.; UCHIDA, S. An empirical survey of data augmentation for time series classification with neural networks. *PLOS ONE*, v. 16, n. 7, p. e0254841, 15 jul. 2021.

JACKSON, D. A.; GLICKMAN, S. L.; DALE JR, J. L. *Method and system for measuring caster trail*. . [S.l.]: Google Patents. , dez. 2003

JAMBUKAR, S.; CHANDRAMOHAN, S. *Effects of Kingpin Inclination and Caster Angle on Kinematics and Lateral Dynamics of Long Wheelbase School Bus*. . [S.l: s.n.], 2019.

JAMES, S. S.; ANDERSON, S. R.; DA LIO, M. Longitudinal vehicle dynamics: A comparison of physical and data-driven models under large-scale real-world driving conditions. *IEEE Access*, v. 8, p. 73714–73729, 2020.

JAMSON, A. *Motion cueing in driving simulators for research applications*. 2010. PhD. Thesis – University of Leeds, Leeds, 2010.

JANARTHANAM, B.; GHODEKAR, S. K.; APTE, A. A. *Virtual development of optimum twist beam design configuration for a new generation passenger car*. . [S.l: s.n.], 2007.

JAZAR, R. N. *Vehicle dynamics: theory and application*. [S.l.]: Springer, 2017.

JONES, I. S.; KORDING, K. P. Can single neurons solve mnist? the computational power of biological dendritic trees. *arXiv preprint arXiv:2009.01269*, 2020.

JR, W. P. C.; LOSEKANN, C. R. *Eixo Temático: Sistema de suspensões*. Florianópolis: CEFET/SC, 2003. v. 1.

KAMBLE, S. S.; GUNASEKARAN, A.; GAWANKAR, S. A. Sustainable Industry 4.0 framework: A systematic literature review identifying the current trends and future perspectives. *Process Safety and Environmental Protection*, v. 117, p. 408–425, 2018.

KATZ, J.; GARCIA, D. Aerodynamic effects of Indy car components. *SAE Transactions*, p. 2322–2330, 2002.

KHAYYAM, H. *et al.* A novel hybrid machine learning algorithm for limited and big data modeling with application in industry 4.0. *IEEE access*, v. 8, p. 111381–111393, 2020.

KIM, D. *et al.* Design of a Human Evaluator Model for the Ride Comfort of Vehicle on a Speed Bump Using a Neural Artistic Style Extraction. *Sensors*, v. 19, n. 24, 2019a.

KIM, D. *et al.* Design of a Human Evaluator Model for the Ride Comfort of Vehicle on a Speed Bump Using a Neural Artistic Style Extraction. *Sensors*, v. 19, n. 24, p. 5407, 8 dez. 2019b.

KIM, G. *et al.* Study on durability and reliability of strut type suspension noise based on experimental methods. *Journal of mechanical science and technology*, v. 26, n. 1, p. 21–29, 2012.

KIM, J.-H.; SONG, J.-B. Control logic for an electric power steering system using assist motor. *Mechatronics*, v. 12, n. 3, p. 447–459, 2002.

KLOCKE, F. *et al.* Simplified life cycle assessment of a hybrid car body part. *Procedia CIRP*, v. 15, p. 484–489, 2014.

KOUTSOUKAS, A. *et al.* Deep-learning: investigating deep neural networks hyper-parameters and comparison of performance to shallow methods for modeling bioactivity data. *Journal of cheminformatics*, v. 9, n. 1, p. 1–13, 2017.

KRÖNK, M. *Camber & Toe*. . [S.l: s.n.]. Disponível em: <https://virtualracingschool.com/academy/iracing-career-guide/setups/camber-toe/>. , 2017

KUMAR, A. *et al.* Prediction of Drivers' Subjective Evaluation of Vehicle Reaction Under Aerodynamic Excitations. *Human Factors: The Journal of the Human Factors and Ergonomics Society*, p. 001872082311579, 20 fev. 2023.

LANEVE, R. *Traction Control System development for an AWD hybrid vehicle*. 2020. Dipartimento di Ingegneria Meccanica e Aerospaziale, Politecnico di Torino, Torino, 2020.

LEAL, V. *Estudo cinemático de suspensões veiculares do tipo eixo de torção*. 2007. Programa de Pós-Graduação em Engenharia Mecânica, Pontifícia Universidade Católica de Minas Gerais, Belo Horizonte, 2007.

LEDWABA, R. *Demystifying the Fourth Industrial Revolution. Available in <https://www.gfpafoundation.org/aviation-aerospace-news/industry-news/78-demystifying-the-fourth-industrial-revolution>*.

LELEDAKIS, A. *mploying Optimization in CAE Vehicle Dynamics*. 2014. Programa de Pós-Graduação em Engenharia Mecânica, Technical University of Crete School of Production Engineering & Management, Göteborg, 2014.

LIU-HENKE, X. *et al.* Driving-Simulator-in-the-Loop — Virtual Function Design with Consideration of Human Behaviour. 12 out. 2020, [S.l.]: IEEE, 12 out. 2020. p. 1–6.

LÖCKEL, S. *et al.* Identification and modelling of race driving styles. *Vehicle System Dynamics*, v. 60, n. 8, p. 2890–2918, 3 ago. 2022.

LUCAS, G. *et al.* A simulation sickness study on a driving simulator equipped with a vibration platform. *Transportation Research Part F: Traffic Psychology and Behaviour*, v. 68, p. 15–22, jan. 2020.

MACFARLANE, A. *Modular Electric Automatic Guided Vehicle Suspension-Drive Unit*. 2016. Built Environment & Information Technology Department, Nelson Mandela Metropolitan University, Port Elizabeth, 2016.

MAHARANA, K.; MONDAL, S.; NEMADE, B. A review: Data pre-processing and data augmentation techniques. *Global Transitions Proceedings*, v. 3, n. 1, p. 91–99, jun. 2022.

MANCA, R. *Design and implementation of an Electric Power Steering system for a Formula Student Driverless vehicle*. 2020. 1–85 f. Masters – Politecnico di Torino, Torino, 2020.

MARINKOVIĆ, Z. *et al.* A review on the artificial neural network applications for small-signal modeling of microwave FETs. *International Journal of Numerical Modelling: Electronic Networks, Devices and Fields*, v. 33, n. 3, 6 maio 2020.

MARQUES, F. *et al.* Modeling and analysis of friction including rolling effects in multibody dynamics: a review. *Multibody System Dynamics*, v. 45, n. 2, 22 fev. 2019.

MASSARO, M.; LIMEBEER, D. J. N. Minimum-lap-time optimisation and simulation. *Vehicle System Dynamics*, v. 59, n. 7, p. 1069–1113, 3 jul. 2021.

MCCULLOCH, W. S. a. P., WH (1943)." A logical calculus of the ideas immanent in nervous activity.". *Bulletin of Mathematical Biophysics*, v. 5, n. 115–133, 1943.

MENG, J.; DASGUPTA, A. MEMS Packaging Reliability in Board-Level Drop Tests Under Severe Shock and Impact Loading Conditions—Part II: Fatigue Damage Modeling. *IEEE Transactions on Components, Packaging and Manufacturing Technology*, v. 6, n. 11, p. 1604–1614, nov. 2016.

MILLIKEN, W.; MILLIKEN, D. *Chassis Design: Principles and Analysis*. Warrendale: Society of Automotive Engineers, 2002.

MURRAY, M.; ABROL, V.; TANNER, J. Activation function design for deep networks: linearity and effective initialisation. *arXiv preprint arXiv:2105.07741*, 2021.

NEVES, E. *Análise da dinâmica veicular e motion cueing para um simulador veicular dinâmico de 9 GDL*. 2018. Programa de Pós-Graduação em Engenharia Mecânica, Pontifícia Universidade Católica de Minas Gerais, Belo Horizonte, 2018.

NHU, V.-H. *et al.* Effectiveness assessment of Keras based deep learning with different robust optimization algorithms for shallow landslide susceptibility mapping at tropical area. *Catena*, v. 188, p. 104458, 2020.

NI, J.; HU, J.; XIANG, C. Robust Control in Diagonal Move Steer Mode and Experiment on an X-by-Wire UGV. *IEEE/ASME Transactions on Mechatronics*, v. 24, n. 2, p. 572–584, abr. 2019.

NOVI, T. *et al.* Real-time control for at-limit handling driving on a predefined path. *Vehicle System Dynamics*, v. 58, n. 7, p. 1007–1036, 2 jul. 2020.

ÖZCAN, D.; SÖNMEZ, Ü.; GÜVENÇ, L. Optimisation of the nonlinear suspension characteristics of a light commercial vehicle. *International Journal of Vehicular Technology*, v. 2013, 2013.

OZTEMEL, E.; GURSEV, S. Literature review of Industry 4.0 and related technologies. *Journal of Intelligent Manufacturing*, v. 31, n. 1, p. 127–182, 2020.

PACEJKA, H. B. *Tyre and vehicle dynamics, Elseiver Butterworth*. [S.l.]: Heinemann, 2006.

PAGLIARECCI, N. *et al.* Test methodology for the vehicle-tire handling performance evaluation: objectification of driver's subjective assessment. *IFAC-PapersOnLine*, v. 53, n. 2, p. 14394–14400, 2020.

PARRA, A. *et al.* Modelling and Validation of Full Vehicle Model based on a Novel Multibody Formulation. out. 2019, [S.l.]: IEEE, out. 2019. p. 675–680.

PASZKIEL, S. The Use of Facial Expressions Identified from the Level of the EEG Signal for Controlling a Mobile Vehicle Based on a State Machine. [S.l: s.n.], 2020. p. 227–238.

PAUCA, G.-S.; CARUNTU, C.-F. MPC-Based Dynamic Velocity Adaptation in Nonlinear Vehicle Systems: A Real-World Case Study. *Electronics*, v. 13, n. 15, p. 2913, 24 jul. 2024.

PENG, H.; EISELE, D. D. Vehicle dynamics control with rollover prevention for articulated heavy trucks. 2000, [S.l: s.n.], 2000.

PICCAROZZI, M.; AQUILANI, B.; GATTI, C. Industry 4.0 in management studies: A systematic literature review. *Sustainability*, v. 10, n. 10, p. 3821, 2018.

PINTO, L. M. B. *Redes neurais artificiais para o monitoramento do acúmulo de danos em ativos*. 2019. Programa de Pós-Graduação em Engenharia Mecânica, Pontifícia Universidade Católica de Minas Gerais, Belo Horizonte, 2019.

PULVERMÜLLER, F. *et al.* Biological constraints on neural network models of cognitive function. *Nature Reviews Neuroscience*, p. 1–15, 2021.

PURUSHOTHAM, A. Comparative simulation studies on MacPherson suspension system. *International Journal of Modern Engineering Research (IJMER)*, v. 3, n. 3, p. 1377–1381, 2013.

QUEZADA, V.; NICOLAS, M. *Comprehensive Assessmentof Comfort (Motion Sickness) in Vehicles.* 2024. Examensarbete för masterexamen - Master's Thesis – Chalmers University of Technology, Gothenborg, 2024.

RAABE, J. *et al.* Contribution to the Objective Evaluation of Combined Longitudinal and Lateral Vehicle Dynamics in Nonlinear Driving Range. *SAE International Journal of Vehicle Dynamics, Stability, and NVH*, v. 7, n. 4, p. 10- 07- 04–0034, 19 out. 2023.

RAI, R. *et al.* Machine learning in manufacturing and industry 4.0 applications. *International Journal of Production Research*, 2021.

RAKHMATOV, R.; BOKAREV, A.; MARTYNOV, E. Method of Improvement of Vehicle Vibroacoustic (NVH) Comfort When Crossing Single Irregularities. [S.l: s.n.], 2024. p. 195–218.

REDDY, K. V. *et al.* A comprehensive kinematic analysis of the double wishbone and MacPherson strut suspension systems. *Mechanism and Machine Theory*, v. 105, p. 441–470, 2016.

REIMPELL, J.; STOLL, H.; BETZLER, J. *The automotive chassis: engineering principles*. [S.l.]: Elsevier, 2001.

RIBEIRO, M. M. *Comparação entre um sistema PID e um sliding mode control para o controle de estabilidade aplicado a um simulador de din veicular*. 2019. Programa de Pós-Graduação em Engenharia Mecânica, Pontifícia Universidade Católica de Minas Gerais, Belo Horizonte, 2019.

RYU, Y. I. *et al.* Development of analytical process to reduce side load in strut-type suspension. *Journal of mechanical science and technology*, v. 24, n. 1, p. 351–356, 2010.

SAE INTERNATIONAL. *J266_199601: Steady-State Directional Control Test Procedures for Passenger Cars and Light Trucks*. *SAE International*. [S.l: s.n.]. , 1996

SAIFIA, D. *et al.* Fuzzy control for electric power steering system with assist motor current input constraints. *Journal of the Franklin Institute*, v. 352, n. 2, p. 562–576, 2015.

SANDU, C.; ANDERSEN, E. R.; SOUTHWARD, S. Multibody dynamics modelling and system identification of a quarter-car test rig with McPherson strut suspension. *Vehicle System Dynamics*, v. 49, n. 1–2, p. 153–179, 2011.

SARKER, I. H. Deep cybersecurity: a comprehensive overview from neural network and deep learning perspective. *SN Computer Science*, v. 2, n. 3, p. 1–16, 2021.

SCHURMANN, R. *et al.* Objectification and prediction of the subjective criticality of axle damages using artificial neural networks as well as multibody- and real-time simulations. *International Journal of Vehicle Performance*, v. 9, n. 4, p. 376–403, 2023.

SCHWARK, J. *et al.* An Investigation of Operator Performance in All-terrain Vehicle (ATV) Handling and Control. *Procedia Manufacturing*, v. 3, 2015.

SCHWARZSCHILD, A. *et al.* Can You Learn an Algorithm? Generalizing from Easy to Hard Problems with Recurrent Networks. *arXiv preprint arXiv:2106.04537*, 2021.

SCIKIT. *Documentation: Scikit. Available at <https://scikit-learn.org/stable/modules/generated/>*.

SEREDYNSKI, P. *Multimatic opening new Michigan virtual vehicle-dynamics development center*.

SERJE, D.; ACUÑA, E. Driving and Flying Simulators: A Review on Relevant Considerations and Trends. *Transportation Research Record: Journal of the Transportation Research Board*, v. 2676, n. 3, p. 551–570, 30 mar. 2022.

SHAIKH, I. J.; PARVEZ, M. S.; SHAKEBUDDIN, M. A literature review on collapsible steering column. *International Journal for Innovative Research in Science & Technology*, v. 2, n. 5, 2015.

SHAO, Y. *et al.* Evaluation method of handling and stability performance of special vehicle with large inertia based on the combination method of rank correlation coefficient. 2018.

SHEAHAN, H. *et al.* Neural state space alignment for magnitude generalization in humans and recurrent networks. *Neuron*, v. 109, n. 7, p. 1214–1226, 2021.

SHIM, T.; GHIKE, C. Understanding the limitations of different vehicle models for roll dynamics studies. *Vehicle system dynamics*, v. 45, n. 3, p. 191–216, 2007.

SKRICKIJ, V. *et al.* Improving Vehicle Stability and Comfort through Active Corner Positioning. 9 abr. 2024, [S.l: s.n.], 9 abr. 2024.

SOCIETY OF AUTOMOTIVE ENGINEERS. *SAE J 1441-2016: Subjective Rating Scale For Vehicle Ride And Handling*. *Society of Automotive Engineers*. SAE J 1441-2016: [s.n.]. , 2016

SONG, H.; MONTENEGRO-MARIN; ENRIQUE, C. Secure prediction and assessment of sports injuries using deep learning based convolutional neural network. *Journal of Ambient Intelligence and Humanized Computing*, v. 12, n. 3, p. 3399–3410, 2021.

SONY, M.; NAIK, S. Key ingredients for evaluating Industry 4.0 readiness for organizations: a literature review. *Benchmarking: An International Journal*, 2019.

SORRENTINO, V. *Development of a torque-vectoring logic for a hybrid vehicle*. 2020. Corso di Laurea Magistrale in Ingegneria Meccanica, Politecnico di Torino, Torino, 2020.

SPERINGER, M.; SCHNELZER, J. *Differentiation of Industry 4.0 Models. The 4th Industrial Revolution from different Regional Perspectives in the Global North and Global South*. . [S.l: s.n.], 2019.

STERTHOFF, J.; HENZE, R.; KÜÇÜKAY, F. Vehicle handling improvements through Steer-by-Wire. *Automotive and Engine Technology*, v. 6, n. 1–2, p. 91–98, 6 jun. 2021.

STRUBLE, D.; STRUBLE, J. *Automotive Accident Reconstruction: Practices and Principles*. Second ed. Boca Raton: CRC Press, 2020.

SUGIURA, H. *et al. Trailing twist axle suspension design using ADAMS*. . [S.l: s.n.], 2000.

SUH, K.-H.; LEE, Y.-K.; YOON, H.-S. *Optimization of Front Bump Steer Using Design of Experiments*. . [S.l: s.n.], 2000.

SUN, X. *et al.* Piecewise affine modeling and hybrid optimal control of intelligent vehicle longitudinal dynamics for velocity regulation. *Mechanical Systems and Signal Processing*, v. 162, p. 108089, 2022.

SUNG, K.-G.; SEONG, M.-S.; CHOI, S.-B. Performance evaluation of electronic control suspension featuring vehicle ER dampers. *Meccanica*, v. 48, n. 1, p. 121–134, 2013.

TALARICO, E. M. *et al.* A Virtual Development Approach Using Advanced HiL Steering Bench. [S.l: s.n.], 2022. p. 454–478.

TOTA, A. *et al.* An Intelligent Predictive Algorithm for the Anti-Rollover Prevention of Heavy Vehicles for Off-Road Applications. *Machines*, v. 10, n. 10, p. 835, 21 set. 2022.

USTEBAY, S.; TURGUT, Z.; AYDIN, M. A. Cyber Attack Detection by Using Neural Network Approaches: Shallow Neural Network, Deep Neural Network and AutoEncoder. [S.l: s.n.], 2019. p. 144–155.

VAN DE BURGT, Y.; GKOUPIDENIS, P. Organic materials and devices for brain-inspired computing: From artificial implementation to biophysical realism. *MRS Bulletin*, v. 45, n. 8, p. 631–640, 2020.

VARGAS, V. *Efeitos da flexibilidade estrutural em simulações de dinâmica lateral de veículo de transporte de carga*. 2011. 1–132 f. MSc – Universidade Federal do Rio Grande do Sul, Porto Alegre, 2011.

VEPA, R. *Flight dynamics, simulation, and control: For Rigid and Flexible Aircraft*. First ed. Boca Raton: CRC Press, 2015.

VI-GRADE. *VI-Grade provides to FCA Latam and PUC Minas the first dynamic driving simulator to be ever installed in Latin America*.

VILELA, D.; BARBOSA, R. S. Analytical models correlation for vehicle dynamic handling properties. *Journal of the Brazilian Society of Mechanical Sciences and Engineering*, v. 33, n. 4, p. 437–444, 2011.

WANG, M. *et al.* Frequency-Based Modeling of a Vehicle Fitted With Roll-Plane Hydraulically Interconnected Suspension for Ride Comfort and Experimental Validation. *IEEE Access*, v. 8, p. 1091–1104, 2020.

WANG, Q. *et al.* Optimal Coordinated Control of ARS and DYC for Four-Wheel Steer and In-Wheel Motor Driven Electric Vehicle With Unknown Tire Model. *IEEE Transactions on Vehicular Technology*, v. 69, n. 10, p. 10809–10819, out. 2020.

WANG, Y. *et al.* The influence of the activation function in a convolution neural network model of facial expression recognition. *Applied Sciences*, v. 10, n. 5, p. 1897, 2020.

WEI, C.; TAGHAVIFAR, H. A novel approach to energy harvesting from vehicle suspension system: Half-vehicle model. *Energy*, v. 134, p. 279–288, set. 2017.

XIANG, X. *et al.* Research on vehicle comfort testing and evaluation based on the characterization of passenger motion sickness degree. 13 jul. 2024, [S.l.]: SPIE, 13 jul. 2024. p. 112.

YANG, M. *et al.* A hybrid approach to building simplification with an evaluator from a backpropagation neural network. *International Journal of Geographical Information Science*, p. 1–30, 2021.

YING, X. An overview of overfitting and its solutions. 2019, [S.l: s.n.], 2019. p. 22022.

YU, B. *et al.* Modeling study of sandstone permeability under true triaxial stress based on backpropagation neural network, genetic programming, and multiple regression analysis. *Journal of Natural Gas Science and Engineering*, v. 86, p. 103742, 2021.

ZALEWSKI, J. Analysis of the Motor Vehicle Dynamics on the Example of a Fish Hook Maneuver Simulation. [S.l: s.n.], 2017. p. 248–259.

ZHANG, B.; LUO, M.; TAN, C. A. Ride comfort and energy harvesting of inflatable hydraulic-electric regenerative suspension system for heavy-duty vehicles. *Journal of Mechanical Science and Technology*, v. 38, n. 5, p. 2277–2289, 3 maio 2024.

ZHANG, N.; DONG, G.-M.; DU, H.-P. Investigation into untripped rollover of light vehicles in the modified fishhook and the sine maneuvers. Part I: Vehicle modelling, roll and yaw instability. *Vehicle System Dynamics*, v. 46, n. 4, p. 271–293, 2008.

ZHANG, X. *et al.* Vehicle Handling Indexes Mining and Consistency of Subjective and Objective Evaluation. [S.l: s.n.], 2020. p. 1302–1312.

ZHANG, X. *et al.* Vehicle roll centre estimation with transient dynamics via roll rate. *Vehicle System Dynamics*, v. 60, n. 2, p. 699–717, 1 fev. 2022.

ZHAO, J. *et al.* Exploring the Relationships between Subjective Evaluations and Objective Metrics of Vehicle Dynamic Performance. *Journal of Advanced Transportation*, v. 2018, 19 set. 2018.

ZHAO, L. *et al.* Truck Handling Stability Simulation and Comparison of Taper-Leaf and Multi-Leaf Spring Suspensions with the Same Vertical Stiffness. *Applied Sciences*, v. 10, n. 4, p. 1293, 14 fev. 2020.

ZHOU, C.; LIU, X.; XU, F. Intervention criterion and control strategy of active front steering system for emergency rescue vehicle. *Mechanical Systems and Signal Processing*, v. 148, p. 107160, 2021.

ZHOU, W. *et al.* A novel objective evaluation method of drivability for passenger cars considering subjective and objective consistency. *Proceedings of the Institution of Mechanical Engineers, Part D: Journal of Automobile Engineering*, v. 237, n. 4, p. 607–621, 16 mar. 2023.